Three-Dimensional Vestibulo-Ocular Reflex in Humans: a Matter of Balance

Janine Goumans

Three-Dimensional Vestibulo-Ocular Reflex in Humans:
a Matter of Balance

Thesis: Erasmus Univeristy Rotterdam, The Netherlands

Cover: R.S. Kromowirjo
Printed by Whörmann print service (www.wps.nl)
ISBN: 978-90-9025087-8

Three-Dimensional Vestibulo-Ocular Reflex in Humans: a Matter of Balance

Vestibulo-Oculaire Reflex in Drie Dimensies bij de Mens: een Kwestie van Evenwicht

Proefschrift

ter verkrijging van de graad van doctor aan de
Erasmus Universiteit Rotterdam
op gezag van de
Rector Magnificus

Prof.dr. H.G. Schmidt

en volgens besluit van het College voor Promoties

De openbare verdediging zal plaatsvinden op

woensdag 14 april 2010 om 15.30 uur

door

Janine Goumans

geboren te Amsterdam

Promotiecommissie

Promotoren:	Prof.dr. J.G.G. Borst Prof.dr. L. Feenstra
Overige leden:	Prof.dr. M.A. Frens Prof.dr. P.J. Koudstaal Prof.dr. ir. M. Mulder
Copromotor:	dr. J. van der Steen

The study described in this thesis was supported by Dutch NWO/ZonMW Grants number 912-03-037 and 911-02-004.

Publication of this thesis was financially supported by:
ALK-Abelló B.V., Atos Medical B.V., GlaxoSmithKline, Schering-Plough en de Nederlandse Vereniging voor KNO-heelkunde en Heelkunde van het Hoofd-Halsgebied.

Contents

Chapter 1

General introduction

Objective

The objective of this thesis was to quantify three-dimensional ocular stability in response to head movements in healthy human subjects and in patients with various types of peripheral vestibular disorders. Despite a large increase in our knowledge from animal and human studies about the neuronal circuitry that regulates three-dimensional (3D) vestibular organization (for a recent review see Angelaki and Cullen 2008), its application to clinical practice is still a long way ahead. In order to bridge this gap, we explored in healthy subjects the naturally occurring variability in 3D vestibulo-ocular stabilization and compared these results with changes that occur in 3D vestibulo-ocular stabilization in patients with various types of unilateral vestibular disorders.

To keep the human body in an upright position and maintain spatial orientation during voluntary and involuntary movements a joint effort of three sensory modalities is required. These three senses are vision, proprioception and the sense of equilibrium (vestibular system). The combined information of these three sensory systems is processed by the central nervous system (brain) to generate appropriate motor commands that help us to maintain spatial orientation (Figure 1).

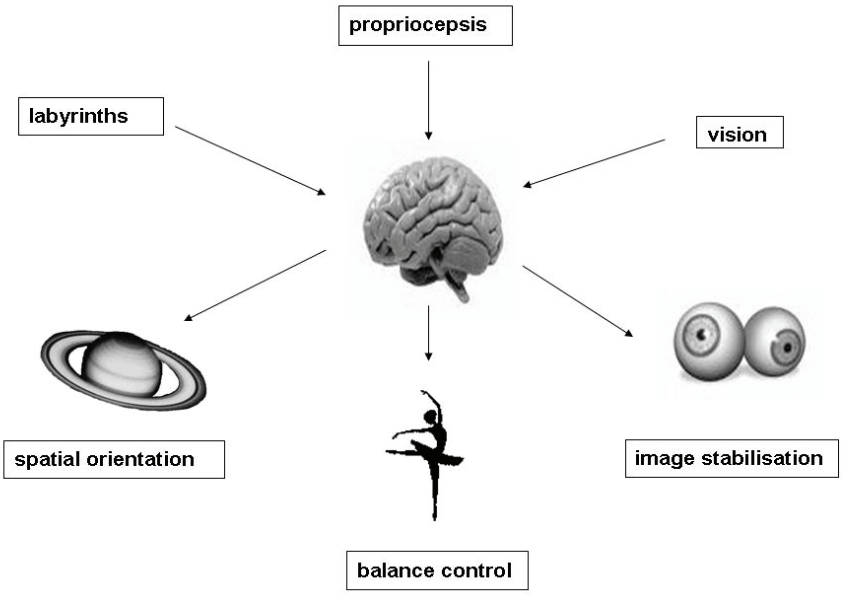

Figure 1. Schematic illustration of the multisensory interaction for maintaining balance and spatial orientation.

At first the anatomy and physiology of how the vestibular system allows it to function as an organ that senses head rotations and translations in three

dimensions is described. An explanation how vestibular driven compensatory eye movements are organized and how these movements can be measured follow this.

The vestibular system

Vestibular signals are generated in specialized areas of the inner ear. These are the three semicircular canals and the two otolith organs, the utriculus and sacculus (Figure 2). Together they form the equilibrium organ. Together with the hearing organ it is enclosed in the petrosal bone, which is part of the temporal bone.

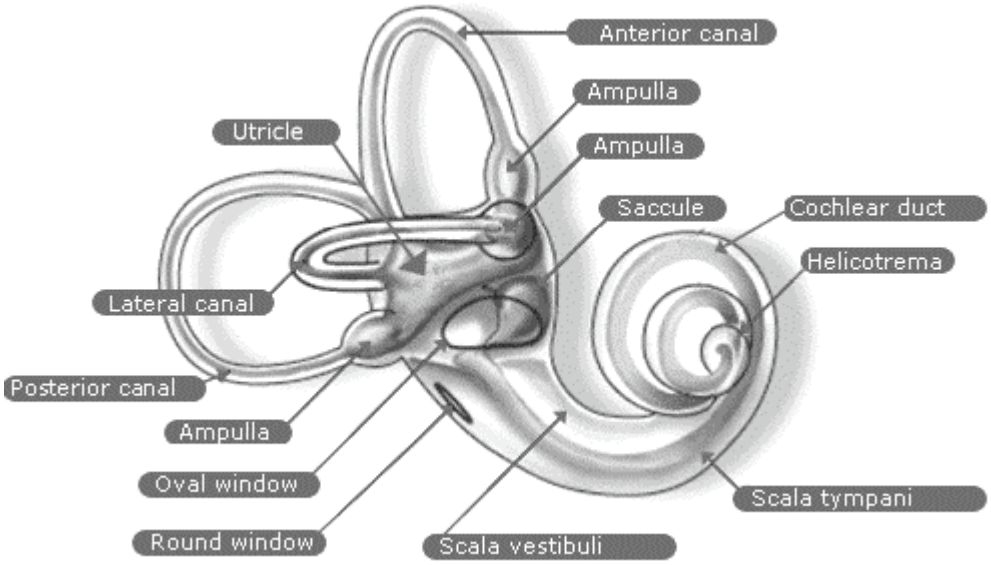

Figure 2. Illustration of the parts of the equilibrium organ. Note the close relation to the inner ear (cochlea) as illustrated by the continuity of the endolymph in hearing and equilibrium organ. Source: www.asc-csa.gc.ca.

The semicircular canals are small membranous tubes with an inner diameter of 0.4 mm and an outer diameter of 6.5 mm. The horizontal canal has a backward tilt of 19.9° when the head is in an upright position with the nasal-occipital axis, the superior and posterior semicircular canal make an angle of 94° (Della Santina et al. 2005).
The semicircular canals register angular accelerations during head movements in 3D (Breuer 1874; Egmond et al. 1949). The capability of the semicircular canals to detect angular accelerations is due to the small diameter of the canals and the viscosity of the endolymph fluid within the canals.
The hair cells in the sensory epithelium of the canals are positioned on a crest-like septum, the crista, which is positioned perpendicular to the longitudinal axis of the canal in an enlarged part of the canal, the ampulla. The hair cells consist of multiple stereocilia and one kinocilium protruding into

a gelatinous mass, the cupula, which reaches onto the roof of the canal (Ramprashad et al. 1984; Mc Laren and Hillman 1979). When there is a sudden head displacement the motion of endolymph will lag behind. This leads to a deflection of stereocilia and the kinocilium located on the apical side of each hair cell (Breuer 1874; Rasmussen and Windle 1960) (Figure 3). The stereocilia are very sensitive: a deflection of one Angstrom (1 Å = 10^{-10} m) can be detected. Deflection of the stereocilia leads to a cascade of cellular events causing receptor potentials at the base of the cell. The larger the deflection of the stereocilia, the larger the change in membrane potential.

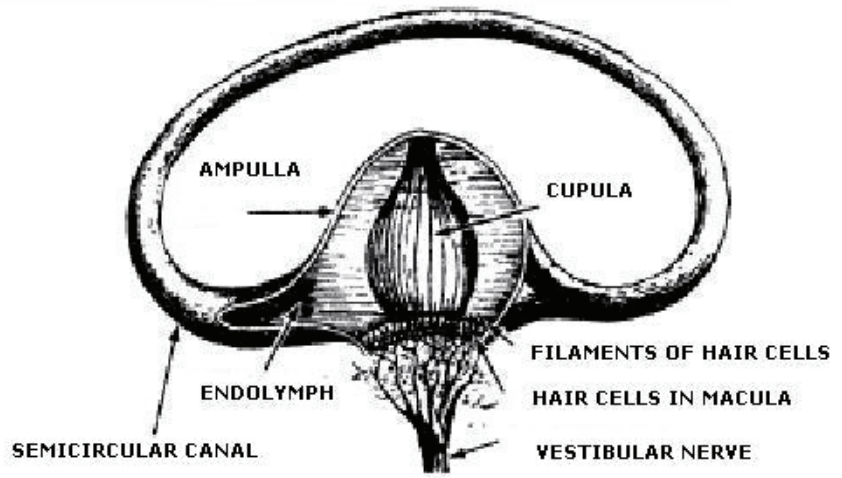

Figure 3. Schematic illustration of the sensory epithelium of a semicircular canal. During a sudden head movement the endolymph temporarily lags behind, which leads to a deflection of the stereocilia and kinocillia of the hair cells.
Source: www.cami.jccbi.gov/aam-400/phys_intro.htm

The utriculus and sacculus are two separate globular cavities in the vestibule part of the membranous labyrinth. The sacculus lies inferior to the utriculus on the medial wall of the vestibule (Figure 2). The sensory epithelium of both otoliths consists of a row of hair cells. These cells are oriented towards a line, the striola. The hair cells on each side of the striola are oriented to have their kinocilia point in opposite direction. Because of this orientation, the afferent output of one otolith is the difference between excitation on one side of the striola and inhibition on its other side. The stereocilia are within the otolithic membrane. The otolithic membrane contains the otoconia, small calcium carbonate crystals, ranging from 0.5 to 30 micrometers in diameter, which have a density of more than twice that of water (de Vries 1950). During accelerations or changes in position in relation to gravity, the higher mass of these crystals causes a deflection of the stereocilia. Bending of the stereocilia towards the kinocilium results in an increase of the spontaneous firing rate of vestibular nerve fibers; bending into the opposite direction results in a decrease of the firing rate (Lowenstein and Wersall 1959).

The function of the otoliths is to detect linear accelerations in all three dimensions and also to detect changes in position with respect to gravity. The axes of optimum sensitivity of the sensory epithelium of both sacculus and utriculus are curved: that of the sacculus lies predominantly in a vertical position. The sensory epithelium of the utriculus is predominantly in horizontal direction (Figure 4). The curved axes of optimum sensitivity allow the otoliths to cover three-dimensional orientation in space.

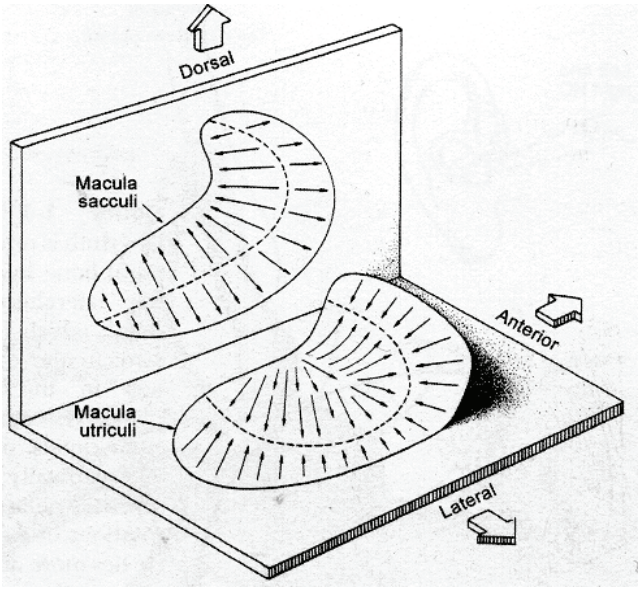

Figure 4. Schematic illustration showing the organization of the hair cells in the two otoliths and their orientation sensitivity. Source: Baloh RW, Honrubia V. Clinical Neurophysiology of the vestibular system, third edition 2001 Oxford.

Vestibular function

A more detailed insight in vestibular function can be gained from studying the vestibular reflexes and in particular the vestibulo-ocular reflex (VOR). The VOR is a reflex eye movement system that stabilizes images on the retina during head movement by producing an eye velocity that is equal and opposite to head velocity, thus preserving the image on the centre of the visual field (Crawford and Vilis 1991; Angelaki 2004). When there is continuous motion of the head a nystagmus occurs. Nystagmus is a slow eye movement (the vestibular component) in opposite direction, with a fast movement (the resetting component) in the same direction as the head movement.
The basic elements of the vestibulo-ocular reflex are a hair cell, an afferent bipolar neuron, an interneuron and an effector neuron (Lorente De No 1993). Because of the small number of elements in this reflex arc, the VOR is a fast reflex, which is necessary to maintain clear vision during head movements. There are two types of VOR: the rotational VOR due to stimulation of the

semicircular canals and the translational VOR due to stimulation of the otoliths.
Figure 5 shows schematically how the VOR works during a horizontal head movement.

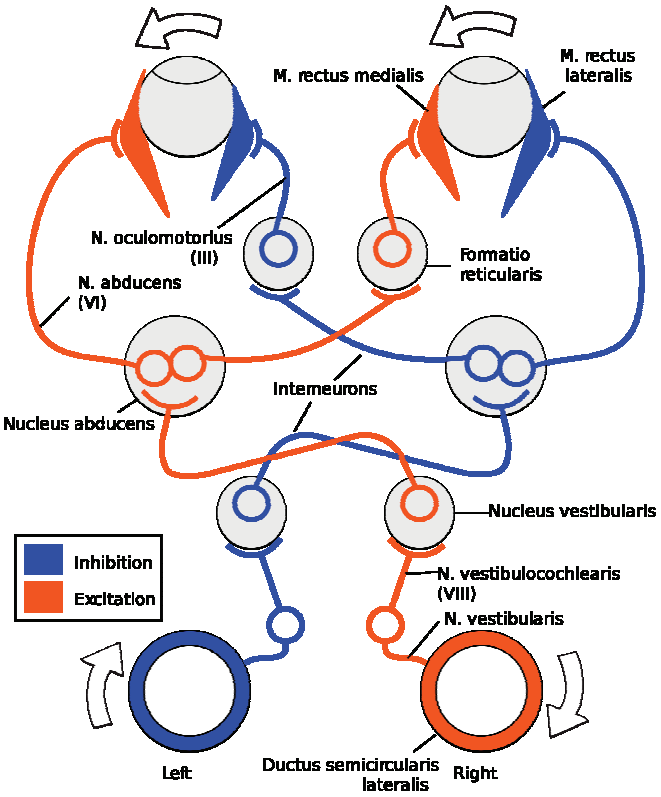

Figure 5. Schematic illustration of the three neural arc reflex of the vestibulo-ocular reflex. Source: www.en.wikipedia.org/wiki/Vestibulo-ocular_reflex.

If, for example, the head rotates to the right then excitatory impulses are sent from the horizontal semicircular canal on the right side via the vestibular nerve through Scarpa's ganglion to the vestibular nuclei in the brainstem. From these nuclei excitatory fibers cross to the left abducens nucleus, which projects to and stimulates the rectus lateralis muscle of the left eye. In addition, via an internuclear pathway to the oculomotorius nerve (III) running through the medial longitudinal fascicle (MLF), the rectus medialis muscle of the right eye is also stimulated. At the same time, neurons from the right vestibular nucleus directly stimulate the right rectus medialis muscle and inhibit the right nucleus abducens. As a result both eyes turn to the left, the opposite direction of the head movement.
This three-neural arc works similarly for vertical and torsional as well as for translational head movements, although it makes use of different pathways. For instance, rotational acceleration of the superior semicircular canal results in contraction of the ipsilateral rectus superior muscle and contralateral oblique inferior muscle and relaxation of the ipsilateral rectus inferior muscle

and contralateral oblique superior muscle, resulting in an upward torsional eye movement. Rotational acceleration of the posterior semicircular canal results in contraction of the ipsilateral oblique superior muscle and contralateral rectus inferior muscle and relaxation of the ipsilateral oblique inferior muscle and contralateral rectus superior muscle, resulting in a downwards torsional eye movement. Both labyrinths work together intensively and are each other's antagonists. Stimulation of one side directly results in inhibition of the other side, the so-called push-pull system. This principle is possible because the afferent fibers of the vestibular nerve have high spontaneous activity (Hoagland 1932) with a resting rate up to 90 spikes/sec (Goldberg and Fernandez 1971).

Disorders of spatial orientation and equilibrium

If there is a failure somewhere in the process of sensory-motor integration, complaints of dizziness and/or unsteadiness occur. These complaints can range from a feeling of lightness in the head during sudden head movements to disabling complaints which can prevent people to continue their daily activities such as taking a shower or driving a car.
Dizziness is a common complaint for the family physician. In the Netherlands the incidence is 27 per 1000 inhabitants (Verheij et al. 2002).
One general problem in quantifying vestibular complaints is the ambiguity in the term dizziness, as perceptions related to our sense of equilibrium are difficult to verbalize. Therefore, it is often difficult to determine the exact cause of dizziness from patient's descriptions. Indeed, it is much easier to describe changes in visual acuity or hearing disabilities.
Other problems are the many causes of dizziness and the not infrequently encountered fact that more than one cause can be simultaneously active within one patient. For example, a head trauma can have its impact on the brain, one or both labyrinths and the neck musculature.
In this thesis we tested two groups of patients: patients with vestibular Schwannoma and patients with superior canal dehiscence syndrome (SCDS). Vestibular Schwannoma is usually a benign tumor that arises from the sheath of the eighth cranial nerve; this tumor usually grows very slowly. Although the most frequent reason why patients go to a doctor is sensorineural hearing loss, in 49 -66% of the patients this is accompanied by dizziness (Humphriss et al. 2003). SCDS is caused by partial or complete absence of bone overlying the superior semicircular canal, which results in characteristic balance and/or hearing problems (Minor et al. 1998; Brantberg et al. 2001; Mikulec et al. 2004). Common symptoms are dizziness following a sound stimulus ('Tullio phenomenon') or following changes applied to the external ear ('Hennebert's sign'), increased sensitivity for bone-conducted sounds and/or decreased sensitivity for air-conducted sounds, autophony or pulse-synchronous tinnitus. The underlying cause for these symptoms is that the dehiscence of bone of the superior canal acts as a 'third window', leading to pressure changes within the vestibular part of the labyrinth in stead of only into the cochlea (oval and round window) (Minor et al. 2003; Rosowski et al. 2004).

Measuring the VOR

Directly studying the stabilizing reflexes, such as the VOR, also can give more insight into causes of vestibular dysfunction. The quality of the VOR is expressed as the gain of the reflex, which is defined as the ratio between the velocity in the eye rotation and velocity in the head rotation. Ideally, the gain of the rotational VOR is 1. The gain of the horizontal and vertical VOR is close to one, but the gain of the torsional VOR is generally much lower (Crawford and Vilis 1991; Ferman et al. 1987; Tabak and Collewijn 1994; Paige and Seidman 1999; Misslisch and Hess 2000; Roy and Tomlinson 2004).
To measure the VOR accurately, one needs an eye measurement device with sufficient precision to measure each eye movement component separately. In clinical practice electronystagmography is still used very often to quantify vestibular function on the basis of the VOR. A major drawback of this technique, however, is its relative inaccuracy of the system, especially for the non-horizontal eye movements. This limits the diagnostic value of the VOR to abnormalities in the horizontal plane.
Currently, the golden standard for measuring eye movements is the scleral search coil technique (Robinson 1963; Collewijn et al. 1975). This consists of a single copper coil embedded in a soft silicon annulus. Horizontal and vertical eye movements can be measured as changes in magnetic field. After modification of this technique the torsional component of the eye movement could also be measured (Ferman et al. 1987; Collewijn et al. 1985). The advantage of this technique is its accuracy and precision, but a disadvantage is limitation of measuring time to 30 minutes, because of its discomfort.
Nowadays, several video-based eye-tracking devices can provide a good alternative to the scleral search coil method for measuring two-dimensional eye movements (van der Geest and Frens 2002). The advantage of video-based techniques is its non-invasive character, but the application for 3D video recording systems are limited, because of the low frame sampling rate (typically about 50 Hz). In 2001, the first version of a novel infrared video-based 3D eye-tracking device with a frame rate of 200 Hz, the Chronos Eye Tracker (Chronos Vision, Berlin, Germany), was introduced. More recently, gain characteristics in the planes of the vertical canals were also measured (Halmagyi et al. 2001; Migliaccio et al. 2004; Houben et al. 2005). This became possible because of the combination of improved eye movement registration equipment and development in techniques for testing the vestibular system in a more natural way.
An important test for the vestibular function is head impulse testing. With this technique the examiner rotates the patients head suddenly with a small rapid impulse while the eye movements are registered continuously. If the first 100 ms of the eye movement response before visual information comes in are considered, head impulse tests allow direct assessment of vestibular function (Tabak and Collewijn 1994; Halmagyi et al. 2002). A drawback of this type of testing is the confounding influence of the neck afferents.

Experimental equipment

A primary goal of this thesis is to develop improved tests for detecting the function of the different semicircular canals. Therefore we introduce a new technique and describe experiments with a motion platform that generates head movements in any possible axis. This platform is capable of generating angular and translational whole body stimulation at a total of six degrees of freedom (6DF). Therefore this device allows testing vestibular function without interference of the visual system and neck afferents (propriocepsis). Eye movements were recorded with 3D scleral search coils, using a two field coil system that was fixated on the motion platform. Figure 6 shows the experimental design schematically. The whole body rotations were delivered about the three cardinal axes (vertical axis = yaw, interaural axis = pitch, nasal-occipital axis = roll) and about intermediate horizontal axes between pitch and roll with increments of 22.5°.

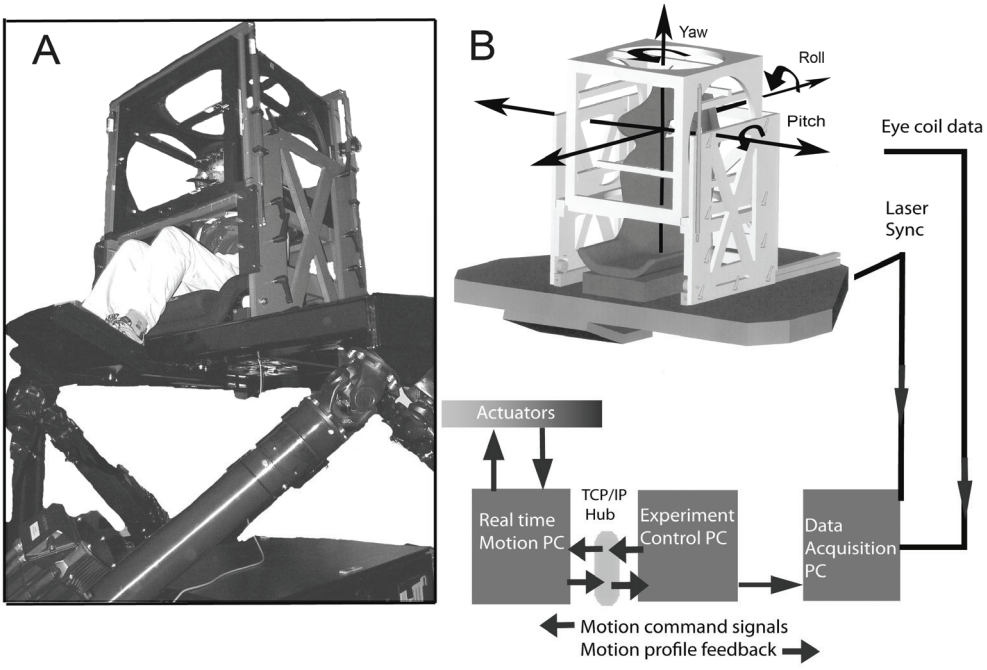

Figure 6. Schematic illustration of the experimental design; 6DF motion platform with the scleral search coil system.

Scope of this thesis

The objective of this thesis is to quantify the 3D ocular stability in response to head movements about a whole range of axes in 3D space in healthy human subjects and in patients with various types of peripheral vestibular disorders.

Chapter 2 gives a comparison of infrared eye tracking and scleral search coils to find the best methodology to measure 3D vestibulo-ocular reflexes accurately and reliably during whole body stimulation and visual tests in healthy subjects.

Chapter 3 reports on the quality of the 3D VOR under dark and light conditions in terms of gain and misalignment during 3D whole body stimulation in healthy subjects.

Chapter 4 describes 3D VOR in patients with partial or total unilateral vestibular dysfunction due to vestibular Schwannoma.

Chapter 5 presents a review of the superior canal dehiscence syndrome (SCDS).

Chapter 6 describes the results from 3D VOR measurements in patients with SCDS.

Chapter 7 describes the results of audiometric measurements in patients with SCDS.

References

Angelaki DE. Eyes on target: what neurons must do for the vestibulo-ocular reflex during linear motion. J Neurophysiol. 2004; 92(1): 20-35.

Angelaki DE, Cullen KE. Vestibular system: the many facets of a multimodal sense. Annual review of neuroscience. 2008; 31: 125-150.

Brantberg K, Bergenius J, Mendel L, Witt H, Tribukait A, Ygge J. Symptoms, findings and treatment in patients with dehiscence of the superior semicircular canal. Acta Otolaryngol. 2001; 121:68-75.

Breuer J. Uber die Funktion der Bogengange des Orhlabyrinthes. Wien med Jarhb 1874; 4: 71.

Collewijn H, Van der Mark F, Jansen TC. Precise recording of human eye movements. Vision Res. 1975; 15: 447-450.

Collewijn H, van der Steen J, Ferman L, Jansen TC. Human ocular counterroll: assessment of static and dynamic properties from electromagnetic scleral coil recordings. Exp Brain Res. 1985; 59: 185-196.

Crawford JD, Vilis T. Axes of eye rotation and Listing's law during rotations of the head. J Neurophysiol. 1991; 65(3): 407-23.

Della Santina CC, Potyagaylo V, Migliaccio AA, Minor LB, Carey JP. Orientation of human semicircular canals measured by three-Dimensional multiplanar CT reconstruction. J Assoc Res Otolaryngol. 2005; 6: 191-206.

De Vries H. The mechanics of the labyrinth otoliths. Acta Otolaryngol (Stockh). 1950; 38: 262.

Egmond AAJV, Groen JJ, Jonkees LBW. The mechanism of the semicircular canal. J Physiol. 1949; 110: 1.

Ferman L, Collewijn H, Jansen TC, Van den Berg AV. Human gaze stability in the horizontal, vertical and torsional direction during voluntary head movements, evaluated with a three-dimensional scleral induction coil technique. Vision Res. 1987; 27: 811-828.

Goldberg JM, Fernandez C. Physiology of peripheral neurons innervating semicircular canals of the squirrel monkey. 1. Resting discharge and response to constant angular accelerations. J Neurophysiol. 1971; 34: 635.

Halmagyi GM, Aw ST, Cremer PD, Curthoys IS, Todd MJ. Impulsive testing of individual semicircular canal function. Ann N Y Acad Sci. 2001; 942: 192-200.

Halmagyi GM, Aw ST, Karlberg M, Curthoys IS, Todd MJ. Inferior vestibular neuritis. Ann N Y Acad Sci. 2002; 956: 306-313.

Hoagland H. Impulses from sensory nerves of catfish. Proc natl Acad Sci USA. 1932; 18: 701.

Houben MMJ, Goumans J, Dejongste AH, Van der Steen J. Angular and linear vestibulo-ocular responses in humans. Ann N Y Acad Sci. 2005; 1039: 68-80.

Humphriss RL, Baguley DM, Moffat DA. Change in dizziness handicap after vestibular schwannoma excision. Otol Neurotol. 2003; 24: 661-665.

Lorente De No R. vestibulo-ocular reflex arc. Arch Neurol Psychiatory 1993; 30: 245.

Lowenstein O, Wersall J. A functional interpretation of the electron microscopic structure of the sensory hairs in the cristae of the

elasmobranch Raja clavata in terms of directional sensitivity. Nature. 1959; 184: 1807.
Mc Laren JW, Hillman DE. Displacement of the semicircular canal cupula during sinusoidal rotation. Neuroscience. 1979; 4: 2001.
Migliaccio AA, Schubert MC, Jiradejvong P, Lasker DM, Clendaniel RA, Minor LB. The three-dimensional vestibulo-ocular reflex evoked by high-Acceleration rotations in the squirrel monkey. Exp Brain Res. 2004; 159: 433-446.
Mikulec AA, McKenna MJ, Ramsey MJ, Rosowski JJ, Herrmann BS. Superior semicircular canal dehiscence presenting as conductive hearing loss without vertigo. Otol Neurotol. 2004; 25: 121-129.
Minor LB. Carey JP, Cremer PD, Lustig LR, Streubel S-O. Dehiscence of bone overlying the superior canal as a cause of apparent conductive hearing loss.Otology & Neurotology. 2003; 24: 270-278.
Minor LB, Solomon D, Zinreich JS, Zee DS. Sound- and/or pressure-induced vertigo due to bone dehiscence of the superior semicircular canal. Arch Otolaryngol head neck surg. 1998; 124: 249-258.
Misslisch H, Hess BJ. Three-dimensional vestibuloocular reflex of the monkey: optimal retinal image stabilization versus listing's law. J Neurophysiol. 2000; 83: 3264-3276.
Paige GD, Seidman SH. Characteristics of the VOR in response to linear acceleration. Ann N Y Acad Sci. 1999; 871: 123-135.
Rasmussen GL, Windle WF(eds). Neural mechanisms of the auditory and vestibular system. Charles C Thomas, Springfield, IL, 1960.
Robinson DA. A method of measuring eye movement using a scleral search coil in a magnetic field. *IEEE Trans Biomed Eng*. 1963; 10: 137-145.
Rosowski JJ, Songer JE, Nakajima HD, Brinsko KM, Merchant SN. Clinical, experimental and theoretical investigations of the effect of superior semicircular dehiscence on hearing mechanisms. Otology & Neurotology. 2004; 25: 323-332.
Roy FD, Tomlinson RD. Characterization of the vestibulo-ocular reflex evoked by high-velocity movements. Laryngoscope. 2004; 114: 1190-1193.
Tabak S, Collewijn H. Human vestibulo-ocular responses to rapid, helmet driven head movements. Exp Brain Res. 1994; 102: 367-378.
Van der Geest JN, Frens MA. Recording eye movements with video-oculography and scleral search coils: a direct comparison of two methods. J Neurosci. Methods. 2002; 114:1 85-195.
Verheij AAA, van Weert HCPM, Lubbers WJ, van Sluisveld ILL, Saes GAF, Eizenga WH, Boukes FS, van Lieshout J. Huisarts en Wetenschap. 2002; 45(11):601-609.

Chapter 2

Recording three-dimensional eye movements: scleral search coils versus video-oculography

Houben MMJ, Goumans J, van der Steen J

Invest ophthalmol Vis Sci, January 2006; 47(1):179-187

Abstract

The purpose of this study was to compare the performance of a video-based infrared three-dimensional eye tracker device (Chronos) with the scleral search coil method.
Three-dimensional eye movements were measured simultaneously with both systems during fixation, saccades, optokinetic stimulation and vestibular stimulation.
Comparison of fixation positions between -15º and +15º showed that horizontal and vertical eye position signals of the two systems were highly correlated (R^2 = 0.99). Torsion values measured by coils and video system were significantly different ($p<0.001$). Saccade main sequence parameters of coil and video signals were in good agreement. Gain of torsion in response to optokinetic stimulation (cycloversion and cyclovergence) were not significantly different ($p>0.05$). Gain values of the vestibulo-ocular reflex as determined from coil and video signals showed good agreement for rotations. However, there was more variability in the video signals for translations, possibly due to relative motion between the head and cameras.
The lower time resolution, possible instability of the head device of the video system and inherent small instabilities of pupil tracking algorithms makes the coil system the best choice when measuring eye movement responses with high precision or involving high frequency head motion. For less demanding and static tests and measurements longer than half an hour, the latest generation infrared video systems (e.g. Chronos) is a good alternative to scleral search coils. However, quality of torsion of the infrared video system is less compared to scleral search coils and needs further technological improvement.

Introduction

Because the oculomotor system is such a good model to relate sensory input to motor output, eye movement measurements are an important tool to study brain function. In humans, eye movement recordings are extensively used in behavioral and cognitive neuropsychological experiments. In addition, eye movement recordings are an important and sensitive tool to diagnose neurological, ophthalmologic and vestibular disorders.
For a long period the scleral search coil technique has been regarded as the golden standard for measuring eye movements. The scleral search coils were introduced by Robinson[1] and were modified by Collewijn and colleagues[2] into its present form: a single copper coil embedded in a soft silicon annulus. This initiated measurement of horizontal and vertical eye movements with unprecedented precision[2] in many laboratories all over the world. With a modified version of the coil it became possible to also measure torsional components.[3,4] Since then, three-dimensional (3D) coils have proved to be of indispensable value to study 3D kinematics of eye movements. [5,6,7,8,9,10,11]
Despite its precision and low signal-to-noise ratio, a drawback of the scleral search coil is that because of their invasive nature they can only be used for a maximum duration of 30 to 60 minutes. Therefore, there has always been a search for alternative, non-invasive recording techniques capable of accurate measurement of three-dimensional eye movement. Although several video-based eye-tracking devices now exist that can provide a good alternative to the scleral search coil method for measuring two-dimensional (2D) eye movements,[12] when it comes to recording 3D eye movements, choices of commercially available video recording systems are limited. The main problem of 3D infrared (IR) eye measurement systems was their low frame sampling rate (typically about 50 Hz). In 2001, the first version of a novel infrared video-based 3D eye-tracking device with a frame rate of 200 Hz, the Chronos Eye Tracker (Chronos Vision, Berlin, Germany), was introduced. Since then, numerous improvements have been made on its hardware and software.
IR eye movement trackers in general and 3D IR eye trackers in particular are increasingly used in fundamental investigations as well as for clinical diagnosis. Therefore, we performed a comparison of 3D eye movements measured by the scleral search coil method with eye movements measured simultaneously by the video-based Chronos system. To allow a good overall comparison of performance, we tested the two methods simultaneously under static (fixations and saccades) and dynamic (optokinetic and vestibular stimulation) conditions.

Methods

Subjects

Four healthy subjects (three male, one female) without any history or clinical signs of oculomotor or vestibular abnormalities participated in the experiment. Ages were 25, 29, 46, and 53 years. Three subjects had brown eyes, the other subject blue eyes. One subject had corrected vision (refractive error of −3D and −5D for left and right eye, respectively), but did not wear his glasses during our experiments. Three subjects had worn scleral

search coils before. All subjects participated on voluntary basis and gave their informed consent. Experimental procedures were approved by the Medical Ethical Committee of the Erasmus University Medical Center and adhered to the Declaration of Helsinki for research involving human subjects.

Eye movement recordings

Images of both eyes were recorded with an infrared video-based eye-tracking system (Chronos Vision, Berlin, Germany), capable of 3D eye position measurement. The Chronos system is available in two versions. One is a standalone system, which plugs in to the parallel board of a personal cmoputer. The other version, which we used, is a personal computer based system with dedicated hard- and software. In our experiment subjects wore the head device delivered with the system. It has laterally mounted digital infrared cameras (Figure 1) ensuring a free field-of-view and allowing measurement of eye rotations of at least ±30 degrees horizontally and ±25 degrees vertically. The head was immobilised using an individually moulded silastic dental-impression bite bar. The image sequences of both eyes were sampled at a frequency of 200 Hz and stored to hard disk for off-line extraction of eye positions. For recording and off-line calculation we used software supplied by Chronos Vision in 2004: "etd2.exe", version 3.4.0.0 and "iris.exe", version 2.1.6.1, respectively.

Chronos' off-line algorithm for calculation of horizontal and vertical eye position is based on a circle approximation technique (Hough transform), which fits a circle to the pupil perimeter.[13] Eye responses to calibration data were used during off-line evaluation by the Chronos software for correction of the geometric projection error in tertiary eye positions and for the transformation from pixel to Euler co-ordinates. Torsional eye positions were calculated by correlation of an iris signature (iris luminance profile derived from circular sampling around the iris) of the current frame with a predefined reference signature.[13] The resulting raw 3D eye positions are expressed in Fick angles. The inset of Figure 1 shows an example image during off-line analysis of an eye recorded by the Chronos system and with the pupil fit and iris signature indicated. Although the Chronos software provides scleral marker tracking as an alternative to the iris segment correlation, we did not use it as the software did not allow us to get a wide-angle video image of the eye and it would invalidate the non-invasiveness of the video system.

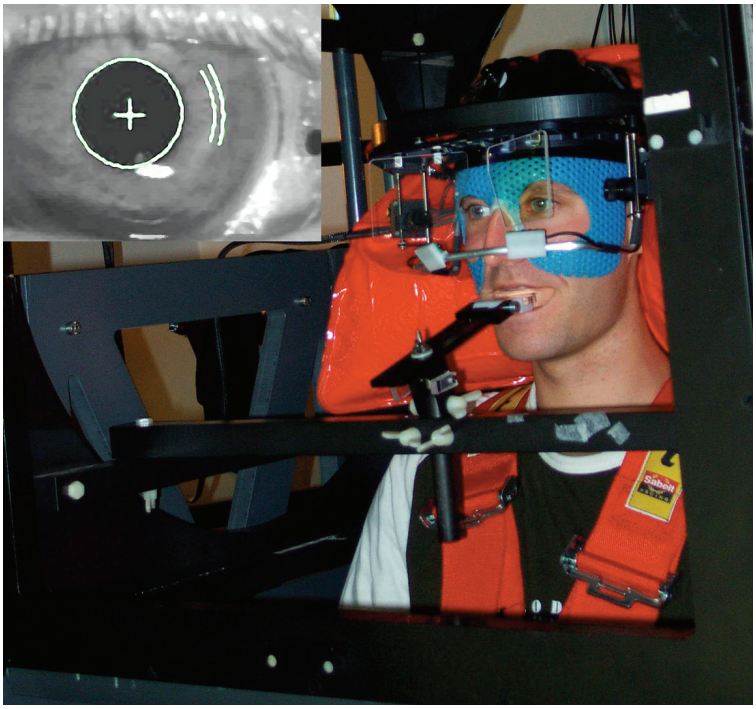

Figure 1. Photograph of the setup with the eye movement recording devices. A subject who is held in place with a bite bar wears the Chronos head device and is surrounded by a cubic frame containing the field coils. The inset shows an image recorded and used by Chronos' recording and analysis software, of a subject's eye with scleral search coil inserted (partially visible around the limbus). Also shown is the fit through the pupil (white circle) and its center position (white cross) as well as an iris signature with two segments (curved white lines to the right of the pupil).

As the scleral search coils do not cover the pupil and iris, we were able to measure three-dimensional eye positions simultaneously with the video system and scleral search coils (see Figure 1). We used a standard 25 kHz two field coil system based on the amplitude detection method by Robinson.[1] (Model EMP3020, Skalar Medical, Delft, The Netherlands). Standard dual coils embedded in a silicone annulus (Skalar Medical, Delft, The Netherlands) were inserted in each eye. Before insertion the eyes were anaesthetised with a few drops of oxybuprocain (0.4%) in HCL (pH 4.0). Both coils were pre-calibrated in vitro by mounting them on a gimbal system placed in the centre of the magnetic fields. The coil signals were passed through an analog low-pass filter (cut-off 500 Hz) and sampled on-line at a frequency of 200 Hz and with 12 bit precision by the analog to digital converter (ADC) board provided in the Chronos system. Thus, we obtained synchronous IR video and search coil signals. In addition, we also sampled the coil data at 1000 Hz on a CED system (Cambridge Electronic design, Cambridge). All data were stored to hard disk for off-line analysis.

Stimuli
Visual stimuli were back-projected onto a translucent screen in front of each subject at a distance of 189 cm. The centre of the visual target was horizontally and vertically aligned with the centre point between the subject's eyes. Subjects were tested under the following static and dynamic conditions.

Fixations
Subjects viewed a succession of 25 white dots, one at a time, against a black background. The horizontal and vertical position of the dots was at eccentricities of -15º, -7.5º, 0º, 7.5º and 15º, together forming a grid of 5 x 5 targets. Each target was visible for 4 s. Subjects were asked to fixate the targets as accurately as possible.

Voluntary saccades
We tested voluntary saccades in full detail in one subject. While looking at a grid pattern with horizontal and vertical grid lines at 5º intervals, the subject was instructed to make voluntary saccades at random towards the cross-sections of horizontal and vertical grid lines. In this way, saccades with amplitude over a range of 5º to 30º in any direction were recorded.

Optokinetic stimulation
Two identical patterns of 1000 random dots were presented dichoptically on the projection screen. Subjects looked at the centre of the patterns, whereas the patterns oscillated sinusoidally in the same direction (cycloversion) or opposite direction (cyclovergence) about the line of sight. The frequency was 0.24 Hz and the peak-to-peak amplitude was 4° for the cycloversion condition and 2° for the cyclovergence condition. The duration of each stimulus was 70 s.

Vestibular stimulation
To deliver vestibular stimuli, a motion platform (FCS, Schiphol, The Netherlands) capable of rotatory and linear motion in any direction was used. Subjects were seated in a rigid chair mounted on the platform and securely fastened with heavy-duty seatbelts as used in racing cars. Further fixation of subjects during the whole-body motion was ensured by a bite bar connected to a solid cubic frame rigidly mounted on the platform and a vacuum cushion folded around the head and around a ring that was fixed to the chair. The centre of rotation for all axes of rotation of the platform was set under software control to be midway between the ears. We performed sinusoidal tests on all subjects in the light as well as in darkness. In the light condition, subjects fixated a target that was projected onto the screen in an otherwise darkened room. The platform was sinusoidally rotated or translated about or along one of three orthogonal axes in space: the gravity aligned axis ("yaw" rotation and "heave" translation), the naso-occipital axis ("roll" rotation and "surge" translation), and the interaural axis ("pitch" rotation and "sway" translation). Naming of rotation and translation axes is in accordance with definitions used in aviation and simulation (see also description by Houben et al.[14]). Stimulation frequency was 0.5 Hz, duration 14 s (including 2 s of fade-in and fade-out time). Stimulus peak-to-peak amplitude was 8° for rotations and 0.2 m for translations (resulting in peak accelerations of respectively 40 °/s^2 and 1.0 m/s^2).

We determined coil artefacts induced by motion of the platform (and cubic frame containing the field coils) with one search coil attached to the bite bar and another one attached to the forehead of the subject. Peak-to-peak artefacts due to the motion as measured by the coils were less than 0.1º in any direction.

Data analysis

Eye movement signals obtained with the Chronos infrared video system were analysed with the supplied analysis software. The software converts the raw pixel data per eye into Fick co-ordinates by using a five-target calibration. For this, we used five targets from the fixation condition (with the 5x5 visual targets): the centre target and the four targets 7.5° left, right, above and below the centre.

For the coil system, eye responses to all 25 fixation targets were used to iteratively calculate the sensitivities and the misalignment of the coils minimising the deviations in horizontal and vertical eye positions from the target positions. By means of a three-dimensional matrix conversion to correct for misalignment of the coils, coil voltages were transformed into Fick angles.[24,26] The simultaneous use of the Chronos system with the search coils resulted in small inhomogeneties of the magnetic field caused by the metal in the Chronos head device. This induced small aberrations in especially the vertical eye positions. We compensated for these small inhomogeneties and nonlinearities in the magnetic fields by two three-layer back propagation neural networks that fitted the fixation data to the target locations.[15]

Velocity signals were calculated as a 5-point central difference of eye position samples (low pass characteristics of 50 Hz).[16] Fixations (defined as intersaccadic intervals) were marked automatically in the coil signal by detection of saccades using a velocity threshold of 100°/s and a minimum fixation length of 2 s. The same fixation intervals were taken for the video signal. Mean horizontal, vertical and torsional positions during each fixation were calculated independently for the coil and video signal.

For analysis of optokinetic stimulation, torsion signals of both eyes were used to yield cycloversion (average of left and right eye torsion, clockwise motion defined as positive) and cyclovergence signals (difference between left and right eye torsion, convergence defined as positive). From the cycloversion coil signal, saccades were removed using a velocity threshold of 20 º/s. In the cyclovergence signal no saccades were present because by taking the difference between the left eye and right eye torsion, saccades were automatically eliminated.

For analysis of vestibular stimulation, stimulus amplitude during translations (in meters) was translated into the geometrically required angle (in degrees) by taking into account the distance of 189 cm from the subject's eyes to the projection screen. This allowed easier comparison of the results for angular and linear stimulation as well as derivation of the gain of eye responses during translations in terms of required eye rotation at the used viewing distance. Saccades were removed from the raw data by using a velocity threshold of 12 °/s[16] and the smooth components as well as the stimulus signal were converted to the frequency domain using a Fast Fourier Transform (FFT). Gain and phase of left and right eye responses were calculated from the real and imaginary components.[17]

Results

Fixations

Eye positions for right and left eye as recorded with the coil and IR video system simultaneously during fixation of a target grid are shown in Figure 2 The target grid of 5x5 targets was scanned row by row from bottom left to top right target. This pattern can be observed in the time traces. The top two panels show the coil data, whereas the lower two panels give the video data. The coil and video signals are comparable, but at larger eccentricities occasionally erroneous eye positions can be observed in the video data, especially for torsional eye positions.

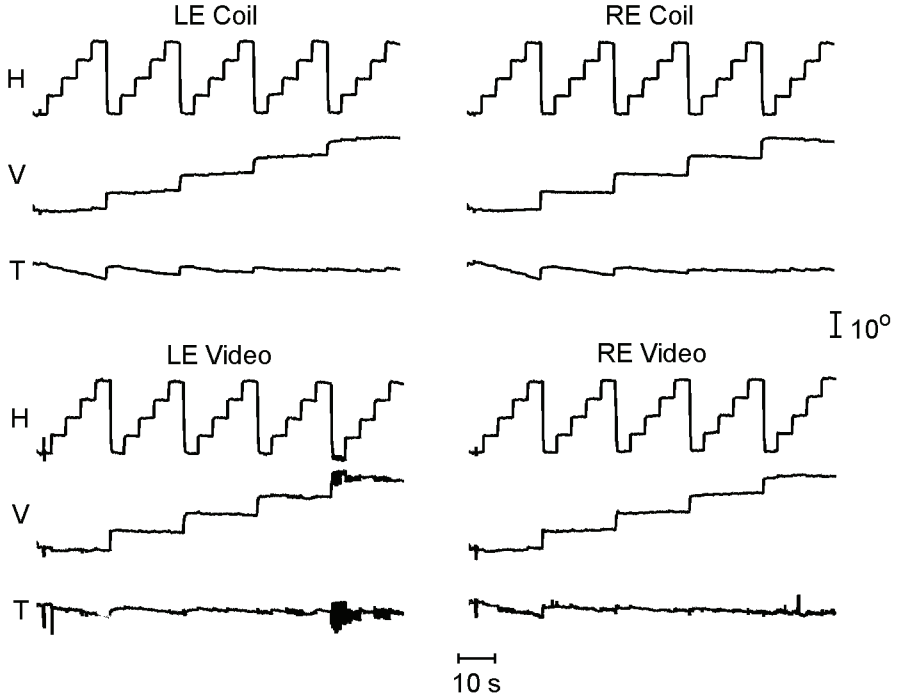

Figure 2. Example time traces of eye positions of subject JS during fixation of the 5x5 target matrix. LE = left eye, RE = right eye, Coil = positions as measured by the coil system, Video = positions as measured by the video system. H = horizontal (up = rightward), V = vertical, T = torsional (up = clockwise) eye positions.

In Figure 3 vertical eye positions during fixation are plotted as function of horizontal eye positions, thus revealing the target grid. The extracted fixation positions (indicated by crosses) correspond to the presented grid of fixation targets (indicated by the intersections of the dashed lines). The mean square differences between the true and actual fixation positions, averaged over left and right eye of all subjects, is 0.56° (horizontal) and 0.62° (vertical eye positions) for the video system and 0.096° (horizontal) and 0.080° (vertical eye positions) for the coil system. Although differences between positions recorded by the coil and video system can be observed (compare upper to

lower panels of Figure 3) within 10° from the centre position the fixation positions as determined from the coil and video signals are very similar. The mean square differences between coil and video for each fixation position, averaged across subjects, is 0.55° for horizontal and 0.61° for vertical eye positions.

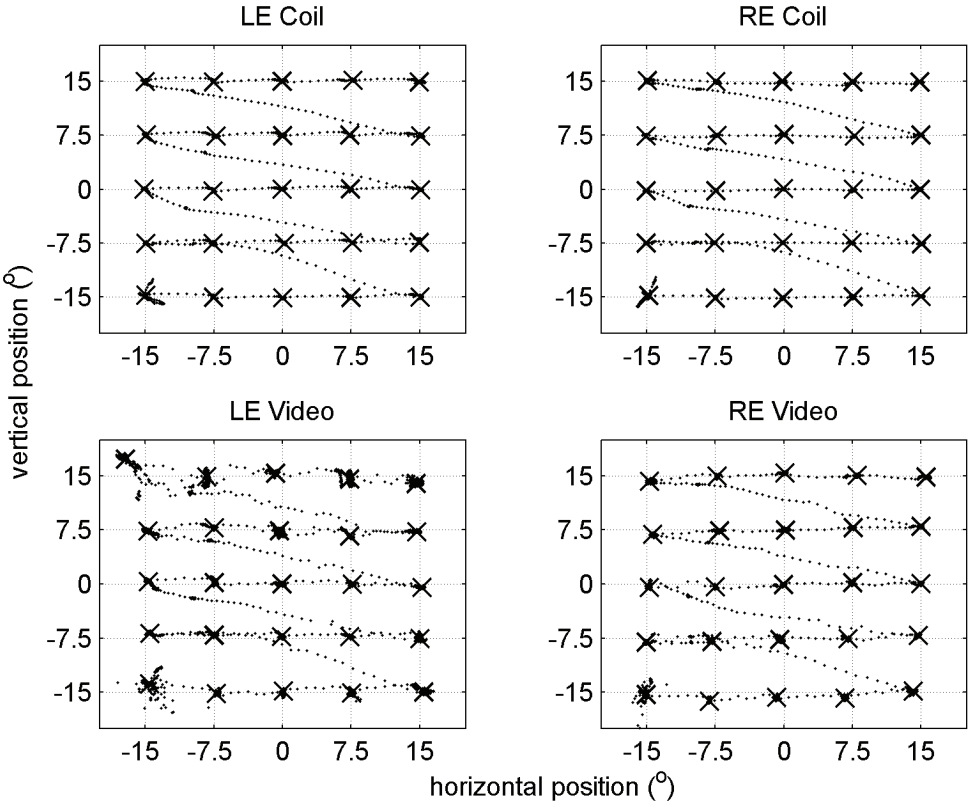

Figure 3. Horizontal versus vertical eye positions of subject JS during fixation. Crosses indicate extracted fixation positions (i.e. mean eye positions during each fixation epoch, see "Data Analysis" Section). Left panels: left eye (LE) data, right panels: right eye (RE) data. Top panels: coil data, bottom panels: video data.

In contrast, the correspondence between torsional eye positions measured by coil and video data during fixation was considerably less than for horizontal and vertical positions. Mean torsion at the fixation positions (Figure 4) show larger discrepancies between coil and video data. Especially for tertiary positions occasionally large discrepancies (up to 5°) are observed. Please note that the seemingly dramatic differences in torsional positions shown in Figure 4 have an exaggeration factor of 10 and are actually very small. The mean square differences between coil and video for each fixation position, averaged across subjects, is 1.9° for torsional eye positions.

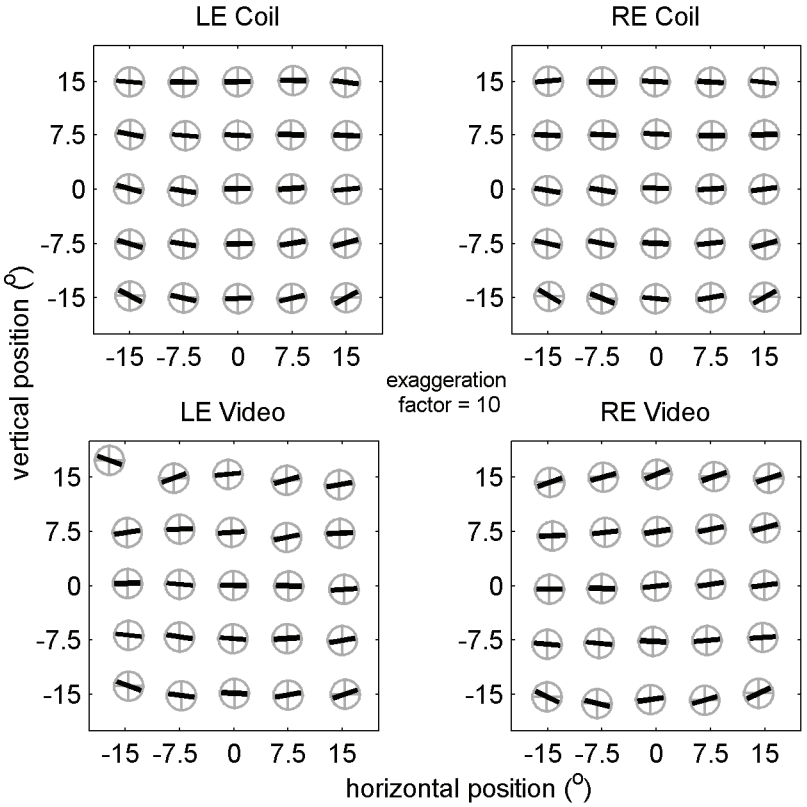

Figure 4. Mean torsion of the left eye (left panels) and right eye (right panels) of subject JS during fixation as function of the horizontal and vertical position of the eye as derived from the coil (upper panels) and video (lower panels) signals. The rotation angle of the depicted tilted bar compared to horizontal equals the torsion multiplied by an exaggeration factor of 10 for better visibility (clockwise torsion as seen from the subject is clockwise deviation from horizontal).

A quantitative comparison between measured eye positions of both systems during fixations is given in Figure 5. This figure shows that, although there is a good linear relationship throughout the measured range between coil and video signal for horizontal and vertical fixation positions (slopes near one), for torsion it is much lower. Individual fit parameters are listed in Table 1. The mean slope (averaged over right and left eye of all subjects) does not significantly differ from 1.0 at the 1% level for horizontal (Student's two-tailed t-test, $p=0.14$, $t=1.66$, $df=7$) and vertical positions ($p=0.58$, $t=0.59$, $df=7$), but does for torsion ($p<0.001$, $t=7.58$, $df=7$).

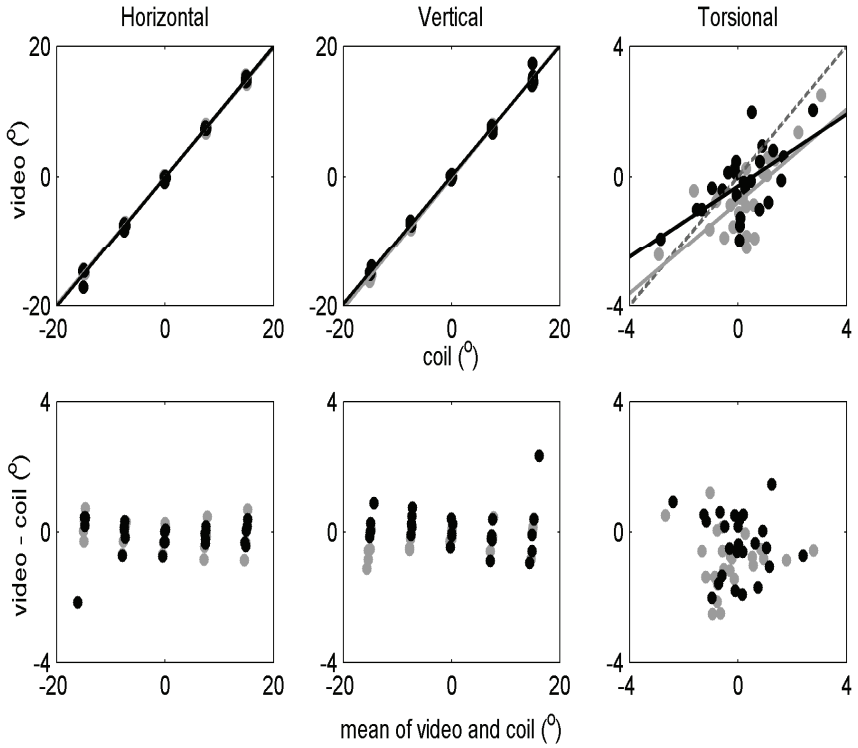

Figure 5. Upper three panels: correlation between coil and video data regarding horizontal (top left), vertical (top middle) and torsional (top right panel) eye positions of subject JS during fixation. Measured fixation positions are shown by dots (gray = right eye, black = left eye). Also shown are the unity line (dashed gray line) and straight lines fitted through the data points. Lower three panels: corresponding discrepancies between video and coil data as function of eccentricity (that is, mean position of video and coil data).

	Horizontal				Vertical				torsional			
	slope		R^2		slope		R^2		slope		R^2	
	left	right	left	right	left	right	left	right	left	right	left	right
JS	1.0	0.99	1.0	1.0	1.0	1.0	0.99	1.0	0.55	0.71	0.38	0.53
JR	0.96	0.99	0.99	0.99	1.0	0.99	0.99	0.99	0.11	0.58	0.0025	0.24
BW	0.99	0.96	0.99	1.0	0.96	1.0	0.99	0.99	0.12	0.31	0.026	0.49
JB	0.97	1.0	1.0	0.99	0.98	1.0	1.0	0.97	0.51	0.21	0.42	0.032
mean	0.98		1.0		0.99		0.99		0.39		0.27	

Table1. Fit parameters per subject. A straight line is fitted through the video fixation positions as a function of the coil fixation position. Slopes and R^2 of the fitted lines for horizontal, vertical and torsional eye positions are given for the left and right eye seperately. Horizontal and vertical eye positions larger than 20° and torsions larger than 10 ° in absolute value where discarded. Mean values averaged over right and left eye of all subjects are shown in the bottom row.

Voluntary saccades

Figure 6 shows a detailed saccade profile of a 30° saccade with two corrective saccades measured simultaneously with coils and video system. Although the overall shape of the saccade measured with the two systems is very similar, small differences exist in the details of the saccades. These differences have an impact on a quantitative saccade analysis. For instance, the alignment of the two eyes directly after the first saccade is different. This results in a 5°/s higher peak velocity of the left eye for the video signal compared to the coil signal. Note that this difference cannot be due to the load of the coil, as coil and video signals were measured simultaneously. Neither can it be caused due to differences in temporal resolution as both signals were collected with the same sampling frequency. To compare the coil and video system over a range of saccades we plotted the main sequence of horizontal and vertical saccades (Figure 7). Absolute values of left and right saccades as well as up and down for vertical saccades were pooled. Figure 7 shows that the results obtained with coils and video signals are very similar (t-test, p=0.94 or higher, see Table 2). Still, small differences can be observed. Firstly, for large horizontal saccades there is a tendency of higher peak velocities for video than for coil signals. Secondly, saccades measured with the video system have slightly longer duration at large amplitudes.

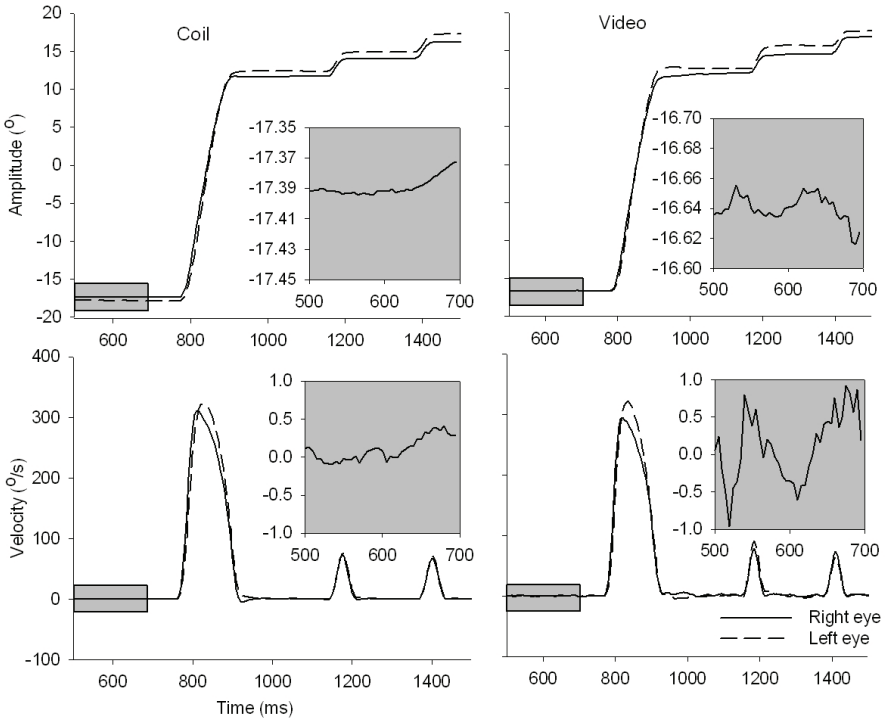

Figure 6. Example saccade made by subject JS. Shown are right (solid line) and left (dashed line) eye position (top panels) and velocity (bottom panels) as a function of time, measured by the coil (left panels) and video (right panels) system. Shaded insets show a magnification of the signals measured while the eyes fixate.

One possible cause for this variability is differences in signal noise. For this reason, we determined the signal noise levels of the two systems. The insets in Figure 6 show a high magnification of the position and velocity signals of the right eye. In this subject, the noise level measured with the coil on the eye was less than 0.02°. When we mounted the scleral coil on a gimbal system noise levels were a factor of 10 smaller (0.002°). Actual eye positions during fixation measured with the Chronos system resulted in noise levels of 0.2°. This value is approximately 30 times higher than the reported noise levels of 0.006° measured on a gimbal system.[13]

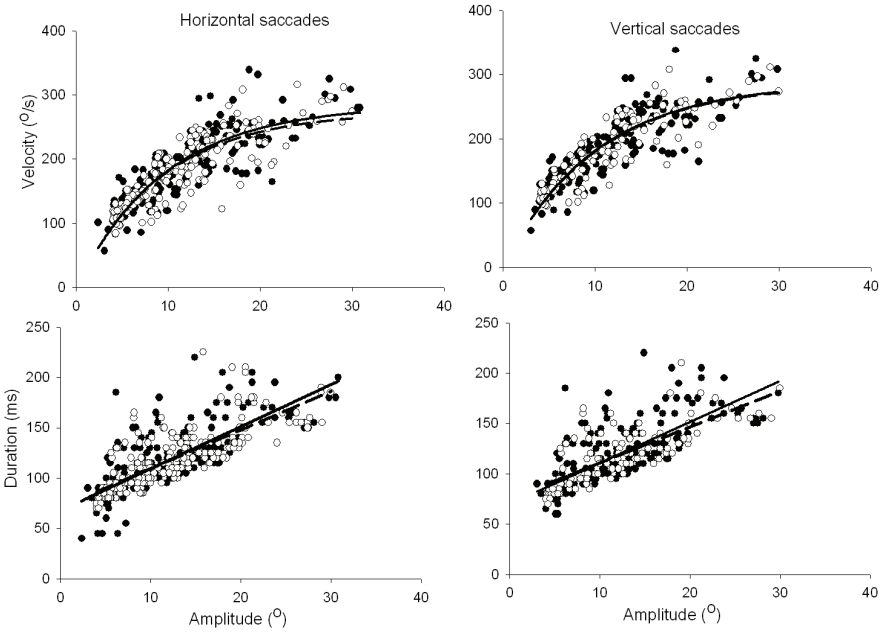

Figure 7. Main sequence plots of horizontal and vertical saccades made by subject JS. The top panels show amplitude peak-velocity relationships of horizontal (left panels) and vertical (right panels) saccades. The lower panels show amplitude versus duration. Solid circles show video data, coil data by open circles. The data in the top panels were fitted with an exponential curve, the lower two panels with a linear equation. Solid and dashed lines show fits through video and coil data points, respectively.

In summary, in a real eye movement recording on a human subject noise levels of the Chronos video signals are a factor of 10 higher than noise levels of the coil signals. The differences in noise levels are even more clearly visible in the velocity signals. On average we found a 1 °/s basic noise level during fixation for the video signals compared to 0.1°/s for the coil signals. When averaged across subjects the overall differences in noise were less pronounced. The standard deviation around the mean during each fixation interval, averaged over all targets and left and right eyes, was for the coils 0.25º (horizontal), 0.10º (vertical) and 0.22º (torsional eye positions). For the video signals these values were 0.32º, 0.26º and 0.41º, respectively.

Note that in this situation microsaccades, drift and blinks may all contribute to the variability.

Velocity		a	b	R^2	p value t-test
Horizontal	Coil	274	9.23	0.76	0.99
	Video	284	9.69	0.75	
Vertical	Coil	285	10.0	0.76	0.99
	Video	287	10.0	0.76	
Duration		c	d	R^2	p value t-test
Horizontal	Coil	75	3.7	0.59	0.99
	Video	71	3.8	0.63	
Vertical	Coil	75	3.7	0.59	0.94
	Video	70	3.2	0.57	

Table 2. Parameters of lines fitted through the data in Figure 7, as well as R^2 of fit. We fitted an exponential function for the amplitude-velocity data points: Vel = a (1-$e^{-Amp/b}$), where Vel is the fitted peak velocity (º/s), Amp is the saccade amplitude (º), and a and b are the fitted parameters (the saturation level (º/s) and the length constant (º), respectively) and a first order polynomial for the amplitude-duration data points: Dur = c + d Amp, where c is the intercept with the y-axis (ms) and d is the slope of the line (ms/º).

Optokinetic Stimulation

We also compared torsion signals in response to visual stimulation about the visual axis. Torsion signals of both eyes, as measured by the coil and video system, were used to yield cycloversion and cyclovergence signals. Figure 8 shows the cycloversion and cyclovergence as function of time for one subject. One major drawback of the video signals compared to the coil signals was the noise level. To reduce the noise in the cycloversion and cyclovergence signals of the video system, the signals were low pass filtered (using a fifth order low pass digital Butterworth filter) with cut-off frequency of 20 Hz. The figure shows that although the video signals indeed contained much more noise, they do contain the shape of the coil data as apparent in the envelopes. Gain values (ratio of spectral magnitude between torsional component of eye movement and stimulus movement at the stimulus frequency of 0.24 Hz) are shown in Figure 9. Individual gains as well as the mean and standard deviation are depicted for the cycloversion (left) and cyclovergence (right) condition. Although in both conditions the mean gain is lower for the video system compared to the coil system, the difference is not significant at the 0.05 level for both cycloversion (Student's paired t-test, p = 0.19, t = 1.67,

df = 3) and cyclovergence (p = 0.11, t = 2.24, df = 3). Notice that although the coil and video system lead to comparable results with regard to the gain of torsional eye responses, the high noise levels prohibit the use of saccade removal software routines for the video signals.

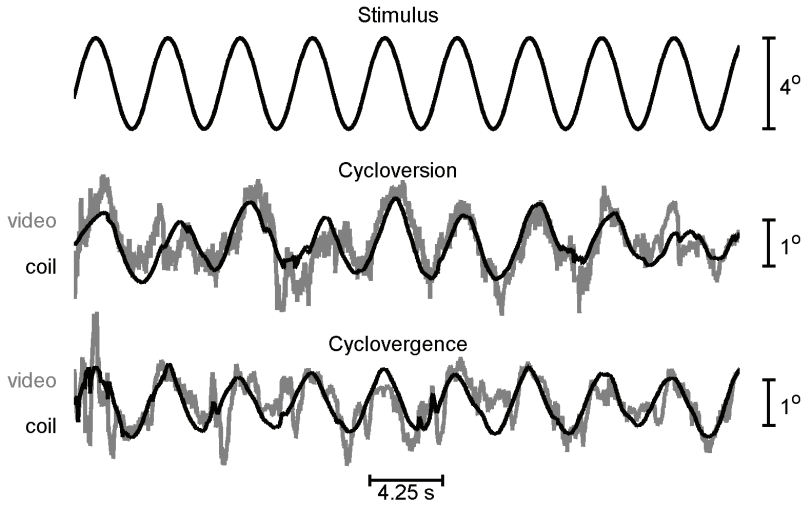

Figure 8. Stimulus, cycloversion and cyclovergence as function of time for subject JR. Video data are shown in gray and coil data superimposed in black.

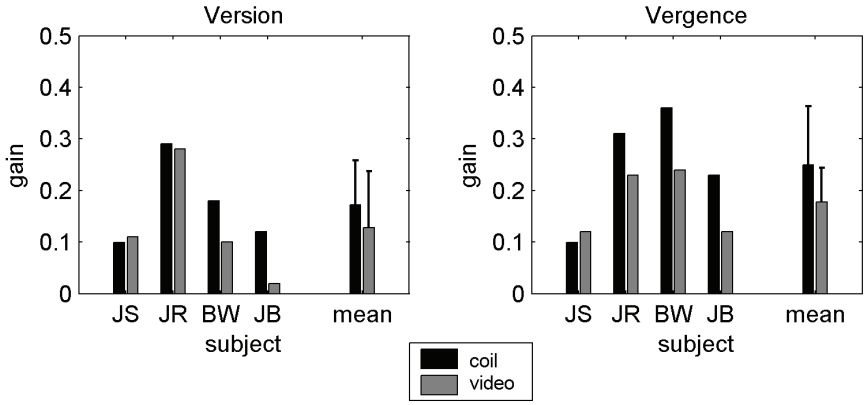

Figure 9. Individual and mean gains with standard deviation for cycloversion (left panel) and cyclovergence (right panel) as calculated from coil (black) and video (gray) data.

Vestibular Stimulation

Figure 10 shows example traces of responses to vestibular sinusoidal rotatory stimulation (called the vestibulo-ocular reflex, VOR). The left panel shows that horizontal eye movement responses to yaw stimulation in the light are fully compensatory (gain of about 1). Responses to roll stimulation in the light (right panel) show compensatory torsion with a gain of about 0.4. For horizontal and vertical eye movement components the simultaneously recorded coil and video data are virtually identical. Also torsion signals are comparable although there is a slightly increased noise level in the video signal compared to the coil signal.

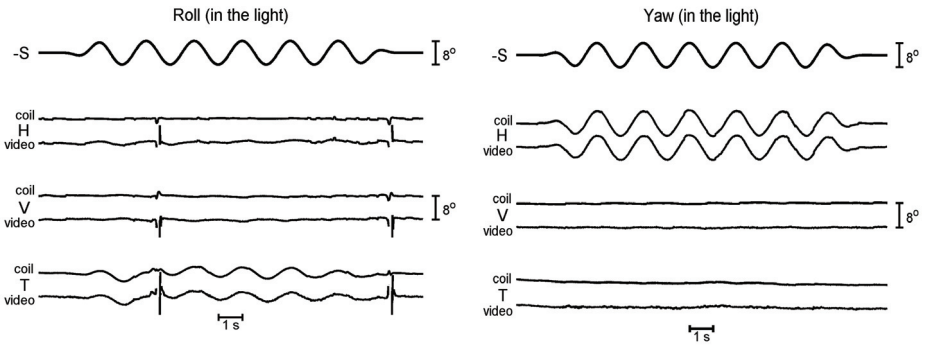

Figure 10. Example responses of the right eye of subject JS to sinusoidal yaw (left traces) and roll (right traces) rotations in the light. Horizontal (H), vertical (V) and torsional (T) eye positions as measured by the coils and the IR video systems are shown in separate traces. The stimuli trace (-S) is the inverse rotation of the platform (and thus the head of the subject) about the yaw (earth-vertical) or roll (nasal-occipital) axis. Note, that during roll measurement, two eye blinks occurred (vertical peaks).

Figure 11 shows gain averaged over left and right eye of all subjects for horizontal, vertical and torsional eye movements obtained from the coil and the video data. To be able to calculate a gain for tranlational stimuli, we used the eye position in degrees that is geometrically required for full compensation (see Data Analysis). Differences, by means of Student's paired t-tests (df=7) between gains as determined from the coil and the video signs that are significant at the 0.05 level are indicated in Figure 11 by asterisks, differences significant at the 0.01 level are indicated by double asterisks. The gains for rotations in the light calculated from the stimulus and eye responses are in a comparable range for the coil and video data. Significant differences exist for translations in light and dark.
During whole-body translation, differences may occur as a result of possible slippage between the headband and skin with the IR video system. This problem is inherent to all video-based eye trackers mounted on the head and is caused by relative motion between camera and eye, which results in incorrect measurement of eye movements. This may explain the larger discrepancies between gains calculated from coil and video signals during translations compared to rotations.

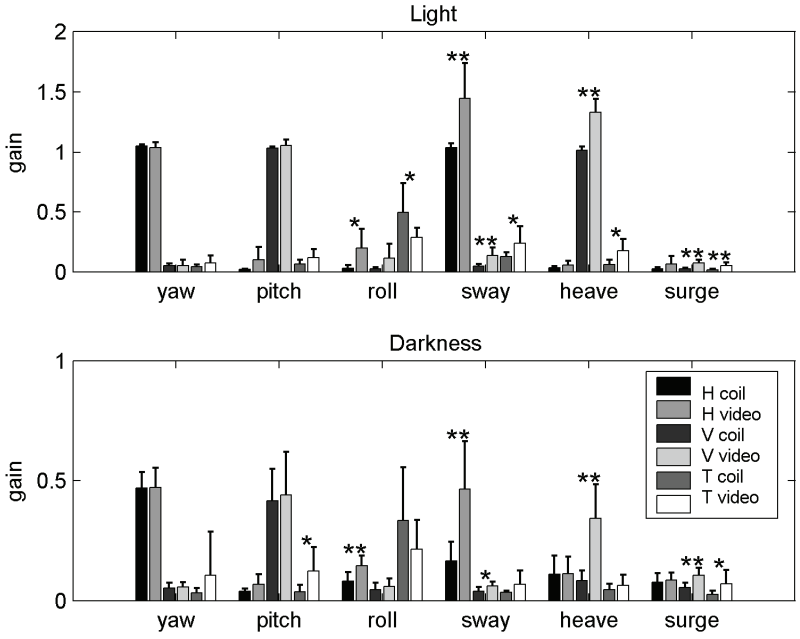

Figure 11. Gain of eye responses during sinusoidal stimulation in the light (upper panel) and in darkness (lower panel) grouped per motion type. Mean responses of eight eyes are shown. Error bars indicate one standard deviation. Significant differences between gains calculated from coil and video data at the 0.05 (*) and 0.01 (**) significance level are marked by asterisks. Note the different y-axis scaling.

Discussion

This study was driven by the question how good IR video eye movement recording devices are in comparison to the scleral search coil method. This question has become an actual issue because IR video systems become increasingly popular in research laboratories and in the clinical setting. Previous studies reported a good performance of video-oculography compared to scleral search coils. Van der Geest and Frens[12] compared the performance of a 2D video-based eye tracker (EyeLink, SR Research Ltd/SMI) with 2D scleral search coils. They found a very good correspondence between the video and the coil output, with a high correlation of fixation positions (average discrepancy < 1º over a tested range of 40 by 40º of visual angle) and linear fits near one (range 0.994 to 1.096) for saccadic properties. However, the video system they used, with a sampling rate of 250 Hz, was not capable of measuring torsion. Clarke et al.[13] tested the Chronos system we used. They did this in a highly conditional set-up comprising an artificial eye in front of an imaging camera. The artificial eye with clear iris landmarks was mounted on a three-axis gimbal and aligned orthogonal to the imaging camera. The measurement resolution for the horizontal, vertical and torsional positions was 0.006º, 0.005º and

0.016º, respectively. In this ideal set-up, measurement error for positions in the range of -20º to 20º was 0.1º for horizontal and vertical positions and 0.4º for torsional positions. They also compared the Chronos system with scleral search coils, much like our verification test with fixations. Subjects successively fixated targets arranged in a 5º-interval grid with horizontal range of -20º to 20º and vertical range of -15º to 15º. Eye movements were recorded simultaneously by scleral search coils and the Chronos. In the coils that they used, black markers were embedded. Off-line, eye positions were calculated by tracking these markers using marker-tracking software. The eye positions were recorded at a sampling rate of 50 Hz instead of 200 Hz. The measured system noise was in the order of 0.1º for both coil and video signals. This is in contrast to the smaller noise levels of coils compared to video signals we found. One problem comparing signal noises in the two systems is that the sources of noise are different. In coil signals there is a physically extremely low signal noise, which is dependent on the magnetic field strength and the number of coil windings. The same applies to the extraction of a position signal with the Chronos video system from a stationary artificial eye. The differences arise when one wants to measure the movements of a real eye in human subjects. Variations in coil signals are mainly determined by the ability of the subjects to hold fixation. This means that the signal noise of a coil attached to a real eye calculated over a short time span is low (<0.02°). In contrast, because the extraction of position signals by the video system is based on tracking of the pupil with continuous variations in diameter, video signals show a larger variability, which is inherent to measuring a biological signal. A comparison of noise levels over longer periods of time gives another picture, because then the noise is more governed by fixation stability. When we calculated the noise by taking the standard deviation around the mean during each fixation interval and averaging over all targets and all eyes, average noise levels for coil signals during fixation were 0.25º, 0.10º and 0.22º for horizontal, vertical and torsional eye positions. For the Chronos signals measured at 200 Hz, these values were 0.32º, 0.26º and 0.41º, respectively. These numbers are higher than the value of 0.1º reported by Clarke et al., [13] for both coil and video signals, which may be partially due to the lower sampling rate of the video signals in their experiment.

The simultaneous measurement of saccades by the Chronos video system and scleral search coils shows that saccade parameters such as peak velocity and duration are not completely identical. The video system gives slightly higher peak velocities at larger amplitudes. In contrast, durations are slightly shorter for saccades measured with the search coil. Van der Geest and Frens found the same amplitude velocity and duration relationships.[12] They explained this difference between coil and video signals by assuming that the load of the coil would influence saccade dynamics. In their study, coil and video data were not measured simultaneously from the same eye. In contrast, we did measure both coil and video signals simultaneously and still found differences. This means, that the explanation of differences in load is not the direct explanation for the observed differences in peak velocity and duration. In our view differences in noise level are a more likely explanation. A general conclusion, which can be drawn from our data on saccades, is that when it comes to fine details, coil signals provide a better signal stability.

Therefore, coil signals are better suited for the analysis of fine details of eye movements, e.g. vergence.
Some critical notes to our comparison study should be made. First, although the scleral search coil method is generally accepted as the gold-standard for accurate eye movement measurements in oculomotor research, insertion of a coil may slightly influence the dynamics of the eye.[18,19] However, as we recorded simultaneously with the coil and video systems, this does not affect our comparison of the two systems. Secondly, possible slippage of the coils, especially during eye blinking and the influence of orientation of the exiting wire of the scleral search coil annulus on torsion measurement after saccades,[20,21] may reduce the accuracy of measurement of eye movement and consequently affect our comparison between coil and video system. Finally, we are aware of the fact that simultaneous recording by scleral search coil and video system may influence the video measurements due to distortion of the image of the eye and may increase the risk that the image is not properly focused. This may make it harder for the Chronos software to track the pupil's position, particularly the torsional component. On the other hand, the inner ring of the coil was at the limbus and thus outside the part of the image used for tracking the eye by the IR video system. We tested the influence of the coil on the video system performance in one subject by recording both eyes with the video system during fixation, with a coil inserted in only one eye. Differences in mean fixation positions between the two eyes were not significant for any eye movement direction (Student's paired t-test, $p=1$).
One of the results of our study is that measurement of torsion by the iris segment correlation technique, as applied by the Chronos system, may have to be improved to be reliable enough for research on eye movements. Bos and De Graaf[22] have shown that when the centre of the pupil is not well defined, the use of a single segment in the iris may result in relatively large errors in calculated torsion. These errors were shown to be sinusoidally dependent on the location of the segment on an imaginary circle around the rotation centre. That is, errors in diametrically positioned segments are equal in magnitude, but opposite in sign. Therefore, a fairly simple strategy to overcome these errors is to not restrain the analysis to one single segment of the iris, but to average two or more diametrically positioned iris segments. An automatic procedure for using this technique which selects and recovers a set of 36 distinct iris segments is described by Groen et al.[23] This technique will also overcome incorrect torsion calculation resulting from occlusion of the pupil by eyelids. The manufacturer is aware of this problem[13] and intends to include this algorithm in the Chronos software in the near future. However, it may be difficult to find multiple paired areas on the iris that can be used as iris segments, due to continuous occlusion by eyelids, eyelashes and corneal reflection.
The alternative method to obtain torsional eye positions is the use of scleral markers. This is available in the Chronos software.[13] However, this technique needs a clear marker being put on the sclera. In the current study a marker was imbedded in the annulus of the scleral search coil, but as the marker was on the edge of the recorded frame we could not test this method. The software version we had at the time of our experiments ("etd2.exe", v.3.4.0.0) did not store the entire image of the eye, but only a part of it around the on-line calculated pupil centre. New software, v.3.7.0.2, available

by the manufacturer at the moment of this writing, has the option to set the proportion of the image that will be recorded. A general disadvantage of the use of markers is that it breaches the non-invasiveness of the video system above the coil system.
Based on our experience in recording with both systems we give a brief overview of advantages and disadvantages of video-oculography and scleral search coil recordings.
The main disadvantage of video recordings compared to coils is their limited sampling frequency (currently 200 Hz for the Chronos system, unlimited for coils, that is, limited by the sampling rate of the ADC-board). This is especially of importance when investigating fast eye movements such as saccades or responses to impulsive vestibular stimulation where accurate latency and gain measurements over a short time span are required. Another disadvantage of IR video systems is the difficulty in tracking eye positions in the dark because of large pupils and increased occlusion of the pupils by eyelids. If eyelashes or droopy eyelids partly occlude the pupil, proper detection of eye position may be deteriorated. Also, dark eyelashes may be problematic as these may be confused with the pupil. With IR video systems, subjects generally cannot wear glasses due to obstruction by the head device. On the other hand, soft contact lenses do not seem to influence performance. In contrast, with scleral search coils only hard lenses can be used.
A disadvantage of coil measurements is the possible lower acceptance of coils over video recordings by volunteers and patients due to the invasive nature of coils. Also the fact that measuring time is limited to about 30 to 60 min with scleral search coils limits the experimental design. Other disadvantages of coils are, in our opinion, their limited lifetime and vulnerability. Advantage of video systems over the coil system is their non-invasive nature and ease of use in healthy subjects and patients. Also, because no large set-up is needed, such as magnetic fields in the coil system, the video system with its head device with cameras and personal computer allows bedside testing.
The accuracy of the off-line analysis techniques is similar in both systems. IR video systems generally come with software that allows one to calibrate eye positions and the data are automatically transformed into eye position data (usually Fick angles). Algorithms for 3D corrections of coil data have been extensively described in the literature[4,24,25,26] but requires skilled expertise to write the appropriate software. An additional advantage of the Chronos system is that it, unlike other on-line pre-calibrated video based systems, stores video images on disk and extracts eye positions from these recordings off-line. Although this procedure is disk space and time consuming, it may be advantageous because of the possibility to reanalyse data.
In conclusion, the lower time resolution and possible fixation problem of the Chronos system makes the coil system the best choice when measuring 3D eye movements, especially for high sensitivity, high frequency and/or short duration dynamic responses. For less time and velocity demanding tests and measurements longer than half an hour, the non-invasive IR Chronos system is a good alternative to scleral search coils. Further technical improvements are underway in the Chronos video system for the measurement of torsion.

References

1. Robinson DA. A method of measuring eye movement using a scleral search coil in a magnetic field. *IEEE Trans Biomed Eng*. 1963;10:137-145.
2. Collewijn H, Van der Mark F, Jansen TC. Precise recording of human eye movements. *Vision Res.* 1975;15:447-450.
3. Collewijn H, Van der Steen J, Ferman L, Jansen TC. Human ocular counterroll: assessment of static and dynamic properties from electromagnetic scleral coil recordings. *Exp Brain Res.* 1985;59:185-196.
4. Ferman L, Collewijn H, Jansen TC, Van den Berg AV. Human gaze stability in the horizontal, vertical and torsional direction during voluntary head movements, evaluated with a three-dimensional scleral induction coil technique. *Vision Res*. 1987;27:811-828.
5. Bruno P, Van den Berg AV. Torsion during saccades between tertiary positions. *Exp Brain Res.* 1997;117:251-265.
6. Ferman L, Collewijn H, Van den Berg AV. A direct test of Listing's law. II. Human ocular torsion measured under dynamic conditions. *Vision Res*. 1987;27:939-951.
7. Hooge IT, Van den Berg AV. Visually evoked cyclovergence and extended Listing's law, *J. Neurophysiol*. 2000;83:2757-2775.
8. Klier EM, Crawford JD. Human oculomotor system accounts for 3-D eye orientation in the visual-motor transformation for saccades. *J Neurophysiol.* 1998;80:2274-2294.
9. Schmid-Priscoveanu A, Straumann D, Kori AA. Torsional vestibulo-ocular reflex during whole-body oscillation in the upright and the supine position. I. Responses in healthy human subjects. *Exp Brain Res.* 2000;134:212-219.
10. Straumann D, Zee DS, Solomon D, Kramer PD. Validity of Listing's law during fixations, saccades, smooth pursuit eye movements, and blinks. *Exp Brain Res*. 1996;112:135-146.
11. Tweed D, Sievering D, Misslisch H, Fetter M, Zee D, Koenig E. Rotational kinematics of the human vestibuloocular reflex. I. Gain matrices. *J Neurophysiol*. 1994;72:2467-2479.
12. Van der Geest JN, Frens MA. Recording eye movements with video-oculography and scleral search coils: a direct comparison of two methods. *J Neurosci Methods*. 2002;114:185-195.
13. Clarke AH, Ditterich J, Drüen K, Schönfeld U, Steineke C. Using high frame-rate CMOS sensors for three-dimensional eye tracking. *Behav Res Meth Ins C.* 2002;34:549-560.
14. Houben MMJ, Goumans J, De Jongste AHC, Van der Steen J. Angular and linear vestibulo-ocular responses in humans. *Ann NY Acad Sci.* 2005;1039:68-80.
15. Goossens HHLM, Van Opstal AJ. Human eye-head coordination in two dimensions under different sensorimotor conditions. *Exp Brain Res*. 1997; 114:542-560.
16. Van der Steen J, Bruno P. Unequal amplitude saccades produced by aniseikonic patterns: effects of viewing distance. *Vision Res.* 1995;35:3459-3471.

17. Van der Steen J, Collewijn H. Ocular stability in the horizontal, frontal and sagittal planes in the rabbit. *Exp Brain Res*. 1984;56:263-274.
18. Frens MA, Van der Geest JN. Scleral search coils influence saccade dynamics, *J Neurophysiol*. 2002;88:692-698.
19. Smeets JBJ, Hooge ITC. Nature of variability in saccades, *J Neurophysiol*. 2002;90:12-20.
20. Bergamin O, Bizzarri S, Straumann S. Ocular torsion during voluntary blinks in human. *Invest Ophthalmol Vis Sci.* 2002;43:3438-3443.
21. Bergamin O, Ramat S, Straumann S, Zee DS. Influence of orientation of exiting wire of search coil annulus on torsion after saccades. *Invest Ophthalmol Vis Sci.* 2004;45:131-137.
22. Bos JE, De Graaf, B. Ocular torsion quantification with video images. *IEEE Trans Biomed Eng.* 1994;41:351-357.
23. Groen E, Bos JE, Nacken PFM, De Graaf B. Determination of ocular torsion by means of automatic pattern recognition. *IEEE Trans Biomed Eng.* 1996;43:471-479.
24. Haslwanter T. Mathematics of three-dimensional eye rotations. *Vision Res* 1995;35:1727-1739.
25. Hess BJM, Van Opstal AJ, Straumann D, Hepp K. Calibration of three-dimensional eye position using search coil signals in the Rhesus monkey. *Vision Res* 1992;32:1647-1654.
26 Schor RH, Furman JM. The "practical mathematics" of recording three-dimensional eye position using scleral coils. *Methods* 2001;25:164-185.

Chapter 3

Peaks and troughs of three-dimensional vestibulo-ocular reflex in humans

Goumans J, Houben MMJ, Dits J, van der Steen J

J Assoc Res Otolaryngol accepted January 2010

Abstract

The three-dimensional vestibulo-ocular reflex (3D VOR) ideally generates compensatory ocular rotations not only with a magnitude equal and opposite to the head rotation but also about an axis that is collinear with the head rotation axis. Vestibulo-ocular responses only partially fulfil this ideal behaviour. Because animal studies have shown that vestibular stimulation about particular axes may lead to suboptimal compensatory responses, we investigated in healthy subjects the peaks and troughs in 3D VOR stabilization in terms of gain and alignment of the three-dimensional vestibulo-ocular response.
Six healthy upright sitting subjects underwent whole-body small amplitude sinusoidal and constant acceleration transients delivered by a six degrees of freedom motion platform. Subjects were oscillated about the vertical axis and about axes in the horizontal plane varying between roll and pitch at increments of 22.5° in azimuth. Transients were delivered in yaw, roll and pitch and in the vertical canal planes.
Eye movements were recorded in with 3D search coils. Eye coil signals were converted to rotation vectors, from which we calculated gain and misalignment. During horizontal axis stimulation systematic deviations were found. In the light misalignment of the three-dimensional VOR had a maximum misalignment at about 45 degrees. These deviations in misalignment can be explained by vector summation of the eye rotation components with a low gain for torsion and high gain for vertical. In the dark and in response to transients gain of all components had lower values. Misalignment in darkness and for transients had different peaks and troughs than in the light: its minimum was during pitch axis stimulation and its maximum during roll axis stimulation. We show that the relatively large misalignment for roll in darkness is due to a horizontal eye movement component that is only present in darkness. In combination with the relatively low torsion gain this horizontal component has a relative large effect on the alignment of the eye rotation axis with respect to the head rotation axis.

Introduction

One of the goals of the vestibular system is to stabilize the eye by providing information about changes in angular position of the head. This is mediated by the vestibulo-ocular reflex (VOR), which ideally compensates for a given head rotation with an eye velocity that is equal and opposite to head velocity. Most head movements are not restricted to a single rotation about one particular axis such as yaw, pitch or roll, but are composed of three dimensional translations and rotations about an axis with different orientation and amplitudes in three-dimensional space (3D) (Grossman et al. 1989; Crane and Demer 1997). The contribution and interaction of the different parts of the vestibular system (canals and otoliths) on ocular stabilization has been investigated in many studies (Groen et al. 1999; Schmid-Priscoveanu et al. 2000; Bockisch et al. 2005), for a review see also (Angelaki and Cullen 2008). Although the quality of the VOR response is usually quantified by the gain (ratio between eye and head velocity), alignment of the eye rotation axis with respect to the head rotation axis is also an important determinant. Both errors in gain and alignment compromise the quality of image stabilization during head rotations. Several systematic and non-systematic factors cause that even in normal situations the eye rotation axis is not always collinear with head rotation axis. Stimulation about an axis in the horizontal plane is such a situation where stimulus and response axis may not align. In monkey it has been shown that gain and alignment of compensatory eye rotation is directly related to the vector sum of roll and pitch and that misalignment varies with stimulus axis orientation (Crawford and Vilis 1991). This variation in misalignment is caused by the different gain of torsion and vertical eye rotation components.
So far it is unclear if suboptimal gain and misalignment during head rotations about particular axes is caused by orbital-mechanical properties (Crane et al. 2005; Demer et al. 2005; Crane et al. 2006), orientation selectivity, response dynamics of sensory signals or by the process of sensory-motor transformation.
To find the peaks and troughs in gain and alignment we tested six upright sitting healthy subjects in the light and in darkness. Subjects were oscillated about the vertical axis and about axes that incremented in steps of 22.5 degrees from the nasal-occipital to the interaural axis. We systematically investigated the gain and misalignment of the VOR in response to 4 degrees peak-to-peak amplitude sinusoidal stimulation at a frequency of 1 Hz. This frequency and amplitude is close to what is normal for activities such as walking, where the predominant frequency is 0.8 Hz with mean amplitude of 6 degrees (Grossman et al. 1988; Crane and Demer 1997).
To assess the role of vision in quality of 3D ocular stability we compared the responses to sinusoidal stimulation in the light to responses in darkness. In addition, we measured compensatory eye movements in response to whole body transient stimulation with constant acceleration of $100^{\circ}.s^{-2}$ during the first 100 ms of the transient. This technique has the advantage that it measures the VOR during the first 100 ms of the stimulation. In this interval visual contribution is absent. Although in most previous studies head transients have been used with accelerations up to $2500^{\circ}.s^{-2}$ (Tabak et al. 1997b; Tabak et al. 1997a; Halmagyi et al. 2001; Halmagyi et al. 2003), we

used accelerations and peak velocities in the same amplitude velocity range as our sinusoidal stimuli.

Methods

Subjects

Six subjects participated in the experiment. The subject's ages ranged between 22 and 55 years. None of the subjects had a medical history or clinical signs of vestibular, neurological, oculomotor or cardiovascular abnormalities. All subjects gave their informed consent. The experimental procedure was approved by the Medical Ethics Committee of Erasmus University Medical Centre and adhered to the Declaration of Helsinki for research involving human subjects.

Experimental set-up

Stimuli were delivered with a motion platform (see Figure 1A and B) capable of generating angular and translational stimuli at a total of six degrees of freedom (FCS-MOOG, Nieuw-Vennep, The Netherlands). The platform is moved by six electro-mechanical actuators connected to a personal computer with dedicated control software. It generates accurate movements with six degrees of freedom. Sensors placed in the actuators continuously monitor the platform motion profile. Measured by these sensors the device has <0.5 mm precision for linear and <0.05 degrees precision for angular movements. Due to the high resonance frequency of the device (> 75 Hz) vibrations during stimulation were very small (< 0.02 degrees). A comparison between the stimulus signal sent to the platform and the output measured with a search coil fixed in space while oscillating the platform, confirmed that the platform produced a perfect sinusoidal stimulus ($P < 0.001$). During the experiments, platform motion profile was monitored by the sensors in the actuators, reconstructed using inverse dynamics and sent to the data collection computer at a rate of 100 Hz. To precisely synchronize platform and eye movement data, a laser beam was mounted at the back of the platform and projected onto a small photocell at the base of a 0.8 mm pinhole (reaction time 10 μs). Simultaneously with the eye movement data the output voltage of the photocell was sampled at a rate of 1 kHz. This way the photocell signal provided a real time indicator of zero crossings of the platform motion onset with 1ms accuracy. During the offline analysis using Matlab (Mathworks, Natick, MA), the reconstructed motion profile of the platform based on the sensor information of the actuators in the platform was precisely aligned with the onset of platform motion as indicated by the drop in voltage of the photocell.

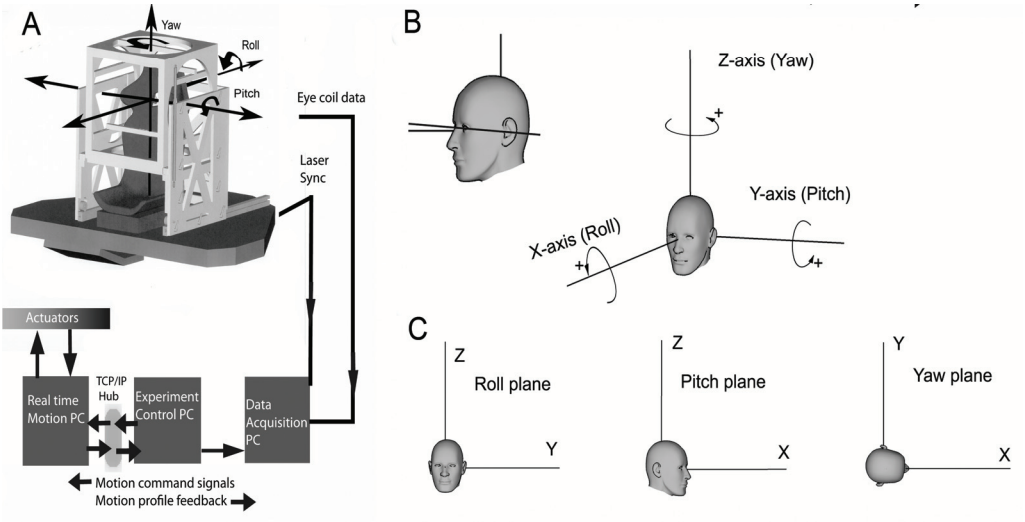

Figure 1. A) Schematic drawing of the 6DF motion platform. The boxes represent the computer hardware and the lines indicate the flow of signals to control the movements of the platform and to monitor platform motion and eye movements. B) The orientation of the subject's head when seated on the platform. In the standard orientation Reid's line (solid line) makes an angle of 7 degrees with earth horizontal. C) Directions of rotations around the cardinal axes according to the right hand rule. Bottom panels show the yaw, roll and pitch projection planes used to plot angular eye velocities during sinusoidal stimulation.

Subjects were seated on a chair mounted at the centre of the platform (Figure 1A). The subject's body was restrained with a four-point seatbelt as used in racing cars. The seatbelts were anchored to the base of the motion platform. A PVC cubic frame that supported the field coils surrounded the chair. The field coil system was adjustable in height, such that the subject's eyes were in the centre of the magnetic field. The head was immobilized using an individually moulded dental-impression bite board, which was attached to the cubic frame via a rigid bar. A vacuum pillow folded around the neck and an annulus attached to the chair further ensured fixation of the subject. In addition, we attached two 3D sensors (Analog devices) directly to the bite board, one for angular and one for linear acceleration to monitor spurious head movements during stimulation.

Eye movement recordings

Eye movements of both eyes were recorded with 3D scleral search coils (Skalar, Delft, The Netherlands) using a standard 25 kHz two field coil system based on the amplitude detection method of Robinson (Model EMP3020, Skalar Medical, Delft, The Netherlands). The coil signals were passed through an analogue low-pass filter with cut-off frequency of 500 Hz and sampled on-line and stored to hard disk at a frequency of 1000 Hz with 16 bit precision (CED system running Spike2 v6, Cambridge Electronic Design, Cambridge). Noise levels of the coil signals during fixation were $0.1°.s^{-1}$. Coil signals were off-line inspected for slippage by comparing the signals of left and right eye. No significant differences were found (P=0.907). Eye rotations were defined

in a head-fixed right-handed co-ordinate system (see Figure 1C). In this system from the subject's point of view a leftward rotation about the Z-axis (yaw), a downward rotation about the Y-axis (pitch) and rightward rotation about the X-axis (roll) are defined as positive. The planes orthogonal to the X, Y and Z rotation axes are respectively the roll, pitch and yaw planes (Figure 1D). Data were also analyzed by projecting them on these three co-ordinate planes.

Experimental protocol

Prior to the experiments, torsion eye position measurement error due to non-orthogonality between the direction and torsion coil was corrected using the Bruno and van den Berg algorithm (Bruno and Van den Berg 1997). At the beginning of the experiment, the horizontal and vertical signals of both coils were individually calibrated by instructing the subject to successively fixate a series of five targets (central target and a target at 10 degrees left, right, up and down) for five seconds each. Calibration targets were projected onto a translucent screen at 186 cm distance.

We determined head orientation with respect to gravity and its rotation centre. Head orientation was as close as possible to the position where subjects felt straight up. In this position we measured Reid's line (an imaginary line connecting the external meatus with the lower orbital cantus) (Fig 1C left panel). In all subjects Reid's line varied between 6 and 10 degrees with earth horizontal. The centre of rotation was defined as the intersection between the imaginary line going through the external meatus and the horizontal line going from the nose to the back of the head. The x, y and z offset of this rotation centre with respect to the default rotation centre of the platform was determined. The offset values were fed into the platform control computer, which then adjusted the centre of rotation. Thus, all stimuli were about the defined head centre of rotation.

Whole-body sinusoidal rotations were delivered about the three cardinal axes: The rostral-caudal or vertical axis (yaw), the interaural axis (pitch) and the naso-occipital axis (roll) and about intermediate horizontal axes between roll and pitch. The orientation of the stimulus axis was incremented in steps of 22.5° azimuth. The frequency of the stimulus was 1 Hz with a total duration of 14 seconds, including two seconds of fade-in and fade-out. Peak-to-peak amplitude of the sinusoidal rotation was 4 degrees (peak acceleration $80^{\circ}.s^{-2}$). Sinusoidal stimuli were delivered in light and darkness. In the light, subjects fixated a continuously lit visual target (a red LED, 2 mm diameter) located 177 cm in front of the subject at eye level close to the eyes primary position. In the dark condition, the visual target was briefly presented (2 s) when the platform was stationary in between two stimulations. Subjects were instructed to fixate the imaginary location of the space fixed target during sinusoidal stimulation after the target had been switched off just prior to motion onset. In a control experiment where we attached one search coil to the bite board and one coil to the forehead, we found that decoupling of the head relative to the platform was $<0.03°$ (see supplement Figure s2).

All subjects were subjected to short duration whole body transients in a dark environment, where the only visible stimulus available to the subject was a visual target located at 177 cm in front of the subject at eye level. Each transient was repeated six times and delivered in random order and with random timing of motion onset (intervals varied between 2.5 and 3.5 s). The

profile of the transients was a constant acceleration of $100^{\circ}.s^{-2}$ during the first 100 ms of the transient, followed by a gradual linear decrease in acceleration. This stimulus resulted in a linear increase in velocity up to $10^{\circ}.s^{-1}$ after 100 ms and was precisely reproducible in terms of amplitude and direction. Transients were well tolerated by our subjects. Decoupling of the head from the bite board was less 0.03° during the first 100 ms of the transient. Peak velocity of the eye movements in response to these transients was 100 times above the noise level of the coil signals (Houben et al. 2006).

Data analysis

Coil signals were converted into Fick angles and then expressed as rotation vectors (Haustein 1989; Haslwanter and Moore 1995). From the fixation data of the target straight ahead we determined the misalignment of the coil in the eye relative to the orthogonal primary magnetic field coils. Signals were corrected for this offset misalignment by three-dimensional counter rotation. To express 3D eye movements in the velocity domain, we converted rotation vector data back into angular velocity ($\boldsymbol{\omega}$). Before conversion of rotation vector to angular velocity, we smoothed the data by zero-phase with a forward and reverse digital filter with a 20-point Gaussian window (length of 20 ms). The gain of each component and 3D eye velocity gain was calculated by fitting a sinusoid with a frequency equal to the platform frequency through the horizontal, vertical and torsion angular velocity components. The gain for each component defined as the ratio between eye component peak velocity and platform peak velocity was calculated separately for each eye. Because left and right eye values were not significantly different ($P = 0.907$), we pooled the left and right eye data.

The misalignment between the 3D eye velocity axis and head velocity axis was calculated using the approach of Aw (Aw et al. 1996b). From the scalar product of two vectors the misalignment was calculated as the instantaneous angle in three dimensions between the inverse of the eye velocity axis and the head velocity axis. Because the calculated values only indicate the misalignment of the eye rotation axis as a cone around the head orientation axis, we also used gaze plane plots to determine the deviation of the eye rotation axis in yaw, roll and pitch planes (see Figure 1D).

Because misalignments could be due to changes in horizontal eye position, we calculated the standard deviation around the mean eye position during each 14-second stimulation period. The variability of eye position around the imaginary fixation point during the dark period was too small to have an effect on misalignment.

All transients were individually inspected on the computer screen. When the subject made a blink or saccade during the transient that trace was manually discarded. This happened on average in one out of 6 cases. Angular velocity components during the first 100 ms after onset of the movement were averaged in time bins of 20 ms and plotted as function of platform velocity (Tabak et al. 1997b). Because the transients had a constant acceleration during the first 100 ms the slopes of the linear regression line fitted through the time bins are a direct measure for eye velocity gain (Tabak et al. 1997b; Tabak et al. 1997a). Left and right eye gains were not significantly different ($P= 0.907$) and were averaged.

The 3D angular velocity gain and misalignment for each azimuth orientation were compared to the gain and misalignment predicted from vector

summation of the torsion and vertical components during roll and pitch (Crawford and Vilis 1991). From this it follows that the orientation of the eye rotation axis aligns with the head rotation axis when velocity gains for roll and pitch are equal, but when the two are different, there is deviation between stimulus and eye rotation axis with a maximum at 45° azimuth.

Statistical analysis

Repeated measures analysis of variance was used to test for significant differences in misalignment data during sinusoidal stimulation in the light and in darkness and in response to transient stimulation.

Results

Sinusoidal stimulation

Sinusoidal stimulation about the vertical axis in the light resulted in smooth compensatory eye movements occasionally interrupted by saccades. The mean gain ± one standard deviation (N=6) was 1.02 ± 0.06 in the light. The responses were restricted to the horizontal eye movement component, with very small vertical and torsion components (gain < 0.05). In darkness, compensatory eye movements were more frequently interrupted by saccades and in most subjects there was a small drift of the other components (see Figure 2A). The standard deviation of the horizontal position change during the 14 s of stimulation was 1.54° in the light and 1.45° in darkness (N=6). Position changes of the vertical and torsion components were <0.28° in the light. Standard deviations of position changes in darkness of the vertical and torsion components were 0.84° for the vertical and 0.38° for the torsion component.

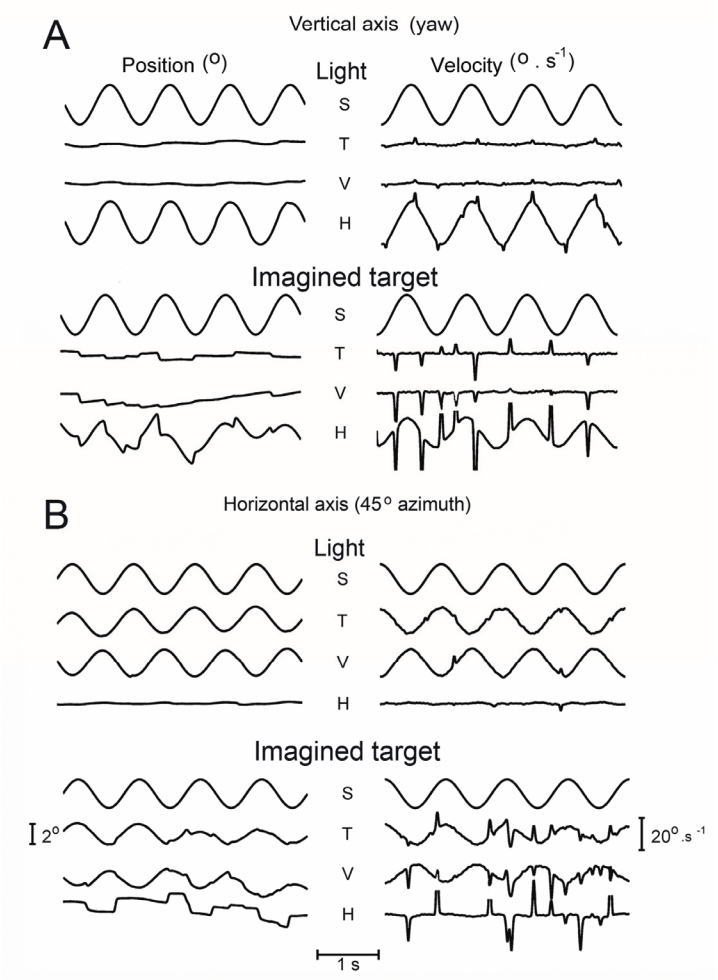

Figure 2. Example of three-dimensional eye movements in response to sinusoidal stimulation about different axes. A) Vertical axis in the light (upper panels) and in the dark while the subject imagined a target (lower panels). B) Horizontal axis oriented at 45° azimuth. Upper panels: light, lower panels: dark.
Left side panels in A and B show the Stimulus (S), Torsion (T), Vertical (V) and Horizontal (H) eye position signals. The right side panels show the corresponding angular velocities. Saccadic peak velocities are clipped in the plots. In this and all subsequent figures eye positions and velocities are expressed in a right-handed, head-fixed co-ordinate system. In this system clockwise, down and left eye rotations viewed from the perspective of the subject are defined as positive values (see also Figure 1). Note that for easier comparison, the polarity of the stimulus signal has been inverted.

Compensatory eye movements had different gains of the horizontal, vertical and torsion components. Gain of the vertical axis VOR in darkness was 0.62° ± 0.16. For horizontal axis stimulation the relative contribution of each component to the overall gain depended on the orientation of the stimulus axis. When the stimulus axis was in the naso-occipital direction (roll), torsion

was the major component of the response at this orientation. The mean gain of torsion was 0.54 ± 0.16 in the light and 0.37 ± 0.09 in darkness. Stimulation about an axis in between the naso-occipital and interaural axis resulted in compensatory eye movements that consisted of a combination of torsion and vertical components. Figure 2B shows examples of eye movements in response to stimulation about an axis oriented at 45° in both the light and in darkness. The torsion component was always smaller than the vertical component, consistent with the differences in gain between pure roll and pitch. We also determined ocular drift that occurred during sinusoidal stimulation in all subjects under light and dark conditions. The standard deviations of respectively torsion, vertical and horizontal gaze positions averaged over all six subjects were 0.72, 0.97 and 1.02 degrees during roll stimulation and 0.45, 1.77 and 1.25 degrees during pitch stimulation in the dark.

During horizontal axis stimulation the eye movements were mainly restricted to vertical and/or torsion eye velocities. Figure 3A (top panel) shows the mean gain of the horizontal, vertical and torsion angular velocity components for all tested stimulation axes in the horizontal plane. The different orientations of the stimulus axis in between pitch and roll resulted in inversely related contributions of vertical and torsion eye movements. Torsion was maximal at 0° azimuth, whereas vertical had its maximum at 90°. The centre panel of Figure 3A shows the 3D eye velocity gain in the light. Gain varied between 0.99 ± 0.12 (pitch) and 0.54 ± 0.16 (roll). The measured data closely correspond to the predicted values calculated from the vector sum of torsion and vertical components (dashed line in centre panel of Figure 3A).

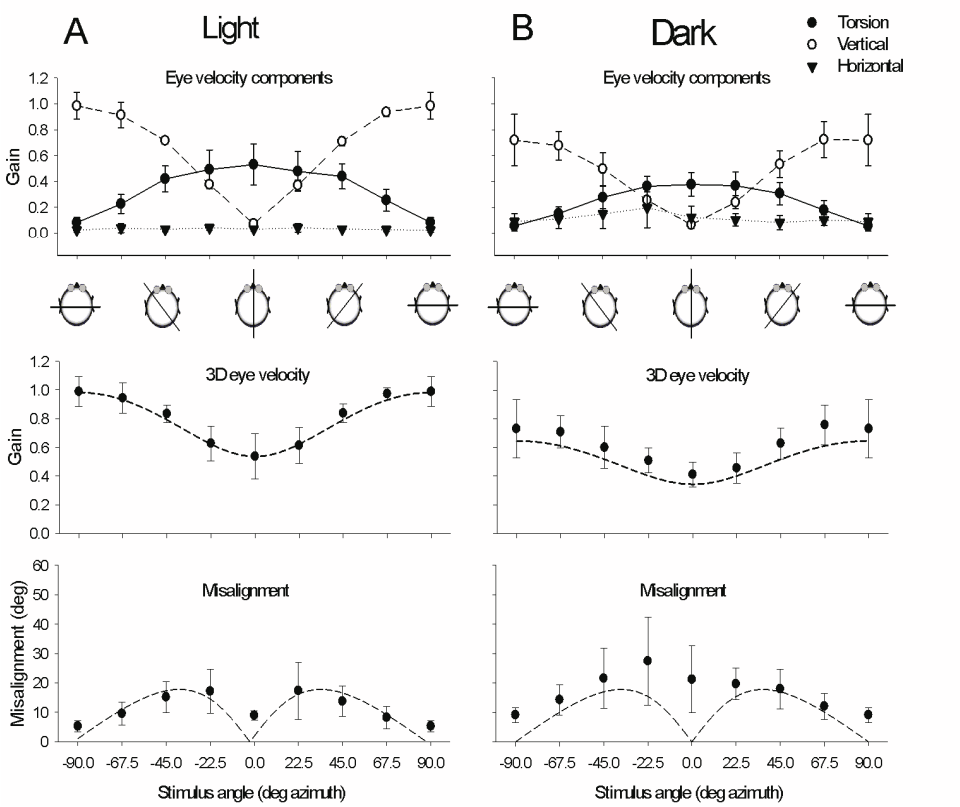

Figure 3. Results of horizontal axis sinusoidal stimulation for all tested horizontal stimulus axes averaged over all subjects (N=6) in the light (A) and in the dark (B). Cartoons underneath the top panels give a top view of the orientation of the stimulus axis with respect to the head. Top panel: mean gain of the horizontal, vertical and torsion eye velocity components. Centre panel: mean 3D eye velocity at each tested stimulus axis orientation. The dashed line represents the vector eye velocity gain response predicted from the vertical and torsion components. Lower panel: misalignment of the response axis with respect to the stimulus axis. The dashed line in the lower panel represents the predicted misalignment calculated from the vector sum of only vertical and torsion eye velocity components in response to pure pitch and pure roll stimulation, respectively. Error bars in all panels indicate one standard deviation.

The misalignment between stimulus and response axis averaged over all subjects is shown in the lower panels of Figure 3. In the light misalignment between stimulus and response axis was smallest (5.25°) during pitch and gradually increased towards roll until the orientation of the stimulus axis was oriented at 22.5° azimuth (maximum misalignment: 17.33°) and decreased towards the roll axis. These values for each horizontal stimulus angle correspond closely to what one would predict from linear vector summation of roll and pitch contributions (dashed line in lower panel of Figure 3A).

In darkness the maximum gain of both the vertical and torsion components was lower than in the light (vertical: 0.72 ± 0.19 torsion: 0.37 ± 0.09) (Figure 3B). Also the 3D eye velocity gain values were significantly lower

than in the light (Student t-test, $p < 0.0001$). Gain was slightly higher than predicted from the vertical and torsion components alone (dashed line in centre panel of Figure 3B). A pronounced difference between sinusoidal stimulation in the light and darkness was a significant (Student t-test, $p < 0.001$) change in misalignment of the eye rotation axis with respect to the stimulus axis (Figure 3A and B, compare lower panels). In the dark the misalignment was minimal at 90° (pitch) and gradually increased to a peak around the 0° axis (roll). The pattern of misalignment in the dark did not correspond to what one would predict from linear vector summation of only roll and pitch components. In contrast to the light, there was a small but systematic horizontal gain component (0.1 < "gain" < 0.23) in the dark condition.
Because the misalignment angle only gives the angle of deviation between head and eye rotation axis, we also plotted the angular velocities projected on the roll, pitch and yaw planes. An example for stimulation about the x-axis (roll) is given in Figure 4. The three top panels show that in the light the angular velocities coincide with the x-axis for each plane. The contributions of yaw and pitch velocities are very small compared to the roll component. In darkness (lower panels) there is considerable more deviation between stimulus and response. There is a small but consistent horizontal velocity component in the dark (left and middle lower panels).

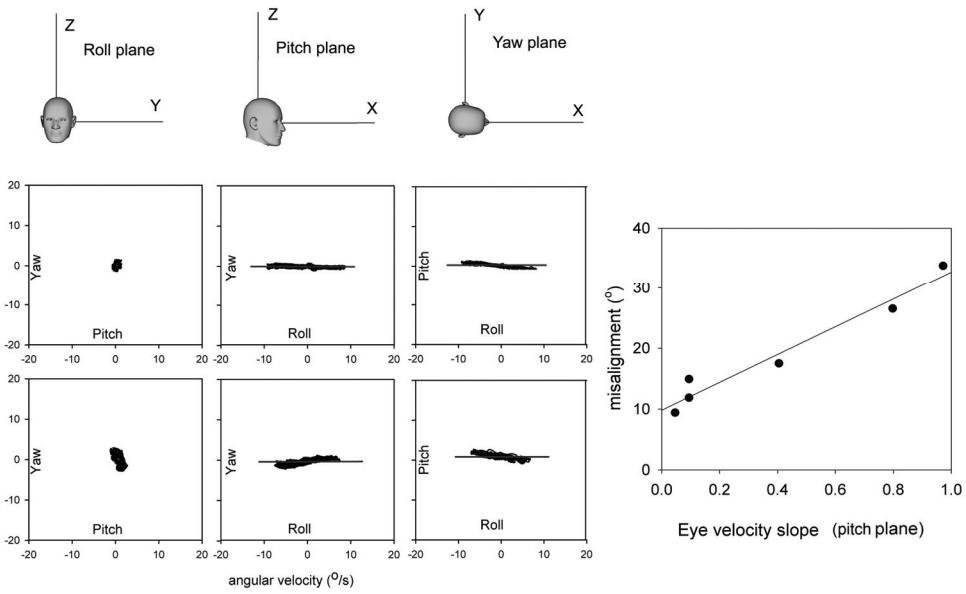

Figure 4. Plots of eye velocities projected on the roll, pitch and yaw plane during sinusoidal stimulation about the roll axis in the light (upper panels) and in darkness (lower panels). The horizontal solid line corresponds to the x-axis shown in the cartoons in the upper panel. Far right panel: correlation between misalignment and the slope of the regression line fitted through eye velocity data obtained during roll stimulation in the dark projected on the pitch plane. Each data point represents one subject.

For each subject the slope of the regression line fitted through the eye velocity points on the pitch plane was plotted as a function of misalignment. There was a strong correlation between misalignment and slope (r^2 = 0.98, intercept 9.8, slope = 22.9).

Transients

Angular rotation head transients about the vertical axis resulted in compensatory horizontal eye movements. The gain of eye versus head velocities in this particular example was 0.76 for rightward and 0.82 for leftward vertical axis (yaw) head transients (Figure 5, bottom left panel). Mean values between left and right averaged over all six subjects were not significantly different.

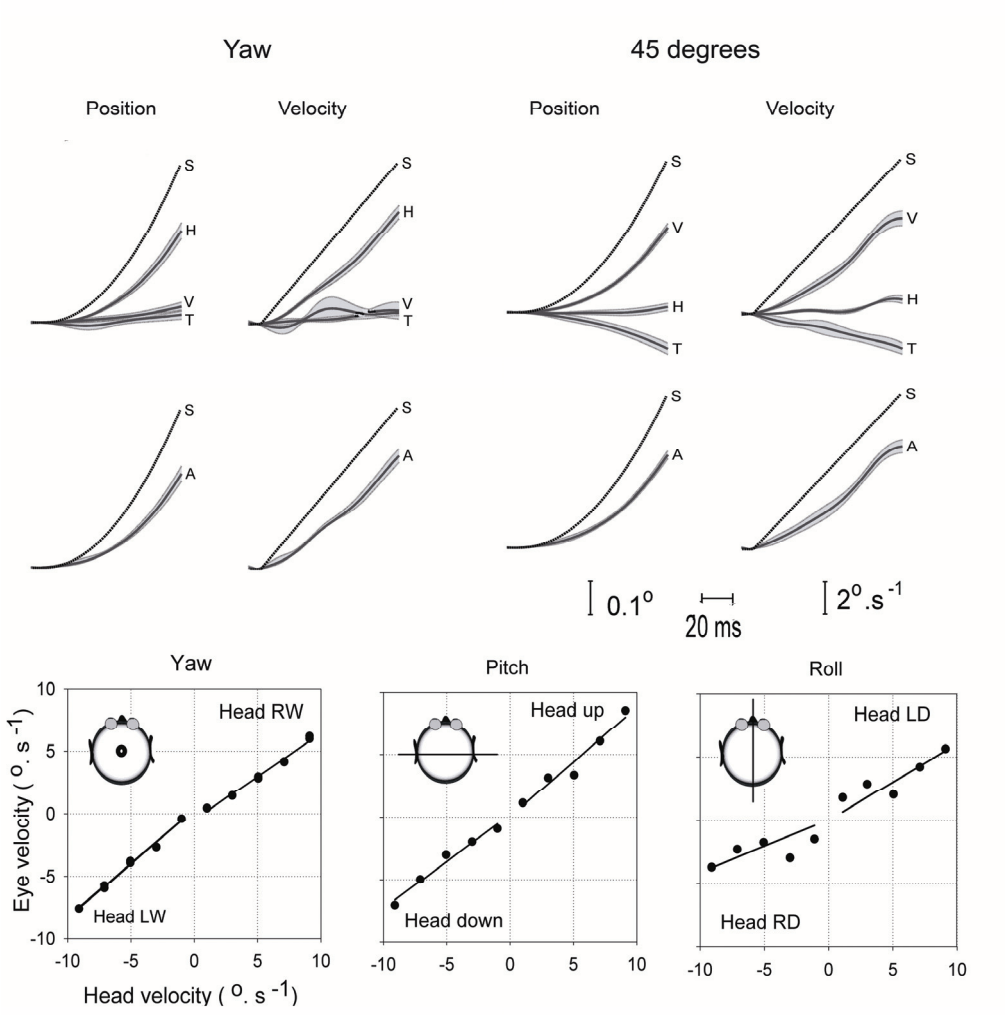

Figure 5. Top panel: example of eye movements in response to a clockwise transient about the vertical axis (yaw) and horizontal axis stimulation at 45° azimuth. Top row of top panel: eye position and eye velocity of respectively horizontal (H), vertical (V) and

torsion (T) components. Lower row of top panel: three-dimensional position and angular velocity of stimulus (S) and eye (A) movements. Grey shaded line is one standard deviation.
Bottom panels: plots of relationship between instantaneous eye and head velocity during angular VOR whole body impulses in one subject. Left panel: vertical axis (yaw) impulse, centre and right panels: interaural axis (pitch) and naso-occipital axis (roll), respectively.
RW = rightward LW = leftward horizontal impulses relative to the head. RD = right side down, LW = left side down torsion impulses relative to the head. Each black filled circle is one bin (bin width = 20 ms) of mean eye velocity of six repetitions of the impulse. Solid line: linear regression fitted through the 20 ms bins. Note that a RW yaw head impulse leads to a LW eye movement, a head up pitch impulse results in a downward eye rotation and a LD roll head impulse leads to a RD torsion eye rotation. These eye movements are according to the right hand rule defined as positive.

Whole body transients about the interaural axis (pitch) resulted in near unity gain for head up and a gain about 0.8 for head down transients. These differences averaged over all subjects (N = 6) between up and down were significant ($P < 0.05$). Transient stimulation about the naso-occipital axis (roll) elicited much lower gain of the compensatory eye movement responses but were symmetrical in both directions. The top right panel in Figure 5 shows the differences in eye angular velocities evoked by the roll and pitch components of a rotational step about a horizontal axis at 45º azimuth. Torsion components were much smaller than vertical components.
Gain and misalignment in response to transients in the horizontal plane are summarised in Figure 6. The top panel shows the mean gain of the horizontal, vertical and torsion eye velocity components. Maximum mean gain for the vertical component alone was 0.85 for pitch (90° azimuth). Maximum gain for torsion was 0.42 for roll (0° azimuth). Vector gains were slightly higher because due to the contribution of all three components. Mean 3D eye velocity gain (N=6) for pitch stimulation was 1.04 ± 0.18 for upward and 0.81 ± 0.14 for downward transients. The mean 3D eye velocity gain in response to roll (N=6) was 0.65 ± 0.39 for head right side down and 0.52 ± 0.16 for head left side down transients. Similar to sinusoidal stimulation in darkness, misalignment was highest during roll (mean 28.2° ± 0.18) and had its minimum value during pitch (mean 11.53°± 0.51).

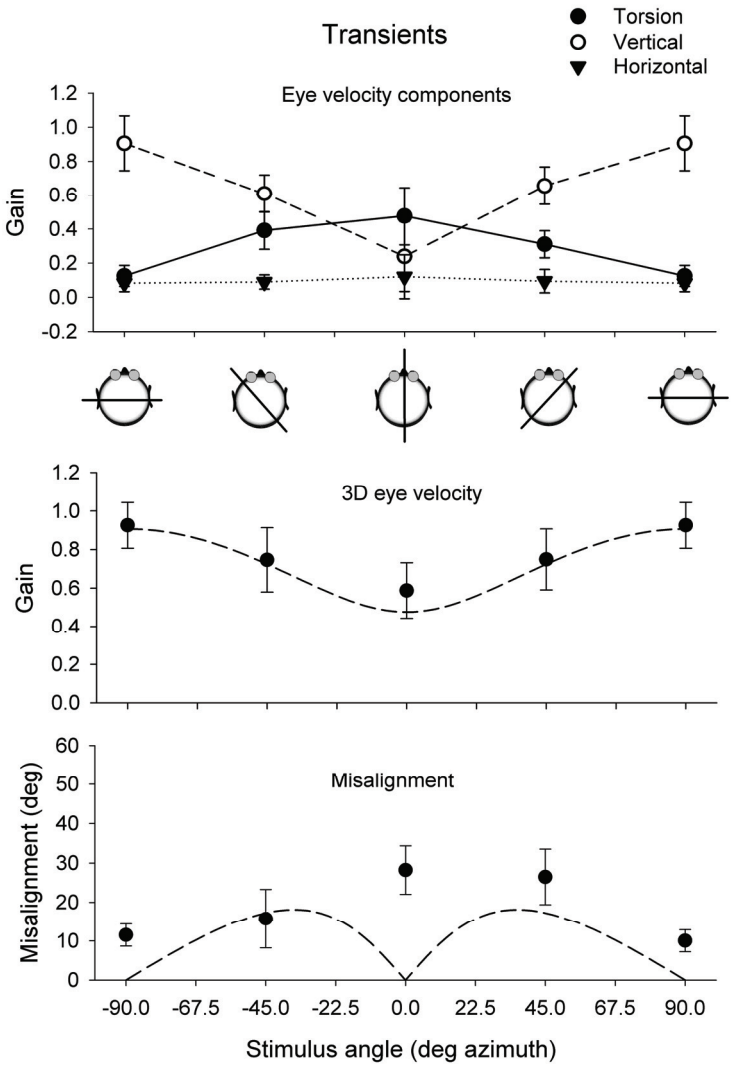

Figure 6. Results of horizontal axis whole body impulse stimulation for all tested horizontal stimulus axes. Top panel: mean gain of the horizontal, vertical and torsion eye velocity components. Middle panel: mean gain of 3D eye velocity for each tested stimulus orientation. The dashed line represents the expected vector eye velocity gain predicted from the vertical and torsion components. The lower panel shows the misalignment of the response axis with respect to the stimulus axis. The dashed line in the lower panel represents the predicted misalignment calculated from the vector sum of vertical and torsion eye velocity components. Error bars in all panels indicate one standard deviation. Cartoons underneath the top panel give a top view of the orientation of the stimulus axis with respect to the head.

In conclusion, we find that the gain and misalignment of eye movements in response to whole body transients follow a similar pattern as responses to sinusoidal stimulation in darkness. In both instances the largest misalignment between 3D head and eye rotation axis occurs during roll stimulation.

To verify that the difference in misalignment between light and dark conditions is related to the absence or presence of a horizontal component, we generated simulated eye movements in response to the same stimulus range as in the real experiment. In the simulation the maximum gain for vertical eye responses was set at 0.99 and for torsion at 0.54. We simulated two conditions: In condition 1 the gain of the horizontal eye movements was set to zero (similar to what we found in the light). In the condition 2 we simulated a horizontal eye rotation component with a gain varying between 0 for pitch to 0.23 for roll. These simulated horizontal, vertical and torsion eye movement data were analyzed with the same analysis software as the real data. In condition 1 the 3D eye velocity gain exactly matched values predicted from roll and pitch components. Also predicted (dashed line) and simulated misalignment (open squares) exactly matched in condition 1. The presence of a horizontal component in condition 2 had only a small effect on 3D eye velocity gain. However, it strongly affected misalignment, with a maximum value towards roll. These simulations show that the changes are due to the presence of a horizontal eye rotation component in the dark.

Discussion

In this paper we show that in humans the quality of the 3D VOR response varies not only in terms of gain, but also in terms of alignment of the eye rotation axis with head rotation axis. Studies in humans on properties of the 3D VOR generally reported on gain and phase characteristics about the cardinal axes that are yaw, roll and pitch (Ferman et al. 1987; Tabak and Collewijn 1994; Paige and Seidman 1999; Misslisch and Hess 2000; Roy and Tomlinson 2004). More recently, gain characteristics in the planes of the vertical canals were measured (Cremer et al. 1998) (Halmagyi et al. 2001; Migliaccio et al. 2004; Houben et al. 2005). All studies on 3D VOR dynamics report a high gain for horizontal and vertical eye movements compared to torsion. This general property has been described in lateral eyed animals (rabbits: (Van der Steen and Collewijn 1984) and frontal eyed animals (monkeys: (Seidman et al. 1995) and humans (Ferman et al. 1987; Seidman and Leigh 1989; Tweed et al. 1994; Aw et al. 1996b). We show that also for small amplitude stimulation the gain of the VOR for stimulation about the cardinal axes is in close agreement with previous studies in humans (Paige 1991; Tabak and Collewijn 1994; Aw et al. 1996a). We found a small but significant higher gain for pitch head up, compared to pitch head down transients (P= 0.05). This is different from earlier reports and possibly related to the fact that our transients were whole body movements in contrast to previous head transient studies that always involved stimulation of the neck (Tabak and Collewijn 1995; Halmagyi et al. 2001).
The second main finding is the systematic variation in misalignment between stimulus and response axis. In the light misalignment between eye and head rotation axis has minima at roll and pitch and its maxima at plus and minus 45° azimuth. This finding is consistent with a co-ordinate system with a head fixed torsion and pitch axis. In this system vector summation of near unity response for pitch and a considerably lower response for roll has an effect on misalignment during stimulation about an axis intermediate between roll and pitch. Quantitatively, the misalignment angles in our study are similar to

those reported in previous studies in monkeys (Crawford and Vilis 1991; Migliaccio et al. 2004).
Quantitative and qualitative differences exist in misalignment between light and dark conditions. Firstly, there is in the dark and during transient stimulation a twofold increase in misalignment compared to sinusoidal stimulation in the light over the whole range of tested axes.
Because in the dark gain is lower, one possibility is that roll and pitch are not proportionally reduced. However, this is not the case: There was on average a 34 % reduction for pitch and a 36 % for roll. Differences were not significantly different (P=0.9). Thus, the larger misalignment is not due to vector summation of different vertical and torsion values.
The second point is the large change in misalignment during roll stimulation in the dark compared to the light. We show that this increase in the dark is due to a horizontal eye movement component. The presence of a horizontal component during roll stimulation in the dark has been reported before (Misslisch and Tweed 2000; Tweed et al. 1994). Misslisch and Tweed (Misslisch and Tweed 2000) suggested that the horizontal cross-coupling between horizontal and torsional eye movements during head roll occurs because "the brain is so accustomed to eye translation during torsional head motion that it has learned to rotate the eyes horizontall during roll even when there is in fact no translation". However, this explanation for the presence of a horizontal component is not very satisfactory.
An alternative possibility is a change of eye in head position in the dark. This change can cause an increase in misalignment as eye position in the orbit has an effect on the orientation of the eye velocity axis (Misslisch et al. 1994). However, this explanation is unlikely because we carefully controlled the central fixation of the subject's eyes by providing a visual fixation target in between stimulus trials. The eyes remained within 1.54 degrees standard deviation around the fixation centre. This value is far too small to explain the observed changes in misalignment.
A second possibility is that otolith signals are part of the response (Angelaki and Dickman 2003; Bockisch et al. 2005). The contribution of tilt VOR to the 3D eye velocity response depends on the orientation of the stimulus axis (Merfeld 1995; Merfeld et al. 2005). In particularly for stimulation about the roll axis (side down) any contribution from tilt VOR would evoke horizontal eye movements. Because otoliths respond to both linear accelerations and tilt (Angelaki and Dickman 2003), we can estimate the contribution of tilt to the horizontal and vertical components from the responses to linear acceleration. Because in our stimulus conditions (1 Hz, 4° peak-to-peak) the estimated horizontal tilt VOR "gain" is only 0.016, tilt VOR can not explain our findings.
Another possibility is that horizontal eye movements during roll depend on head position. A change in pitch head position alters the anatomical orientation of the semicircular canals with respect to gravity. This could have an effect on response vectors of the three semicircular canals, or it could have an effect on the central integration between canal and otolith signals. In our experiments we positioned our subjects as close as possible with the head in an upright position with a seven degree upward inclination of the frontal pole of Reid's line (Della Santina et al. 2005). In this position there is only about 1 degree deviation from the ideal response vector. Thus, the horizontal eye movements cannot be explained by a change in sensitivity vectors due to different canal plane orientation.

This leaves us with the option that horizontal eye movements in darkness are the result of differences in the central processing of 3D canal signals. Afferent signals from the different canal and otolith sensor are to a large extent processed via specific pathways which have connections with different eye muscles (Ito et al. 1976). Recent work on gravity dependence of roll angular VOR in monkey (Yakushin et al. 2009) supports the special organization of the roll angular VOR compared to yaw and pitch angular VOR. These differences are not only reflected in the low gain of torsion and poor adaptive capabilities of roll angular VOR (Yakushin et al. 2009), but also in the poor alignment of the eyes during roll in the dark. In a control experiment we confirmed that there is also in human a gravity dependent effect. We compared two different pitch positions of the head (Reid's line 10 degrees and 25 degrees up). Pitching the head 15 degrees up resulted in a 5 degrees increase in misalignment (see Figure electronic supplement). Only a very small decrease in torsion (0.04) and increase in horizontal (0.05) gain paralleled this increase in misalignment. Theoretically, misalignments due to different head orientations may be counteracted by internal neuronal processing (Merfeld et al. 2005). Our data suggest that these compensations are not very effective for stimulation at 1 Hz in the dark, although the effect on vestibular compensation may be frequency dependent (Groen et al. 1999; Schmid-Priscoveanu et al. 2000; Bockisch et al. 2005; Zupan and Merfeld 2005). This is in line with current ideas that gravito-inertial internal forces play an important role for perceptual representations, whereas head and eye centred reference systems are important for oculomotor stabilization (Angelaki and Cullen 2008).

We agree with the conclusions from Yakushin (Yakushin et al. 2009) that roll angular VOR is different from the yaw and pitch aangular VOR. This is also reflected in the way visual information is integrated with vestibular information. At the subcortical level visual information has a three-dimensional representation of space, similar to that of the semicircular canals, including representation of torsion (roll) (Simpson and Graf 1985; Van der Steen et al. 1994). At the cortical level, the visual system is mainly organized in a two-dimensional system, with little representation of torsion. This organization of the visual system mainly helps to stabilize gaze in yaw and pitch and much less in roll.

References

Angelaki DE, Cullen KE (2008) Vestibular system: the many facets of a multimodal sense. Annu Rev Neurosci 31: 125-150.

Angelaki DE, Dickman JD (2003) Gravity or translation: central processing of vestibular signals to detect motion or tilt. J Vestib Res 13: 245-253.

Aw ST, Halmagyi GM, Haslwanter T, Curthoys IS, Yavor RA, Todd MJ (1996a) Three-dimensional vector analysis of the human vestibuloocular reflex in response to high-acceleration head rotations. II. responses in subjects with unilateral vestibular loss and selective semicircular canal occlusion. J Neurophysiol 76: 4021-4030.

Aw ST, Haslwanter T, Halmagyi GM, Curthoys IS, Yavor RA, Todd MJ (1996b) Three-dimensional vector analysis of the human vestibuloocular reflex in response to high-acceleration head rotations. I. Responses in normal subjects. J Neurophysiol 76: 4009-4020.

Bockisch CJ, Straumann D, Haslwanter T (2005) Human 3-D aVOR with and without otolith stimulation. Exp Brain Res 161: 358-367.

Bruno P, Van den Berg AV (1997) Torsion during saccades between tertiary positions. Exp Brain Res 117: 251-265.

Crane BT, Demer JL (1997) Human gaze stabilization during natural activities: translation, rotation, magnification, and target distance effects. J Neurophysiol 78: 2129-2144.

Crane BT, Tian J, Demer JL (2006) Temporal dynamics of ocular position dependence of the initial human vestibulo-ocular reflex. Invest Ophthalmol Vis Sci 47: 1426-1438.

Crane BT, Tian JR, Demer JL (2005) Human Angular Vestibulo-Ocular Reflex Initiation: Relationship to Listing's Law. Ann N Y Acad Sci 1039: 26-35.

Crawford JD, Vilis T (1991) Axes of eye rotation and Listing's law during rotations of the head. J Neurophysiol 65: 407-423.

Cremer PD, Halmagyi GM, Aw ST, Curthoys IS, McGarvie LA, Todd MJ, Black RA, Hannigan IP (1998) Semicircular canal plane head impulses detect absent function of individual semicircular canals. Brain 121 (Pt 4): 699-716.

Della Santina CC, Potyagaylo V, Migliaccio AA, Minor LB, Carey JP (2005) Orientation of human semicircular canals measured by three-dimensional multiplanar CT reconstruction. J Assoc Res Otolaryngol 6: 191-206.

Demer JL, Crane BT, Tian JR (2005) Human angular vestibulo-ocular reflex axis disconjugacy: relationship to magnetic resonance imaging evidence of globe translation. Ann N Y Acad Sci 1039: 15-25.

Ferman L, Collewijn H, Jansen TC, Van den Berg AV (1987) Human gaze stability in the horizontal, vertical and torsional direction during voluntary head movements, evaluated with a three-dimensional scleral induction coil technique. Vision Res 27: 811-828.

Groen E, Bos JE, de Graaf B (1999) Contribution of the otoliths to the human torsional vestibulo-ocular reflex. J Vestib Res 9: 27-36.

Grossman GE, Leigh RJ, Abel LA, Lanska DJ, Thurston SE (1988) Frequency and velocity of rotational head perturbations during locomotion. Exp Brain Res 70: 470-476.

Grossman GE, Leigh RJ, Bruce EN, Huebner WP, Lanska DJ (1989) Performance of the human vestibuloocular reflex during locomotion. J Neurophysiol 62: 264-272.
Halmagyi GM, Aw ST, Cremer PD, Curthoys IS, Todd MJ (2001) Impulsive testing of individual semicircular canal function. Ann N Y Acad Sci 942: 192-200.
Halmagyi GM, Black RA, Thurtell MJ, Curthoys IS (2003) The human horizontal vestibulo-ocular reflex in response to active and passive head impulses after unilateral vestibular deafferentation. Ann N Y Acad Sci 1004: 325-336.
Haslwanter T, Moore ST (1995) A theoretical analysis of three-dimensional eye position measurement using polar cross-correlation. IEEE Trans Biomed Eng 42: 1053-1061.
Haustein W (1989) Considerations on Listing's Law and the primary position by means of a matrix description of eye position control. Biol Cybern 60: 411-420.
Houben MMJ, Goumans J, Dejongste AH, Van der Steen J (2005) Angular and linear vestibulo-ocular responses in humans. Ann N Y Acad Sci 1039: 68-80.
Houben MMJ, Goumans J, van der Steen J (2006) Recording Three-Dimensional Eye Movements: Scleral Search Coils versus Video Oculography. Invest Ophthalmol Vis Sci 47: 179-187.
Ito M, Nisimaru N, Yamamoto M (1976) Pathways for the vestibulo-ocular reflex excitation arising from semicircular canals of rabbits. Exp Brain Res 24: 257-271.
Merfeld DM (1995) Modeling human vestibular responses during eccentric rotation and off vertical axis rotation. Acta Otolaryngol Suppl 520 Pt 2: 354-359.
Merfeld DM, Park S, Gianna-Poulin C, Black FO, Wood S (2005) Vestibular perception and action employ qualitatively different mechanisms. II. VOR and perceptual responses during combined Tilt&Translation. J Neurophysiol 94: 199-205.
Migliaccio AA, Schubert MC, Jiradejvong P, Lasker DM, Clendaniel RA, Minor LB (2004) The three-dimensional vestibulo-ocular reflex evoked by high-acceleration rotations in the squirrel monkey. Exp Brain Res 159: 433-446.
Misslisch H, Hess BJ (2000) Three-dimensional vestibuloocular reflex of the monkey: optimal retinal image stabilization versus listing's law. J Neurophysiol 83: 3264-3276.
Misslisch H, Tweed D (2000) Torsional dynamics and cross-coupling in the human vestibulo-ocular reflex during active head rotation. J Vestib Res 10: 119-125.
Misslisch H, Tweed D, Fetter M, Sievering D, Koenig E (1994) Rotational kinematics of the human vestibuloocular reflex. III. Listing's law. J Neurophysiol 72: 2490-2502.
Paige GD (1991) Linear vestibulo-ocular reflex (LVOR) and modulation by vergence. Acta Otolaryngol Suppl 481: 282-286.
Paige GD, Seidman SH (1999) Characteristics of the VOR in response to linear acceleration. Ann N Y Acad Sci 871: 123-135.
Roy FD, Tomlinson RD (2004) Characterization of the vestibulo-ocular reflex evoked by high-velocity movements. Laryngoscope 114: 1190-1193.

Schmid-Priscoveanu A, Straumann D, Kori AA (2000) Torsional vestibulo-ocular reflex during whole-body oscillation in the upright and the supine position. I. Responses in healthy human subjects. Exp Brain Res 134: 212-219.
Seidman SH, Leigh RJ (1989) The human torsional vestibulo-ocular reflex during rotation about an earth-vertical axis. Brain Res 504: 264-268.
Seidman SH, Leigh RJ, Tomsak RL, Grant MP, Dell'Osso LF (1995) Dynamic properties of the human vestibulo-ocular reflex during head rotations in roll. Vision Res 35: 679-689.
Simpson JI, Graf W (1985) The selection of reference frames by nature and its investigators. Rev Oculomot Res 1: 3-16.
Tabak S, Collewijn H (1994) Human vestibulo-ocular responses to rapid, helmet-driven head movements. Exp Brain Res 102: 367-378.
Tabak S, Collewijn H (1995) Evaluation of the human vestibulo-ocular reflex at high frequencies with a helmet, driven by reactive torque. Acta Otolaryngol Suppl 520 Pt 1: 4-8.
Tabak S, Collewijn H, Boumans LJ, van der Steen J (1997a) Gain and delay of human vestibulo-ocular reflexes to oscillation and steps of the head by a reactive torque helmet. I. Normal subjects. Acta Otolaryngol 117: 785-795.
Tabak S, Collewijn H, Boumans LJ, van der Steen J (1997b) Gain and delay of human vestibulo-ocular reflexes to oscillation and steps of the head by a reactive torque helmet. II. Vestibular-deficient subjects. Acta Otolaryngol 117: 796-809.
Tweed D, Sievering D, Misslisch H, Fetter M, Zee D, Koenig E (1994) Rotational kinematics of the human vestibuloocular reflex. I. Gain matrices. J Neurophysiol 72: 2467-2479.
Van der Steen J, Collewijn H (1984) Ocular stability in the horizontal, frontal and sagittal planes in the rabbit. Exp Brain Res 56: 263-274.
Van der Steen J, Simpson JI, Tan J (1994) Functional and anatomic organization of three-dimensional eye movements in rabbit cerebellar flocculus. J Neurophysiol 72: 31-46.
Yakushin SB, Xiang Y, Cohen B, Raphan T (2009) Dependence of the roll angular vestibuloocular reflex (aVOR) on gravity. J Neurophysiol 102: 2616-2626.
Zupan LH, Merfeld DM (2005) An internal model of head kinematics predicts the influence of head orientation on reflexive eye movements. J Neural Eng 2: S180-197.

Supplement

Evaluation of factors that may be responsible for the horizontal eye movement component during roll stimulation in darkness.

1- tilt VOR contribution

Sinusoidal oscillation about a horizontal axis not only activates the semicircular canals, but also the otoliths. The latter is due to a change in orientation of the otoliths with respect to gravity. The result is that not only compensatory eye movements are generated with components expected for rotations about that particular axis, but also additional horizontal and/or vertical eye velocity components. For instance, during sinusoidal stimulation about the roll axis a horizontal eye component (H_t) is generated due to otolith contribution.
To estimate the magnitude of this response, we measured the horizontal eye response to pure translation along the same axes as used during rotations in the horizontal plane. The effect on the otoliths is similar because tilt and translation both generate a shear force on the hair cells.
Sinusoidal translations were delivered at a frequency of 1 Hz, amplitude 5 cm, peak acceleration 1.8 m/s^2. The frequency of our angular sinusoidal stimuli was 1 Hz, amplitude 2° (A_r). This stimulus corresponds to a linear acceleration (L_a), which equals the sine of A_r times gravity (g = 9.81 m/s^2).

In formula: $L_a = \sin(A_r) * g = 0.342 \ m/s^2$. (1)

At a target distance of 180 cm and lateral displacement amplitude of 5 cm, the ideal response is a horizontal counter rotation of the eye with an amplitude of atan (5/180) = 1.6°. This is the ideal situation where the "gain" for that viewing distance is 1.
However, the actual "gain" of the horizontal eye movement component as we determined for sinusoidal translations at 1 Hz along the interaural axis in darkness was 0.2 (N=6).

Therefore, the actual response (H_l) is: $(H_l) = 0.2 * 1.6 = 0.32°$. (2)
This is, however, for a peak linear acceleration (a_p) of 1.8 m/ s^2.
From this follows that during sinusoidal stimulation the horizontal VOR component (H_t) due to tilt is:

$H_t = (L_a / a_p) * H_l = (0.342/1.8)*0.32 = 0.061°$. (3)

From this it follows that a sinusoidal stimulation around the roll axis with an amplitude of 2º results in a horizontal gain of 0.061°/ 2° = 0.031 attributable to tilt VOR. This value is much smaller than the horizontal gain of 0.23 we observed.

2- Sensitivity vectors of semicircular canals as function of head pitch orientation

The Della Santina paper (Della Santina et al. 2005) provides a good basis to estimate the orientation effect of the semicircular canals with respect to earth-horizontal. In the study of Della Santina (DellaSantina, Table 1A) individual canal response sensitivities are expressed in Reid's co-ordinate system. Reid's line is the line connecting the meatus externa with the lower rim of the orbital cantus.

Following from the numbers given by Della Santina the contribution from each canal during a rotation expressed in Reid's co-ordinate system is given by the following matrix.

$$\begin{array}{c} \begin{matrix} \text{LA} & \text{LH} & \text{LP} \end{matrix} \\ \begin{pmatrix} -0.58954 & -0.31645 & -0.69611 \\ 0.78750 & 0.04108 & -0.66820 \\ -0.17971 & 0.94772 & -0.26257 \end{pmatrix} \end{array} \begin{matrix} \\ \text{X} \\ \text{Y} \\ \text{Z} \end{matrix} \quad (1)$$

When we assume bi-directional linearity the effects of a pure clockwise (roll) rotation about the x-axis (x = +1, y = 0, z = 0) in Reid's co-ordinates can be approximated by multiplication of matrix 1 with rotation vector (1, 0, 0). After normalisation, the resultant eye movements in torsion, vertical and horizontal components are respectively 0.9998, -00.1488, and 0.0120, which results in about 1-degree deviation of the x-axis with respect to Reid's x-y plane. This value is much smaller than the misalignments we measured in the dark.

3- Gravity dependency of roll angular VOR

The effect of two different head pitch positions (Reid's line 10 degrees and 25 degrees up) on gain and misalignment was measured in three naïve subjects. A summary is shown in Figure S1. Pitching the head up had a small effect on gain: a decrease in torsion of 0.03 ± 0.01 and an increase in horizontal gain of 0.05±0.01. This small change in gain resulted on average in 9.6±2.6 degrees increase in misalignment.

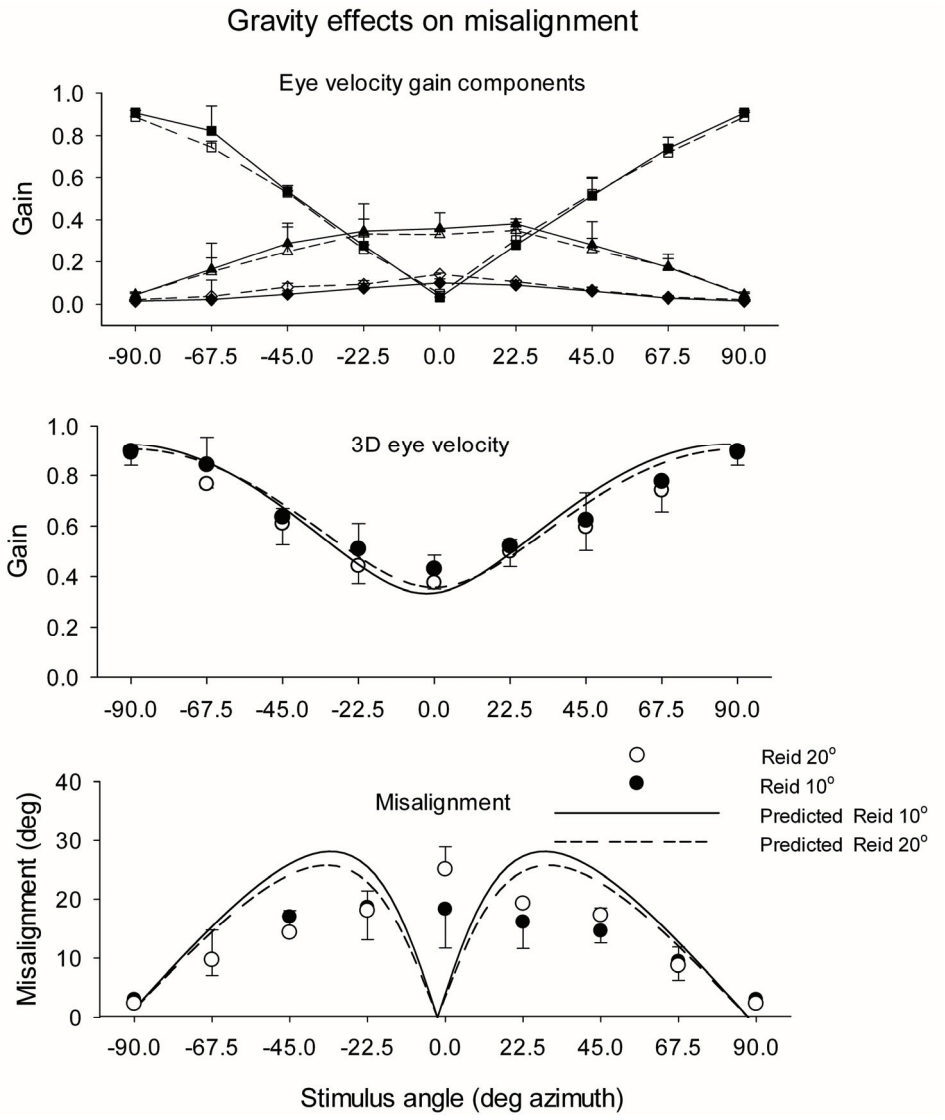

Figure S1. Effects of pitch position of the head on gain and misalignment during horizontal axis sinusoidal stimulation in the dark. Solid line and closed symbols: head oriented with Reid's line at 10 degrees. Dashed line and open symbols: head oriented with Reid's line 20 degrees. Top panel: gain of the horizontal (diamonds), vertical (squares) and torsion (triangles) eye velocity components. Centre panel: 3D eye velocities. Lower panel: misalignment of the response axis with respect to the stimulus axis.

4- Instrument precision

The precision of our stimulation device is shown in Figure S2. The upper left panel shows recordings from an earth fixed search coil mounted in the centre of the field cube. With this stationary search coil in place we applied the stimulus sequence used in our experiments to the platform and search coil data were sampled at 1000 Hz. Because the search coil was stationary in space and not fixed to the platform, any imprecision, vibration, drift or whatever kind of irregularity due to magnetic field coils moving with the platform motion would show up in the coil signal. Coil data were fitted with a sinusoid resulting in a perfect match between measured and fitted data (r^2 = 1.000 and P<0.0001). The plot demonstrates that our platform produces a near perfect a sinusoidal stimulus, without any position drift. The lower left panel in Figure S2 shows the signals in the velocity domain. The black solid line shows that signal noise is about 1 °/s peak-to-peak.

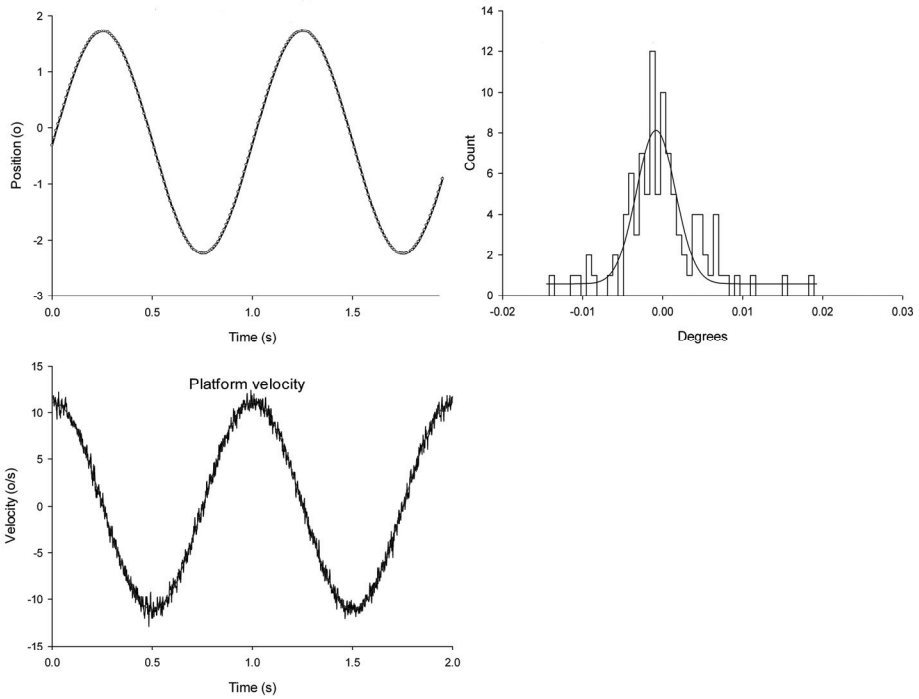

Figure S2. Left panel: recordings from an earth fixed search coil mounted in the centre of the field cube during sinusoidal platform motion at 1 Hz. Top: position data Bottom: velocity data. Right panel: distribution of the difference between the horizontal head coil and bite-board coil signals during sinusoidal oscillation at 1 Hz. The plot is an average of 10 sinusoidal stimulus repetitions. A Gaussian is curve fitted through the data.

Because for the current study stimulus precision is critical to the results, we also determined the amount of relative motion between a coil attached to the bite board and a coil attached to the forehead. Figure S2 (right panel) shows the distribution of the difference between signals of the horizontal head coil and bite-board coil signals. The plot is an average of 10 sinusoidal stimulus repetitions. A Gaussian curve fitted through these data shows that the 95% confidence level is <0.01 degrees. During transients the amount of decoupling was <0.02 degrees during the first 100 ms.

Chapter 4

Three-dimensional vestibulo-ocular stability in operated and not operated unilateral Schwannoma patients

Goumans J, Houben MMJ, Haans R, Feenstra L, van der Steen J

submitted

Abstract

The decision to surgically remove a vestibular Schwannoma is made primarily on its size and the impact of an operation on hearing function. In contrast, its impact on vestibular function has received less attention. Therefore, we tested not operated and operated patients with unilateral vestibular Schwannoma to study the effects of the tumour on gain and misalignment of the vestibulo-ocular response during three-dimensional (3D) vestibular stimulation. The not operated patients had been on a wait and see policy between 8 and 10 years, whereas the operated patients had received a unilateral surgical resection of their tumour and the vestibular nerve 6 to 10 years ago. 3D eye movements were measured with scleral search coils in response to whole-body sinusoidal rotations in healthy controls and in both patient groups, using a motion platform with six degrees of freedom. Subjects were oscillated about the vertical axis and about axes in the horizontal plane between roll and pitch with increments of 22.5° azimuth. Eye movements were converted to rotation vectors and gain and misalignment were determined during sinusoidal stimulation. Ocular stability was impaired in not operated and operated patients. Misalignment of the 3D angular vestibulo-ocular reflex in the not operated Schwannoma patients varied from mild to severe. Gain and misalignment in the three operated patients was closer to values measured in control subjects. The vertical component was relatively well preserved compared to torsional components.

Introduction

Angular motion of the head is sensed by the semicircular canals of the vestibular system. They form the input for a fast reflex loop that stabilizes the retinal image during head movements. Ideally, the angular vestibulo-ocular reflex (VOR) generates an eye velocity equal and opposite to head velocity. This means that the quality of performance is not only determined by the gain and phase of the eye rotation, but also by the accuracy by which input signals from the three semicircular canals are integrated and transformed to eye motor command signals that align the rotation axis of the eye with the rotation axis of the head. The angular difference between eye and head rotation axis is called the misalignment. In healthy subjects both gain and misalignment follow a systematic pattern. In the light three-dimensional (3D) eye velocity gain and misalignment vary as a function of horizontal stimulus axis orientation with the largest misalignment at 45° azimuth. Kinematical properties of the vestibulo-ocular reflex depend on the bilateral input from the peripheral vestibular apparatus. When the vestibular system is completely or partially deprived of its input on one side, ocular instabilities occur, often accompanied by sensations of vertigo. In both animal and human studies, impairments of angular VOR after unilateral vestibular de-afferentation (UVD) have been reported (Cremer et al. 1988; Halmagyi et al. 2003; Aw et al. 1994; Curthoys et al. 1995; Tabak et al. 1997).
Vestibular problems are usually not the main reason for Schwannoma patients to go to the physician. Usually, hearing impairments in one ear leads to these actions.
The reason for this is that vestibular problems usually give rise to much less specific complaints. In addition, in standard clinical practice vestibular clinical tests are usually confined to vertical axis stimulation (yaw or z-axis stimulation), thus measuring only the horizontal canal aspects of the VOR.
In this study we measured the 3D VOR in not operated patients with a partially unilateral vestibular function loss and in patients with surgical resection of the tumour in response to vertical and horizontal axis vestibular stimulation.
We systematically investigated the gain and misalignment of the VOR in response to 4 degrees peak-to-peak amplitude sinusoidal stimulation at a frequency of 1 Hz. This frequency and amplitude is close to what is normal for activities such as walking, where the predominant frequency is 0.8 Hz with mean amplitude of 6 degrees (Grossman et al. 1988; Crane and Demer 1997). The goal of the study was to assess detectable impairments of the 3D VOR in this natural occurring frequency and amplitude range in patients with vestibular Schwannoma.

Methods

Subjects

Fifteen subjects participated in the experiment. All subjects gave their informed consent. The experimental procedure was approved by the Medical Ethics Committee of Erasmus University Medical Centre and adhered to the Declaration of Helsinki for research involving human subjects. Nine subjects served as controls, six subjects had a vestibular Schwannoma (see Table 1).

The age of the control subjects (six males and three females) ranged from 22 to 58 years. None of the control subjects had visual or vestibular complaints. The vestibular Schwannoma patients were selected from a group of 20 patients who were under medical surveillance and/or had received treatment by a multidisciplinary team consisting of an otorhinolaryngologist and a neurosurgeon of the Erasmus University Medical Centre. The age of the patients with Schwannoma varied between 44 and 64 years (five males and one female). In all patients the vestibular Schwannoma was or had been on the right side. Three patients underwent a 'wait and see policy' (Table 1; patients N1-N3) after being diagnosed with vestibular Schwannoma. Their tumour had been stable for over 8-10 years on magnetic resonance imaging. The three other patients (Table 1; group O, patients 1-3) had undergone radical resection of their Schwannoma 6-10 years ago. No recidivate tumour growth was noticed during the control period running from 6-10 years post-operatively. The reason that we have only a small group of patients is that our selection was based on strict exclusion criteria: patients were excluded if there was post-operative damage to other nerves or tissue, or if there were short-term or long-term postoperative facial nerve symptoms.

Patient	Gender	Age (year)	Side of tumour	Tumour size (mm)	Unilateral hearing loss (Fi dB)	Therapy
N1	male	61	right	4	35	wait and see
N2	male	64	right	14	43	wait and see
N3	male	55	right	22	complete	wait and see
O1	male	53	right	4	73	surgery
O2	male	44	right	15	70	surgery
O3	female	46	right	5	40	surgery

Table 1. Clinical data of the not operated group (N) and operated group (O). The unilateral hearing loss is expressed in Fi (= Flechter index, which is mean hearing loss at 500, 1000 and 2000 Hz). Values were determined before any therapy.

In the operated patients the decision to operate had been taken on tumour size and/or severity of tinnitus complaint. Patient O1 was operated using a trans-labyrinth surgical approach, whereas in subjects O2 and O3 a retro-sigmoid approach had been used. Patient O1 had a complete unilateral loss due to the trans-labyrinthine approach. Patient O2 had a relatively large tumour, which made it impossible to spare the nerve. This patient had 70 dB unilateral hearing loss post-operatively. In patient O3 there may have been partial sparing of the auditory nerve because this patient had only partial unilateral hearing loss (40 dB). All operated patients initially had vestibular and postural problems, but in the light there were no long-term vestibular postural stabilization problems.

Experimental set-up

Stimuli were delivered with a motion platform capable of generating angular and translational stimuli with six degrees of freedom (FCS-MOOG, Nieuw-Vennep, The Netherlands).
Subjects were seated on a chair mounted at the centre of the platform. The subject's body was firmly restrained with a four-point seatbelt. The head was

immobilized using an individually moulded dental-impression bite board, which was rigidly connected to the cubic frame. A vacuum pillow folded around the neck and an extra pvc support attached to the chair ensured rigid fixation of the subject's head. The centre of rotation of the platform was set under software control as the intersection point of two horizontal lines connecting the meatus of both ears and the front and back of the head. Head orientation was such that Reid's line made an angle of 7 degrees with earth horizontal (Della Santina et al. 2005).
Whole-body sinusoidal rotations were delivered about the rostro-caudal (yaw), the interaural axis (pitch), the naso-occipital axis (roll) and about horizontal axes intermediate between roll and pitch incremented in steps of 22.5°. Stimulus frequency was 1 Hz with a total duration of 14 seconds, including two seconds of fade-in and fade-out time. Peak-to-peak amplitude of the stimulus for rotatory motion was 4 degrees (peak acceleration $80^{\circ}/s^2$). Sinusoidal stimuli were delivered in light and darkness. In the light, subjects fixated a continuously lit visual target (a red LED, 2 mm diameter) located 177 cm in front of the subject at eye level. During sinusoidal stimulation in the dark, the visual target was briefly presented (2 s) when the platform was stationary during the interval between two consecutive stimulations. Subjects were instructed to fixate the imaginary location of the space fixed target during sinusoidal stimulation after the target had been switched off just prior to motion onset.

Data analysis

All coil signals were converted into Fick angles and then expressed as rotation vectors (Haustein 1989; Haslwanter 1995; Haslwanter and Moore 1995). Eye positions were expressed in a right-handed, head-fixed co-ordinate system. Clockwise, down and left viewed from the perspective of the subject are defined as positive. To express 3D eye movements in the velocity domain, we used angular velocity ($\boldsymbol{\omega}$). Eye velocity gain for sinusoidal stimulation was calculated by fitting a sinusoid with a frequency equal to the platform frequency through the angular velocity components. The gain for each component is defined as the ratio of eye component peak velocity of the sinusoidal fit and platform peak velocity. The misalignment between eye rotation and head rotation axis in three dimensions was calculated as the instantaneous angle in three dimensions between the inverse of the eye velocity axis and the head velocity axis (Aw et al. 1996a). The 3D angular velocity gain and misalignment were compared to the values predicted from linear vector summation of the pure roll and pitch components (Crawford and Vilis 1991). To obtain the predicted eye velocity gain, the length of roll and pitch eye velocity component for a given angle was computed from the orthogonal projection of the head eye velocity vector on the roll and pitch eye velocity axis. Multiplication of these components with the roll and pitch eye velocity vectors resulted in the predicted eye velocities produced by each component individually. Vector summation of the two predicted roll and pitch eye velocity vectors resulted in the predicted eye velocity vector in the plane defined by the roll and pitch axis. Similarly, the angular misalignment was computed from the difference in angular orientation between predicted and measured eye velocity vectors. In addition to this 3D analysis, we also plotted the horizontal, vertical and torsion angular velocities on the yaw, roll and pitch plane.

Results

3D VOR in not operated patients

The magnetic resonance imaging (see top of Figure 1) show the location on the right side and the different size of the tumour in the three not operated patients (see also Table 1 in method section). Complaints of dizziness of these three patients varied. Patient N1 had the smallest intracannicular tumour of the three patients. This patient presented only with unilateral hearing problems and had no vertigo complaints. Patients N2 and N3 also reported mild complaints of vertigo, although neither had a sense of disorientation or vegetative problems.

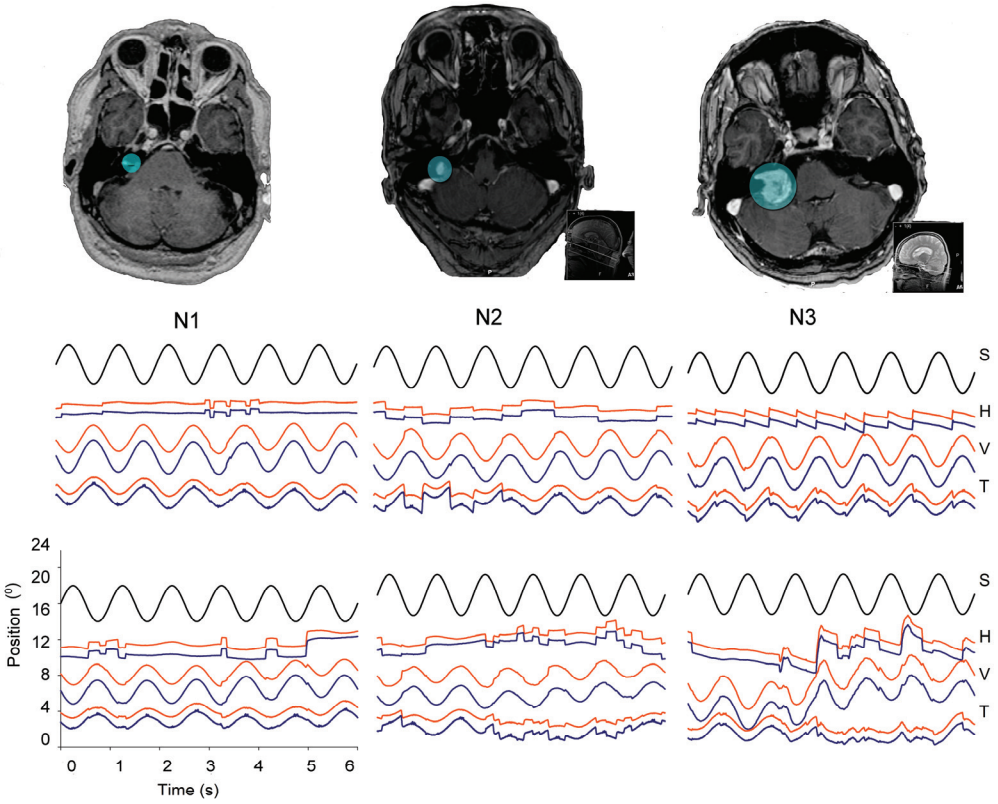

Figure 1. Top panel: magnetic resonance imaging of the three patients with Schwannoma. The circle in each scan indicates the Schwannoma. Lower panels: examples of time plots for the three not operated patients in response to sinusoidal stimulation about a horizontal axis oriented at 45° azimuth. Upper row: light, Lower row: dark. Right (red) and left (blue) eye, horizontal (H), vertical (V) and torsional (T) eye positions are plotted. Stimulus motion is indicated by the top black trace in each panel.

Typical examples of eye position traces for the three not operated patients in response to sinusoidal stimulation about a horizontal axis 45° azimuth are shown in the lower panels of Figure 1. Ideally, this stimulus evokes a combination of vertical and torsional eye movement components and no horizontal eye movements. In the light there were no signs of horizontal eye movement instabilities in patients N1 and N2. Patient N3 had a 2°/s horizontal leftward nystagmus (slow phase to the right) and a 1°/s clockwise (CW) torsional nystagmus (slow phase counterclockwise (CCW).

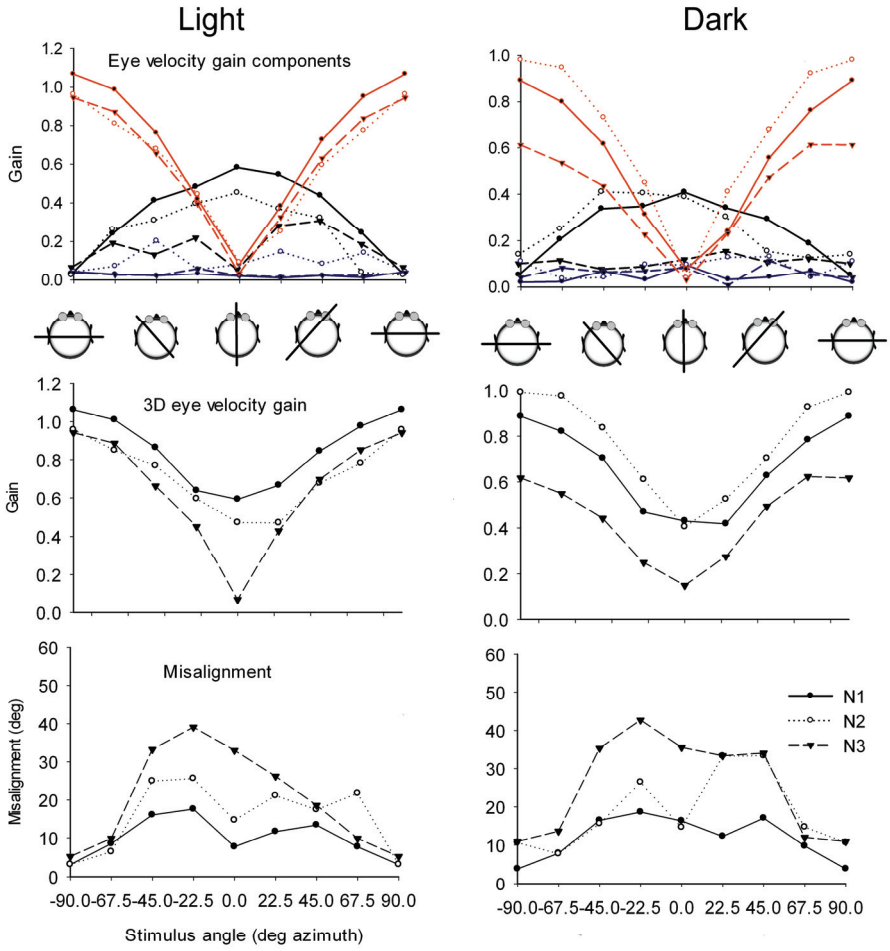

Figure 2. Gain and misalignment of 3D VOR during horizontal axis sinusoidal stimulation in the light (left panels) and dark (right panels) for patients N1, N2 and N3. Top graphs show gain of the horizontal (blue), vertical (red) and torsional (black) eye velocity components. Cartoons underneath give a top view of the orientation of the stimulus axis with respect to the head. Centre graph: 3D eye velocity at each tested stimulus axis orientation. Lower graph: misalignment of the response axis with respect to the stimulus axis.

In the dark torsion drift in patients N1 was 0.5°/s in CCW direction. Drift was corrected by small CW torsional saccades. Instabilities in horizontal, vertical and torsional eye rotation components in patients N2 and N3 were larger and more variable.

Figure 2 shows gain and misalignment in patients N1, N2 and N3. The upper panels show horizontal, vertical and torsion eye velocity gain components. Torsion in patients N2 and N3 was more variable than in patient N1 (Figure 2, black line of top panels). Torsion gain was significantly different from control values in patients N2 and N3 (P= 0.05, one way repeated measures ANOVA). The change in torsion in patients N2 and N3 had a direct impact on 3D eye velocity gain and misalignment, as shown in the centre and lower panels. The close correspondence between predicted and measured 3D eye velocity gain and alignment as seen in subject N1 and in control subjects (see Figure 3) was lost in patients N2 and N3. In patient N2 gain was almost completely determined by the vertical component, whereas in patient N3 3D eye velocity gain had some asymmetric.

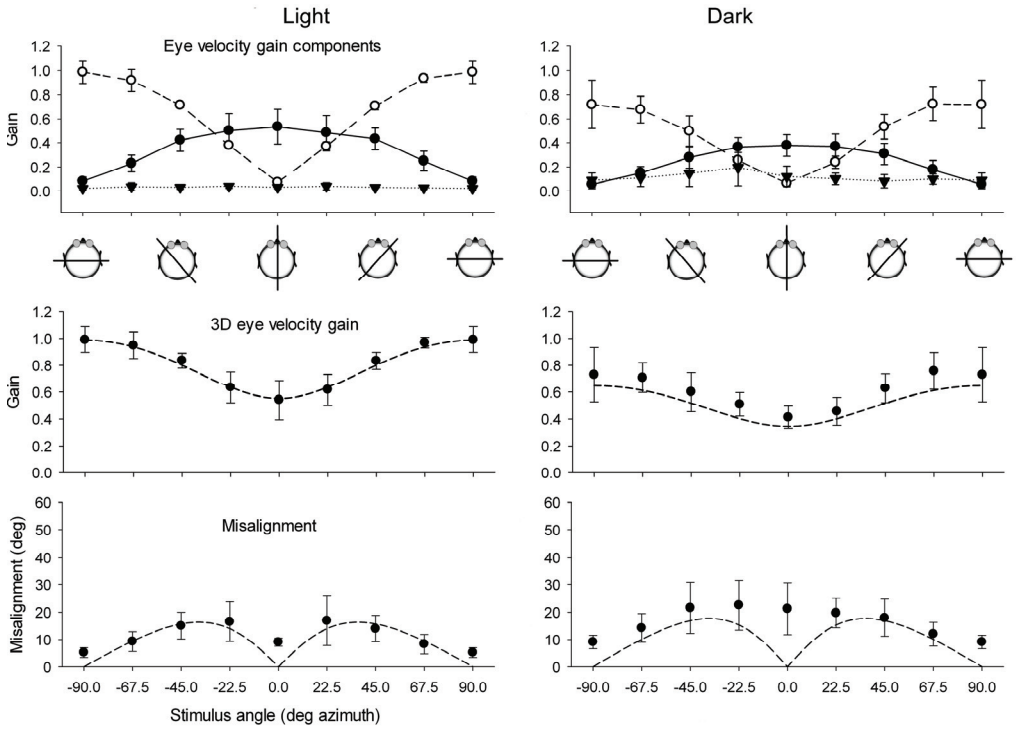

Figure 3. Mean (N=9) gain and misalignment of 3D VOR in control subjects during horizontal axis sinusoidal stimulation in the light (left panels) and dark (right panels). Top graphs show: gains of the horizontal (triangle), vertical (open circle) and torsional (closed circle) eye velocity components in light and darkness. Cartoons underneath give a top view of the orientation of the stimulus axis with respect to the head. Middle graph: mean 3D eye velocity at each tested stimulus axis orientation. Lower graph: misalignment of the response axis with respect to the stimulus.

In the dark, the 3D eye velocity gain in patient N3 was significantly lower ($P < 0.05$, one way repeated measures ANOVA) compared to N1, N2 and control subjects. Changes in gain of torsional and/or vertical components had a strong effect on misalignment. There was a twofold increase in misalignment in patients N2 and N3 compared to N1 and control subjects.

3D VOR in operated patients

3D eye movements in response to sinusoidal vestibular stimulation in the light appeared normal in the three patients who had the tumour surgically removed. There were only in patient O1 weak signs of nystagmus. In darkness all three operated patients had a horizontal nystagmus (Figure 4).

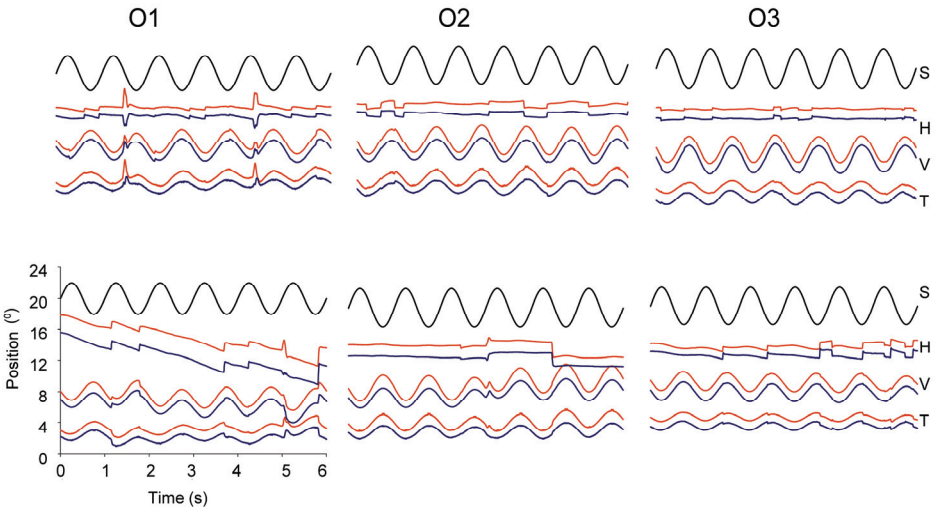

Figure 4. Time series for the three operated patients in response to sinusoidal stimulation about a horizontal axis 45° azimuth. Layout is identical to traces in Figure 1.

Gain of the three operated patients in the light was not significantly different from control subjects ($P > 0.05$). Misalignment had a twofold increase in patients O1 and O3 (Figure 5, lower left panel). This difference was significant ($P < 0.01$).
The smallest angle of misalignment was for pitch (4.68º ± 2.23º). During roll the misalignment was on average 12.36º ± 2.06º.
Pitch stimulation in darkness resulted in compensatory vertical eye movements with a mean gain of 0.73 ± 0.05. The mean gain for torsional eye movements during roll stimulation was 0.30 ± 0.13. The maximum misalignment was during stimulation about the 22.5º axis with a mean of 28.56º ± 10.28º and had its minimum during pitch with a mean of 18.68º ± 3.41º. Values were significantly different from control subjects ($P < 0.05$).

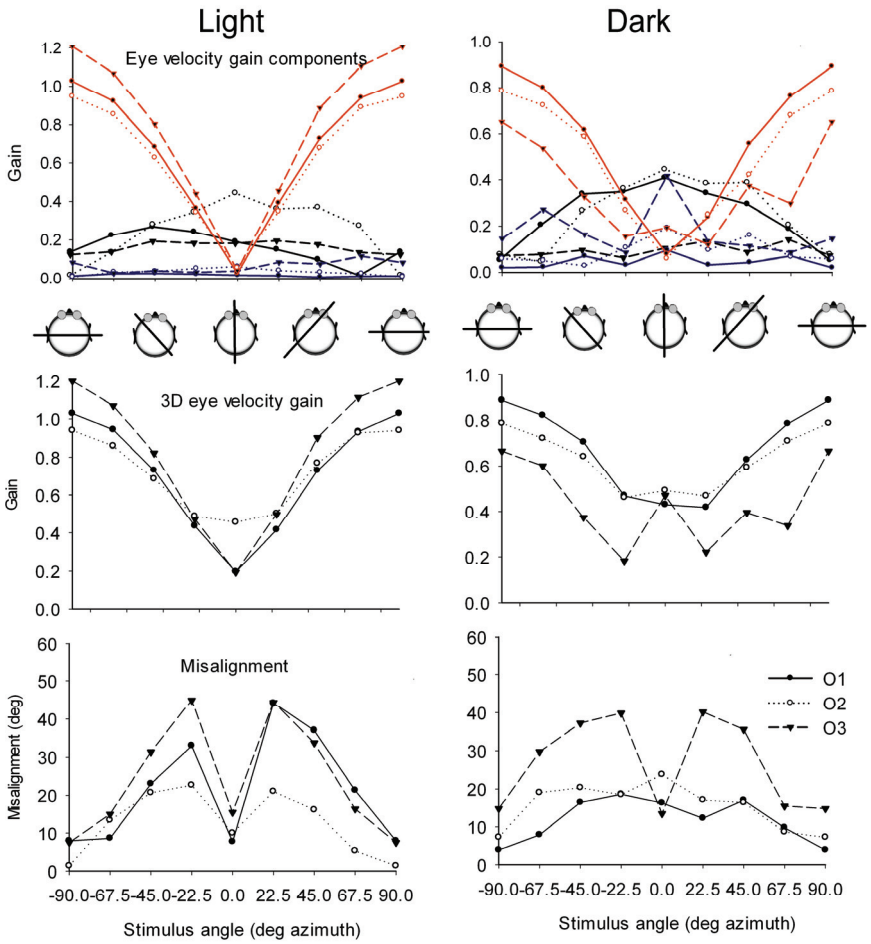

Figure 5. Gain and misalignment in response to horizontal axis sinusoidal stimulation in light and dark for the three operated patients. Layout is identical to Figure 2.

Comparison of ocular stability between vertical and horizontal axis stimulation

The effect of unilateral vestibular Schwannoma on 3D ocular stability in not operated and operated patients is also shown in the plots of angular velocities of control subjects, not operated and operated patients on the yaw, roll and pitch planes. We compared 3D ocular stability in response to vertical axis (z-axis) stimulation with alignment during roll (x-axis) stimulation.

Figure 6 shows a typical example of angular velocities projected on the roll, pitch and yaw plane during vertical axis (z-axis) stimulation. Both in the light and darkness eye velocity in the control subjects was almost collinear with the axis of stimulation. In the roll plane mean (N=3) deviation from earth vertical was 1.58° ± 3.95° in the light and 1.58° ± 3.95° in the dark. In the not operated patients the mean deviation from earth vertical was 3.39° ± 1.69° in the light and 2.06° ± 3.08° in dark and for the operated patients

mean deviation from earth vertical was 1.55° ± 2.06° in the light and 2.25° ± 3.15° in the dark. Changes in orientation of angular velocity were modest and no statistically significant differences were found between control subjects, not operated and operated patients (P > 0.05).

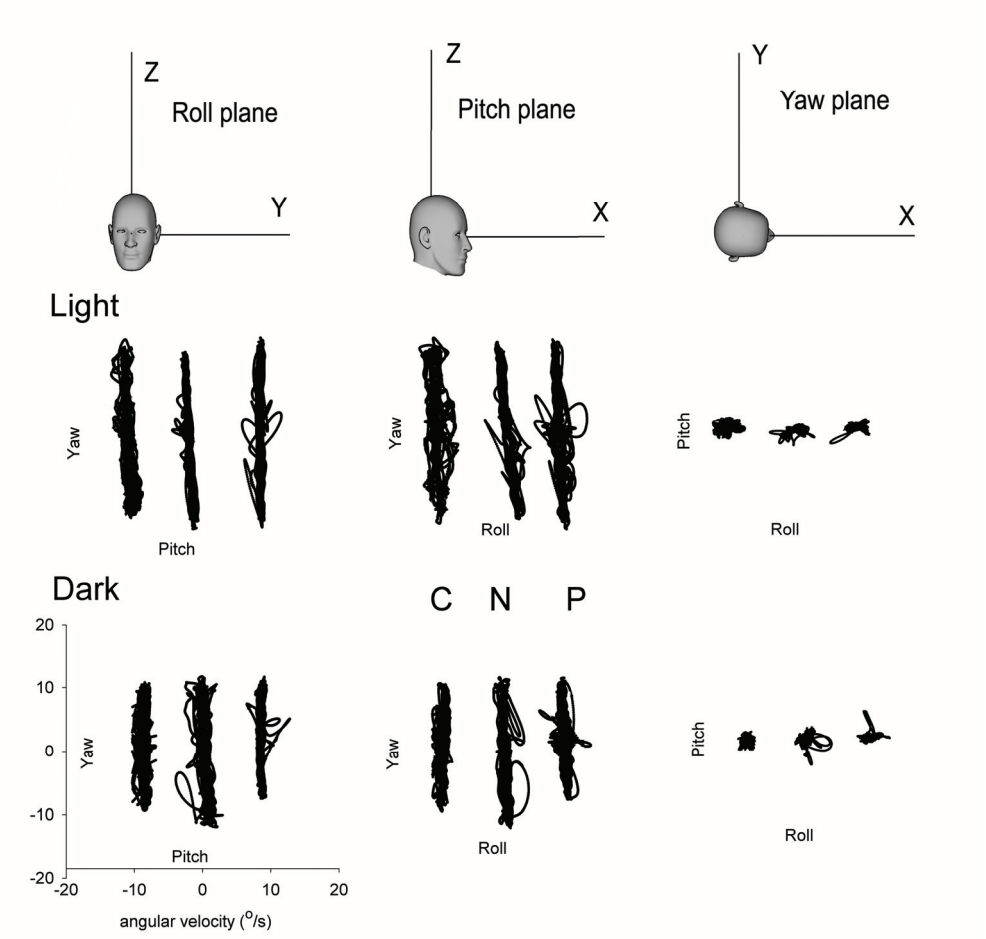

Figure 6. Angular velocity plots during vertical axis stimulation (yaw). The cartoons at the top show the 2D planes on which eye velocities are plotted: these are from left to right the roll, pitch and yaw plane. Eye velocities under light and dark conditions projected on these planes are shown underneath. C= control subject, N = not operated patient and P = operated patient.

Figure 7 shows the effects of unilateral Schwannoma on ocular stability during roll axis stimulation. In the light patient N2 had a pronounced torsion drift interrupted by resetting saccades. In darkness ocular instability during roll increased both in the not operated and operated patients. The most dramatic increase was, however, in the not operated patients. In addition to the larger variability in stability, the orientation of the angular velocities projected on the pitch and yaw planes had changed. In the control subjects the mean deviation in the pitch plane from the z-axis was 3.45° ± 3.85° in the

light and 7.88° ± 4.56° in the dark. In the not operated patients the mean deviation in the pitch plane from the z-axis was 1.85° ± 4.57° in the light and 10.57° ± 5.14° in the dark.
In the operated patients the mean deviation in the pitch plane from the z-axis was 5.58° ± 4.34° in the light and 11.31° ± 5.59° in the dark. Statistically significant differences in orientation in the pitch plane were found between control and not operated and operated patients ($P < 0.05$). Also differences between not operated and operated patients in the pitch plane were significantly different ($P < 0.05$).

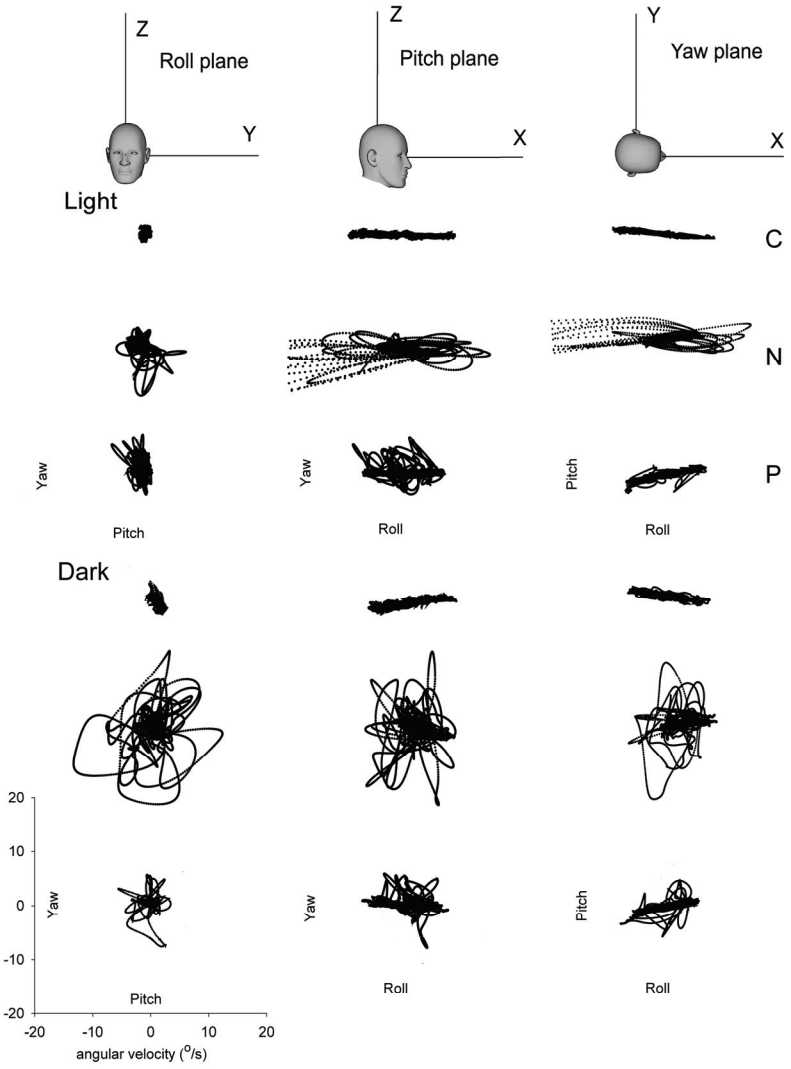

Figure 7. Angular velocity plots during horizontal axis stimulation (roll). Eye velocities under light and dark conditions projected on roll pitch and yaw planes are shown underneath. C = control subject, N = not operated patient and P = operated patient.

Discussion

The goal of this study was to analyse the effects of a vestibular Schwannoma on 3D vestibular function during natural occurring frequencies and amplitudes. We tested the angular VOR over a full range of axes in the horizontal plane. This allowed us to quantify the gain and alignment of the eye rotation axis in 3D with respect to stimulus axis orientation.
One of the main findings is the relatively large increase in misalignment during horizontal axis vestibular stimulation in two out of three patients who were on the 'wait and see' policy. In both cases the effect was strongest during roll stimulation. The main reason is that in these patients the quality of stabilization in torsion was degraded. Both patients (N2 and N3) had torsion drift, both in light and darkness. During roll stimulation misalignment is not only determined by the contribution of the torsion component, but also by the relative contributions of horizontal and vertical components. Because even under normal conditions the gain of torsion is low (Ferman et al. 1987) further degradations of torsion immediately lead to relatively large changes in misalignment.
Most animal (Lasker et al. 2000) and human studies (Cremer et al. 1988; Halmagyi et al. 1990a; Halmagyi et al. 1990b; Tabak et al. 1997; Halmagyi et al. 2003) have studied the effects of UVD on horizontal eye movement instabilities using vestibular stimulation about the vertical axis. Few studies have reported consequences of unilateral impairment of the vestibular organ on 3D aspects of eye rotations (that is including torsion and vertical eye rotations). Aw and colleagues (Aw et al. 1996b; Aw et al. 2003) were the first to describe effects of unilateral vestibular loss and/or selective vertical semicircular canal occlusion on 3D eye movements in patients. They used high acceleration impulses, which resulted in a reduction in gain during ipsi-lesional head impulses, a deviation of the eye rotation axis during ipsi-lesional yaw impulses in the pitch plane away from the rostro-caudal axis towards the naso-occipital axis, as well as a shift in the horizontal plane towards the naso-occipital axis during pitch impulses. Similar to the data of Aw et al., our patients also show a deviation towards the naso-occipital plane during yaw-axis stimulation and a shift towards the naso-occipital axis during roll axis stimulation. Our findings illustrate that even during small amplitude sinusoidal stimulation large deviations in alignment can occur. We attribute these large misalignments to the increased variability of the torsional component.
In terms of misalignment the three operated patients performed better in the light in comparison to two not operated patients. Gain in operated patients in the light was not significantly different from control subjects, whereas the torsional gain in not operated patients was significantly different from control subjects.
Although this result may seem unexpected because generally horizontal drifts have been reported after UVD lesions, both in animal (Lasker et al. 2000) as in human studies (Cremer et al. 1988; Halmagyi et al. 1990a; Halmagyi et al. 1990b; Tabak et al. 1997; Halmagyi et al. 2003), these differences may be attributed to stimulus conditions.

3D VOR function in non operated versus operated patients

It is generally accepted that the vestibular system has a remarkable plasticity (Angelaki and Hess 1996; Angelaki and Hess 1998; Paige 1991; Quinn et al. 1998; Hirata and Highstein 2002). There are different studies reporting on how the VOR adapts after unilateral inactivation. Paige (Paige 1983b) reported good compensation in monkeys following plugging of the horizontal canals, whereas others have reported permanent impairments following horizontal canal inactivation in monkey (Yakushin et al. 1995) and human (Aw et al. 1996a). Recently, Yakushin et al, (Yakushin et al. 2009) found that in monkey adaptive capabilities for roll VOR are structurally different from pitch and yaw VOR.

Our data indicate that recovery of 3D VOR function in terms of alignment can be qualitatively good in operated patients, whereas in the not operated patients the 3D VOR is impaired even in the light. This relatively better recovery in operated patients may be related to stimulus conditions. In the studies by e.g. Aw and colleagues (Aw et al. 1996a) high acceleration stimuli were used. Because such stimuli drive the canal responses into saturation, they are better suited to reveal permanent impairments. Nevertheless, during daily activities patients may avoid high acceleration stimuli and are more likely to be exposed to the low acceleration sinusoidal stimuli we used. Our low acceleration stimulus resembles more the stimulus conditions employed by Paige (Paige 1983a). The other finding is that all patients had a small but persistent drift in the torsional eye movement. Apparently the torsion component is very prone to damage, which may be related to the relatively poor adaptive capabilities of roll angular VOR (Yakushin et al. 2009).

The better 3D VOR responses found in operated patients are also in agreement with findings from a quality of life prospective study (Godefroy et al. 2007). Patients, who received a radical surgical removal of the Schwannoma, may initially have complaints of dizziness, sometimes leading to emesis. These complaints are generally worse in patients who had a small size tumour removed (Andersson et al. 1997). The general long-term outcome is that subjective complaints of dizziness disappear in operated patients. This suggests that subjective complaints are not related to the amount of existing damage to the vestibular nerve, but that it is the amount of change in vestibular information processing that is responsible for the severity of subjective complaints. It agrees with our findings of the close to normal long-term postoperative 3D VOR gain and alignment in response to small amplitude stimulation. The situation may be different when vestibular stimuli are used that drive the system into saturation.

Our results suggest that long term plasticity in the vestibular system, that involve synaptic and/or neuronal modifications in cerebellum (Goossens et al. 2001; van Alphen and De Zeeuw 2002; Weber et al. 2003; Schmolesky et al. 2005; Faulstich et al. 2006) and brainstem (Lisberger and Miles 1980; Lisberger and Pavelko 1986; Lisberger 1995), at least in humans, can only occur when there is a stable situation. In the case of a tumour that gradually compresses more and more of parts of the vestibular nerve, there is a variable information stream from the vestibular system towards the central vestibular system. This variability in signal transduction may prevent central compensation mechanisms to occur.

Clinical implications
Nowadays surgeons generally decide to operate a patient with a vestibular Schwannoma on the size of the tumour and acoustic function loss. We underline the conclusion by Godefroy and colleagues (Godefroy et al. 2007) that surgeons should not only consider tumour size and hearing loss, but also vestibular function loss in their decision to operate on a vestibular Schwannoma. We have shown that drift and instabilities of the torsional eye movement components are a possible cause for vertigo. Our data also suggest that VOR mediated ocular stability in not operated patients is worse compared to patients who had the tumour surgically removed. Further research is needed to find out if these differences are caused by different demands on neural plasticity.

References

Andersson G, Ekvall L, Kinnefors A, Nyberg G, Rask-Andersen H (1997) Evaluation of quality of life and symptoms after translabyrinthine acoustic neuroma surgery. Am J Otol 18: 421-426

Angelaki DE, Hess BJ (1996) Adaptation of primate vestibuloocular reflex to altered peripheral vestibular inputs. II Spatiotemporal properties of the adapted slow-phase eye velocity. J Neurophysiol 76: 2954-2971

Angelaki DE, Hess BJ (1998) Visually induced adaptation in three-dimensional organization of primate vestibuloocular reflex. J Neurophysiol 79: 791-807

Aw ST, Halmagyi GM, Curthoys IS, Todd MJ, Yavor RA (1994) Unilateral vestibular deafferentation causes permanent impairment of the human vertical vestibulo-ocular reflex in the pitch plane. Exp Brain Res 102: 121-130

Aw ST, Halmagyi GM, Haslwanter T, Curthoys IS, Yavor RA, Todd MJ (1996a) Three-dimensional vector analysis of the human vestibuloocular reflex in response to high-acceleration head rotations. II. responses in subjects with unilateral vestibular loss and selective semicircular canal occlusion. J Neurophysiol 76: 4021-4030

Aw ST, Haslwanter T, Halmagyi GM, Curthoys IS, Yavor RA, Todd MJ (1996b) Three-dimensional vector analysis of the human vestibuloocular reflex in response to high-acceleration head rotations. I. Responses in normal subjects. J Neurophysiol 76: 4009-4020

Aw ST, Todd MJ, McGarvie LA, Migliaccio AA, Halmagyi GM (2003) Effects of unilateral vestibular deafferentation on the linear vestibulo-ocular reflex evoked by impulsive eccentric roll rotation. J Neurophysiol 89: 969-978

Crane BT, Demer JL (1997) Human gaze stabilization during natural activities: translation, rotation, magnification, and target distance effects. J Neurophysiol 78: 2129-2144

Crawford JD, Vilis T (1991) Axes of eye rotation and Listing's law during rotations of the head. J Neurophysiol 65: 407-423

Cremer PD, Henderson CJ, Curthoys IS, Halmagyi GM (1988) Horizontal vestibulo-ocular reflexes in humans with only one horizontal semicircular canal. Adv Otorhinolaryngol 42: 180-184

Curthoys IS, Topple AN, Halmagyi GM (1995) Unilateral vestibular deafferentation (UVD) causes permanent asymmetry in the gain of the yaw VOR to high acceleration head impulses in guinea pigs. Acta Otolaryngol Suppl 520 Pt 1: 59-61

Della Santina CC, Potyagaylo V, Migliaccio AA, Minor LB, Carey JP (2005) Orientation of human semicircular canals measured by three-dimensional multiplanar CT reconstruction. J Assoc Res Otolaryngol 6: 191-206

Faulstich M, van Alphen AM, Luo C, du Lac S, De Zeeuw CI (2006) Oculomotor plasticity during vestibular compensation does not depend on cerebellar LTD. J Neurophysiol 96: 1187-1195

Ferman L, Collewijn H, Jansen TC, Van den Berg AV (1987) Human gaze stability in the horizontal, vertical and torsional direction during voluntary head movements, evaluated with a three-dimensional scleral induction coil technique. Vision Res 27: 811-828

Godefroy WP, Hastan D, van der Mey AG (2007) Translabyrinthine surgery for disabling vertigo in vestibular schwannoma patients. Clin Otolaryngol 32: 167-172

Goossens J, Daniel H, Rancillac A, van der Steen J, Oberdick J, Crepel F, De Zeeuw CI, Frens MA (2001) Expression of protein kinase C inhibitor blocks cerebellar long-term depression without affecting Purkinje cell excitability in alert mice. J Neurosci 21: 5813-5823

Grossman GE, Leigh RJ, Abel LA, Lanska DJ, Thurston SE (1988) Frequency and velocity of rotational head perturbations during locomotion. Exp Brain Res 70: 470-476

Halmagyi GM, Black RA, Thurtell MJ, Curthoys IS (2003) The human horizontal vestibulo-ocular reflex in response to active and passive head impulses after unilateral vestibular deafferentation. Ann N Y Acad Sci 1004: 325-336

Halmagyi GM, Curthoys IS, Cremer PD, Henderson CJ, Staples M (1990a) Head impulses after unilateral vestibular deafferentation validate Ewald's second law. J Vestib Res 1: 187-197

Halmagyi GM, Curthoys IS, Cremer PD, Henderson CJ, Todd MJ, Staples MJ, D'Cruz DM (1990b) The human horizontal vestibulo-ocular reflex in response to high-acceleration stimulation before and after unilateral vestibular neurectomy. Exp Brain Res 81: 479-490

Haslwanter T (1995) Mathematics of three-dimensional eye rotations. Vision Res 35: 1727-1739

Haslwanter T, Moore ST (1995) A theoretical analysis of three-dimensional eye position measurement using polar cross-correlation. IEEE Trans Biomed Eng 42: 1053-1061

Haustein W (1989) Considerations on Listing's Law and the primary position by means of a matrix description of eye position control. Biol Cybern 60: 411-420

Hirata Y, Highstein SM (2002) Plasticity of the vertical VOR: a system identification approach to localizing the adaptive sites. Ann N Y Acad Sci 978: 480-495

Lasker DM, Hullar TE, Minor LB (2000) Horizontal vestibuloocular reflex evoked by high-acceleration rotations in the squirrel monkey. III. Responses after labyrinthectomy. J Neurophysiol 83: 2482-2496

Lisberger SG (1995) Learning. A mechanism of learning found? Curr Biol 5: 221-224

Lisberger SG, Miles FA (1980) Role of primate medial vestibular nucleus in long-term adaptive plasticity of vestibuloocular reflex. J Neurophysiol 43: 1725-1745

Lisberger SG, Pavelko TA (1986) Vestibular signals carried by pathways subserving plasticity of the vestibulo-ocular reflex in monkeys. J Neurosci 6: 346-354

Paige GD (1983a) Vestibuloocular reflex and its interactions with visual following mechanisms in the squirrel monkey. I. Response characteristics in normal animals. J Neurophysiol 49: 134-151

Paige GD (1983b) Vestibuloocular reflex and its interactions with visual following mechanisms in the squirrel monkey. II. Response characteristics and plasticity following unilateral inactivation of horizontal canal. J Neurophysiol 49: 152-168

Paige GD (1991) The aging vestibulo-ocular reflex (VOR) and adaptive plasticity. Acta Otolaryngol Suppl 481: 297-300

Quinn KJ, Didier AJ, Baker JF, Peterson BW (1998) Modeling learning in brain stem and cerebellar sites responsible for VOR plasticity. Brain Res Bull 46: 333-346

Schmolesky MT, De Zeeuw CI, Hansel C (2005) Climbing fiber synaptic plasticity and modifications in Purkinje cell excitability. Prog Brain Res 148: 81-94

Tabak S, Collewijn H, Boumans LJ, van der Steen J (1997) Gain and delay of human vestibulo-ocular reflexes to oscillation and steps of the head by a reactive torque helmet. II. Vestibular-deficient subjects. Acta Otolaryngol 117: 796-809

van Alphen AM, De Zeeuw CI (2002) Cerebellar LTD facilitates but is not essential for long-term adaptation of the vestibulo-ocular reflex. Eur J Neurosci 16: 486-490

Weber JT, De Zeeuw CI, Linden DJ, Hansel C (2003) Long-term depression of climbing fiber-evoked calcium transients in Purkinje cell dendrites. Proc Natl Acad Sci U S A 100: 2878-2883

Yakushin S, Dai M, Suzuki J, Raphan T, Cohen B (1995) Semicircular canal contributions to the three-dimensional vestibuloocular reflex: a model-based approach. J Neurophysiol 74: 2722-2738

Yakushin SB, Xiang Y, Cohen B, Raphan T (2009) Dependence of the roll angular vestibuloocular reflex (aVOR) on gravity. J Neurophysiol 102: 2616-2626

Chapter 5

Superior canal dehiscence syndrome

Goumans J, Boumans LJJM, van der Steen J, Feenstra L

Ned Tijdschr Geneeskd, juni 2005 11;149(24):1320-5
(translated from Dutch by permission of the NTvG)

Abstract

In 1998 the superior canal dehiscence syndrome (SCDS) was described for the first time. Dehiscence of the bone overlying the superior semicircular canal creates a 'third mobile window' inducing symptoms of dizziness and oscillopsia when a sound and/or pressure stimulus is given to the involved ear. Characteristic for this syndrome are eye movements with a vertical-torsion direction caused by sound stimuli, pressure changes of the external ear canal and/or the Valsalva manoeuvre. The abnormality is demonstrated with computed tomography scans (CT scan).

Introduction

In 1998 a new syndrome has been described by Minor et al., which they entitled as superior canal dehiscence syndrome (SCDS) [1]. SCDS is caused by a partial or complete absence of bone overlying the superior semicircular canal of the labyrinth (Figure 1 and 2). This results in complaints of dizziness and/or oscillopsia, that occur in reaction to a sound stimulus (Tullio phenomenon) or to pressure changes applied to the external ear canal (Hennebert's sign) and/or Valsalva manoeuvre.

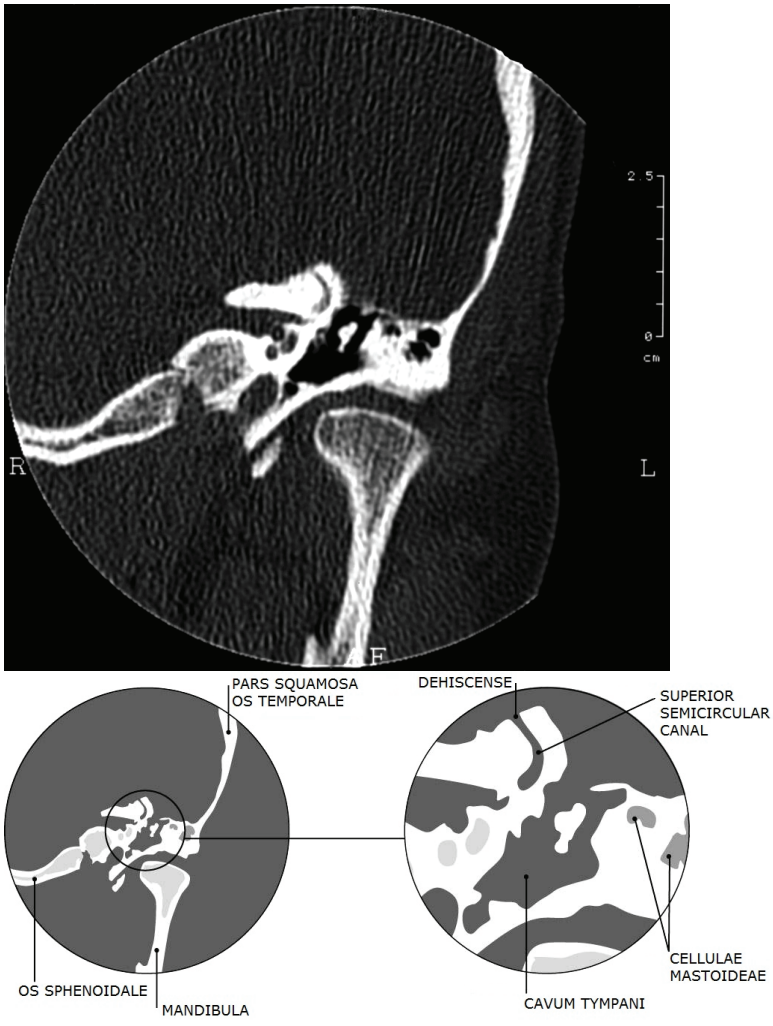

Figure 1. Computed tomography scan (CT scan) of a patient with a dehiscence of bone overlying the superior semicircular canal of the left ear.

Vertigo is the illusion that the environment moves with respect to the individual or vice versa. It generally consists of a sensation of rotation in any direction. Another possibility is a feeling of horizontal or vertical linear displacement. Oscillopsia is the optic illusion that stationary objects seem to move up or down and/or forwards or backwards during walking or with head movements. The pressure sensitivity of the labyrinth can be tested in a number of ways. The Valsalva manoeuvre consists of building intrathoracal pressure with closed epiglottis. This leads to an increase of intracranial pressure, which is propagated to the endolymph via the endolymphatic sac and the perilymph via the cochlear duct. Valsalva's test consists of blowing air through one nostril with a Politzer balloon whereas the pressure of a fingertip closes the other nostril. The air pressure is propagated through the Eustachian tube into the middle ear with displacement of the tympanic membrane outwardly. Pressure on the tragus (fistula symptom) builds up a pressure in the middle ear by pushing the drum inward. During walking the head moves up and down. This may lead to changes in the pressure of the brain on the base of the skull. These pressure changes are propagated through the dehiscence and into the labyrinth (Figure 3). Also the blood flow within the labyrinth can cause intra-labyrinthine pressure changes, resulting in rhythmic eye movements.
The rare Tullio phenomenon consists of a feeling of dizziness or dysbalance after a sound stimulus possibly in combination with abnormal eye- and/or head movements. In the early twenties of the last century this phenomenon has been researched extensively by Tullio and in the Netherlands by Huizinga and co-workers [2,3]. Originally the Tullio phenomenon was demonstrated with pigeons, after fenestration in the plane of the stimulated canal.
The Hennebert sign, described in 1911 was found in patients with hereditary syphilis of the labyrinth. It consists of a sensation of dizziness and nystagmus after pressure changes in the external canal wall with a pneumatic otoscope (fistula symptom) [4].

Etiology

In the literature different hypotheses exist as to the cause of SCDS, such as head – or barotrauma, or postnatal development impairment of the bony labyrinth [1,5,6,7,8]. Carey and co-workers histologically examined one thousand temporal bones [7]. They found in approximately 2% of these a dehiscence or an extreme thin layer of covering bone of the superior semicircular canal. Sometimes a dehiscence is found bilaterally. Children only develop the overlying bone across the superior semicircular canal when over three years of age. These findings plead for postnatal developmental impairment.

A computed tomography scan (CT scan) study of the temporal bone in patients with SCDS supports the hypothesis of a postnatal development impairment [8]. The CT scans show that patients with one-sided SCDS have a significant thinner layer of bone across the semicircular canal at the contralateral ear compared to a control group. In addition, in the control group a significant correlation is found between the amount of bone overlying the left and right superior semicircular canal. Because the syndrome

generally reveals itself at an adult age it is plausible that a head trauma or a sudden change in intracranial pressure precedes the complaints. [7].

Pathophysiology

The bony part of the labyrinth has normally two windows: the oval and round window. Changes in pressure at one window are conducted through the convolutions of the cochlea but not into the vestibular part of the labyrinth.

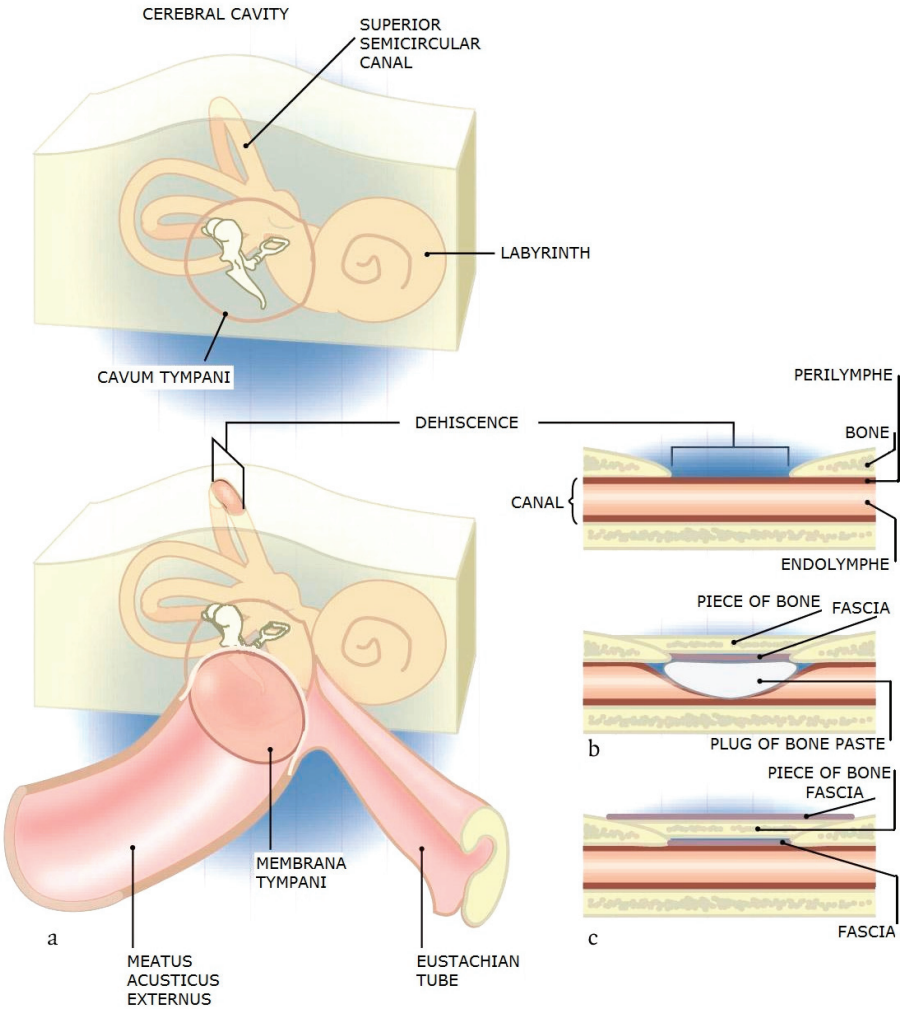

Figure 2. A) Schematic operative correction of a dehiscence of the superior semicircular canal of the right ear; B) plug and compression of the membranous canal of the dehiscence with bone paste; C) reconstruction of the bony wall of the superior semicircular canal with fascia and bone paste.

Lack of overlying bone of the superior canal resulting in a 'third window' in the bony labyrinth leads to pressure changes within the vestibular part of the labyrinth [1,2,4,5,7,9,10]. The hypothesis in literature is that excitation of the superior canal with stimuli like Valsalva's test, resulting in bulging of the membranous labyrinth into the dura mater, lead to conducted endolymphatic ampullofugal deflection of the cupula. On the other hand, stimuli as compression of the jugular vein, Valsalva's manoeuvre or a negative pressure change in the external ear canal lead to a positive pressure gradient at the dehiscence that induces an ampullapetal deflection of the cupula. These pressure changes lead to vertical-torsion eye movements.

Hirvonen et al. studied in nine adult chinchillas the mechanisms of pressure sensitivity of the labyrinth after a three mm fenestration of the overlying bone of the superior canal [11]. Pressure changes causes major activity in the afferents of the superior canal with an endolymph flow according to the above described hypothesis. After surgical repair of the fenestration the pressure sensitivity of the afferents of the superior canal decreased while the physiological detection of rotationally accelerations was normal.

Symptoms and diagnosis

Patients with SCDS complain about vertigo and/or oscillopsia induced by daily sounds such as the ring of a doorbell or traffic noise [12] and/or pressure changes during coughing, sneezing or lifting heavy objects. Squeezing the ear canal can arouse the same feeling of dizziness. Moreover a large portion of the patients complain about a constant feeling of dysbalance and an uncertain feeling with a variety of movements. This is for most of the patients the reason to seek help. Their sensitivity for sound and/or pressure changes usually is admitted only after explicit questioning [1,5]. Some patients complain about hyperacusis; they hear their own voice or heartbeat seemingly reinforced [12,13]. Also a pulse synchronic tinnitus has been described with SCDS patients [6].

With routine vestibular laboratory tests such as electronystagmography the nystagmus preference and the caloric excitability are tested. Patients with SCDS generally do not demonstrate any anomaly [5,6]. In response to sound and/or pressure stimuli in most of the cases a rotational-vertical eye movement occurs that corresponds with the plane of the concerning superior canal [14,15]. This can be easily observed with the use of Frenzel glasses and can be registered with video registration of the eye movements. As the size of the dehiscence is larger than 5 mm, the observation of these specific eye movements decreases or is sometimes confused by eye movements in other directions [9,14].

The threshold for sound induced vestibular evoked myogenic potentials (VEMP) with SCDS patients is lower than normal and their response reaction are enlarged [12,16]. VEMP is a relatively new investigation method for the vestibular system. An ipsilateral relaxation of a tonic contracted sternocleidomastoid muscle is induced by a vestibular controlled reflex after loud clicks (short sound) or a gentle regular tap with a reflex hammer on the mastoid bone.

The tuning fork test of Weber (512 Hz) is usually lateralized to the ear with the dehiscence. Audiometry shows a bass conductive hearing loss with a normal tympanogram and a normal stapedius reflex [6]. This seemingly conductive hearing loss most probably is caused by the loss of acoustic energy within the inner ear [9]. Middle ear inspection of patients with SCDS does not demonstrate any defects and a normal functioning ossicular chain.

With a conventional CT scan of the temporal bone a dehiscence of the overlying bony part of the superior canal can be made visible with coupe slices of 1.0 or 1.5 mm cross-section. However, these have sufficient sensitivity but a relative low specificity to reliably determine the dehiscence of the overlying bony part. To discern a dehiscence from a tiny layer of bone, more reliably coupe slices of 0.5mm scan combined with projections in the plane of the superior canal are preferable. [17].

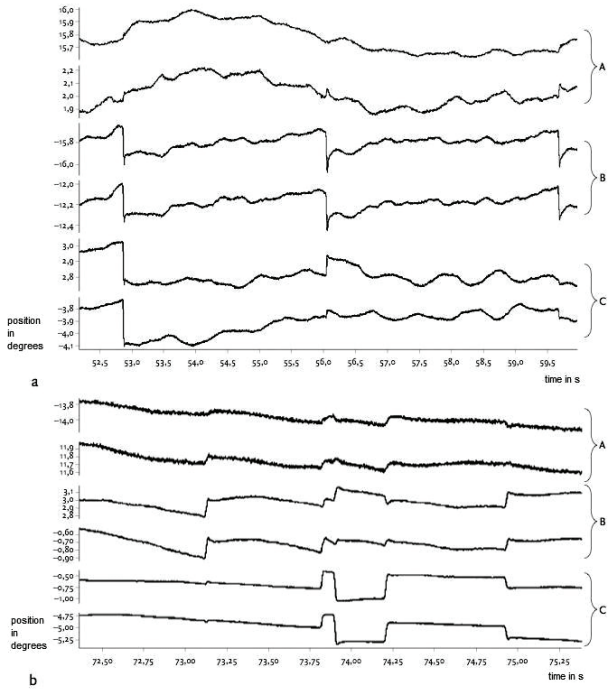

Figure 3. Registration of the eye movements with nystagmography during fixation at a light source at 2 meters distance by (a) a patient with bilateral 'superior canal dehiscence syndrome"; and (b) a control subject under the same conditions. In both panels are the registrations from upward to downwards (A) torsion, (B) vertical and (C) horizontal eye position. Each time the registration of the right comes first, the left eye second. A positive displacement occurs with torsion (A) by ex-cyclorotation of the right eye and in-cyclorotation of the left eye seen from the patient's standpoint. The significance is that the (B) is a vertical an upwards movement and (C) a horizontal movement to the right. The patient has oscillations during fixation corresponding with his own pulse (a), which is not the case with the control subject.

Therapy

Most of the patients with SCDS are satisfied with an explanation of the cause of their complaints and advice how to avoid certain situations that provoke vertigo and/or oscillopsia. For complaints due to increased pressure the placement of a ventilation tube into the drum may be useful [13]. Other surgical treatments do exist. These consist of either eliminating the function of the superior canal by plugging it with bone paste, or to cover the dehiscence with fascia and bone in order to preserve the function of the semicircular canal and the cochlea [5] (Figure 2). The superior vertical canal should be reached using the middle fossa approach.

Conclusion

Superior canal dehiscence is a relatively young entity. Expertise will increase when more patients are diagnosed and treated. The complaints of patients asking for help are a chronic feeling of disability and uncertainty when walking. Unfortunately relative unfamiliarity with this syndrome takes to many patients to a variety of specialists. The dehiscence may be corrected surgically by sealing the dehiscence with fascia and/or bone paste.

Literature

1. Minor LB, Solomon D, Zinreich JS, Zee DS. Sound- and/or pressure-induced vertigo due to bone dehiscence of the superior semicircular canal. Arch Otolaryngol head neck surg. 1998; 124; 249-258
2. Tullio P. Das Ohr und die Enstehung der Sprache und Schrift. Berlin: Urban & Schwarzenberg. 1929
3. Huizinga E. On the sound reaction of Tullio. Acta Otolaryngol (Stokh.). 1935; 22; 359-369
4. Hennebert C. A new syndrome in hereditary syphilis of the labyrinth. Press Med Belg Brux. 1911; 63; 467
5. Minor LB. Superior canal dehiscence syndrome. Am J Otol. 2000; 21; 9-19
6. Brantberg K, Bergenius J, Mendel L, Witt H, Tribukait A, Ygge J. Symptoms, findings and treatment in patients with dehiscence of the superior semicircular canal. Acta Otolaryngol. 2001; 121; 68-75
7. Carey JP, Minor LB, Nager GT. Dehiscence or thinning of bone overlying the superior semicircular canal in a temporal bone survey. Arch Otolaryngol Head Neck Surg. 2000; 126; 137-147
8. Hirvonen TP, Weg N, Zinreich SJ, Minor LB. High-resolution CT findings suggest a developmental abnormality underlying superior canal dehiscence syndrome. Acta Otolaryngol. 2003; 1 23; 477-481
9. Minor LB, Carey JP, Cremer PD, Lustig LR, Streubel S-O. Dehiscence of bone overlying the superior canal as a cause of apparent conductive hearing loss. Otology & Neurotology. 2003; 24; 270-278
10. Rosowski JJ, Songer JE, Nakajima HD, Brinsko KM, Merchant SN. Clinical, experimental and theoretical investigations of the effect of superior semicircular canal dehiscence on hearing mechanisms. Otology & Neurotology. 2004;25: 323-332
11. Hirvonen TP, Carey JP, Liang CJ, Minor LB. Superior canal dehiscence; mechanisms of pressure sensitivity in a chinchilla model. Arch Otolaryngol Head Neck Surg. 2001; 127; 1331-1336
12. Watson SR, Halmagyi GM, Colebatch JG. Vestibular hypersensitivity to sound (Tullio phenomenon): structural and functional assessment. Neurology. 2000; 54(3); 722-737
13. Minor LB, Cremer PD, Carey JP, Della Santina CC, Streubel S-O, Weg N. Symptoms and signs in superior canal dehiscence syndrome. Ann N Y Acad Sci. 2001;942: 259-273
14. Cremer PD, Minor LB, Carey JP, Della Santina CC. Eye movements in patients with superior canal dehiscence syndrome align with abnormal canal. Neurology. 2000; 55; 1833-1841
15. Ostrowski VB, Byskosh A, Hain TC. Tullio phenomenon with dehiscence of the superior semicircular canal. Otology & Neurotology. 2001; 22; 61-65
16. Brantberg K, Bergenius J, Tribukait A. Vestibular-evoked myogenic potentials in patients with dehiscence of the superior semicircular canal. Acta Otolaryngol (Stockh). 1999; 119; 633-640
17. Belden CJ, Weg N, Minor LB, Zinreich SJ. CT evaluation of bone dehiscence of the superior semicircular canal as a cause of sound- and/or pressure-induced vertigo. Radiology. 2003; 226; 337-347

Chapter 6

Effects of superior canal dehiscence syndrome on three-dimensional ocular stability in humans

Goumans J, Feenstra L, van der Steen J

Abstract

Superior canal dehiscence syndrome (SCDS) is a syndrome caused by an opening in the bone overlying the superior semicircular canal. Although it is known that SCDS may affect vestibular function, there are few reports on SCDS in relation to three-dimensional (3D) ocular stabilisation. Therefore, we investigated the effects of dehiscence of the superior canal on ocular stabilisation in 3D in three patients with a unilateral and in one patient with bilateral dehiscence. 3D eye movements were recorded using the scleral search coil technique. We determined the quality of ocular stabilisation in three dimensions in response to sinusoidal vestibular stimulation mediated by the vestibulo-ocular reflex (VOR). In addition, we determined 3D ocular stabilisation during fixation in response to pressure changes in the external meatus (Hennebert sign) and in response to high intensity sound stimuli (Tullio phenonemon).
The gain and misalignment of the VOR during sinusoidal stimulation in the light and in darkness did not differ from healthy control subjects.
In two patients eye movements during fixation oscillated at the same rate as their heartbeat. Hennebert sign was positive in all four patients, but the ocular responses varied: two patients developed a nystagmus, whereas the other two patients had only oscillatory eye movement responses.
The combination of normal 3D VOR during sinusoidal stimulation with ocular instabilities in response to pressure changes in the external meatus or loud sounds suggests that impairments in 3D ocular stabilisation only occur when fluid dynamics of the semicircular canals are disturbed. This finding supports the idea that the dehiscence acts as a third release window.

Introduction

As described in Chapter 5 superior canal dehiscence syndrome (SCDS) is caused by a dehiscence of the petrosal bone overlying one or both the superior semicircular canals (Minor et al. 1998). The majority of patients experience a chronic sensation of disequilibrium and imbalance (Banerjee et al. 2005; Minor 2000). A small fraction of patients complains about hearing their own body sounds at the affected side (Minor et al. 2001; Watson et al. 2000) or having unilateral hearing loss (Minor 2005). A pulse-synchronous tinnitus has also been related to SCDS (Brantberg et al. 2001).
Thus, signs and symptoms in these patients can be divided into auditory and vestibular manifestations. The auditory manifestations are hyperacusis for bone-conducted sounds, autophony, lateralization of the Weber tuning fork test to the affected ear and conductive hearing loss in the low frequency range. Vestibular manifestations are dizziness or oscillopsia combined with eye movement responses in reaction to sound stimuli or changes in the middle ear or intracranial pressure. The most widely accepted theory for the cause of these auditory and vestibular manifestations is that the dehiscence provides a third mobile window in the labyrinth making the vestibular part of the labyrinth more compliant for pressure changes and fluid movements (Carey et al. 2004; Carey et al. 2000; Hirvonen et al. 2001; Rosowski et al. 2004; Songer and Rosowski 2005). Because this third window is located in the superior semicircular canal, this canal is particularly very sensitive for sound stimuli or pressure changes. It has been claimed that this results in abnormal eye movement responses in the plane of that canal (Cremer et al. 2000).
Many patients with SCDS complain about chronic disequilibrium and oscillopsia. One possibility is that oscillopsia and disequilibrium in patients with SCDS are the consequence of changed dynamics of oculomotor compensatory mechanisms during vestibular stimulation: e.g. a lower gain of the vestibulo-ocular reflex (VOR) in the plane of the affected canal. Indeed, a decreased gain of the VOR has been described in a patient with two-sided SCDS (Deutschlander et al. 2004). Therefore, we investigated if the gain and misalignment of the VOR is impaired in patients with SCDS. We thus determined the rotational VOR gain and misalignment in response to sinusoidal stimulation.
A number of investigators has shown that during fixation the eyes of SCDS patients are not stable and also that oscillations can occur following pressure changes or sound stimuli in the affected ear (Banerjee et al. 2005; Brantberg et al. 2001; Cremer et al. 2000; Minor 2005; Minor et al. 1998; Ostrowski et al. 2001; Tilikete et al. 2004). Fixation instabilities are the result of pulsation of the cerebro-spinal fluid and/or blood circulatory system directly impinging on the fenestrated superior canal. A correlation has been found between heartbeat rate and the occurrence of rotatory nystagmus (Younge et al. 2003) or spontaneous vertical oscillations (Tilikete et al. 2004). To investigate the effect of heartbeat on three-dimensional (3D) ocular stabilisation, we measured 3D eye movements at rest during fixation in four patients with SCDS. Pulse rate was monitored with an oxymeter and sampled synchronously with the eye movements.

To investigate the effect of pressure induced changes in ocular stability we measured 3D eye movements in response to active pressure changes in the middle ear cavity (Hennebert sign or Tullio phenomenon).

Methods

Subjects

We tested four adult patients, diagnosed with dehiscence of bone overlying the superior semicircular canal. Three patients came from Erasmus University Medical Centre and one patient came from Universitäts Spital Zürich. The mean age of the patients was 41 years (range 25 – 54). In addition 4 control subjects participated in this study. All gave their informed consent. Experimental procedures were approved by the Medical Ethics Committee of the Erasmus University Medical Centre and adhered to the Declaration of Helsinki for research involving human subjects.

Patient 1, male, 54 year, has a 2 mm bilateral dehiscence of superior semicircular canals. He presented with right ear deafness since early childhood of unknown origin and with a left ear conductive hearing loss of 25 dB between 250 and 1000 Hz. Attacks of dizziness with nausea and vomiting started seven years ago. At present he complains of a chronic feeling of dizziness and unsteadiness. In addition he complains about hearing his heartbeat and eye blinking extremely loud in the left ear. He also perceives a rotation of the environment at the same rhythm as his heartbeat.
Patient 2, female, 48 year, has a left-sided dehiscence of the superior semicircular canal. She has a small conductive hearing loss in the left ear of 15 dB between 250 and 1000 Hz. For three years she complains about hearing echo sounds in her left ear combined with short (< 1 minute) attacks of dizziness. Pressure to the left ear canal gives her a sensation of dizziness and an up and down motion of the environment.
Patient 3, male, 36 year, has a right-sided dehiscence of the superior semicircular canal of 4-5 mm (Figure 1). He has small conductive hearing loss on the right side and normal hearing on the left. Since four years pressure changes in the right ear cause a sensation of dizziness and instability of the environment. Moreover, he hears his own voice and heartbeat loud in the affected ear.
Patient 4, female, 25 year, has a left-sided dehiscence of the superior semicircular canal. Since one year she complains about hearing loss on the left side and attacks of vertigo combined with nausea. She also experiences a feeling of fullness in the left ear and some sounds are very obtrusive. Audiometric tests show a normal hearing in the right ear and perceptive hearing loss in the left ear of 32 dB between 500 and 8000 Hz.

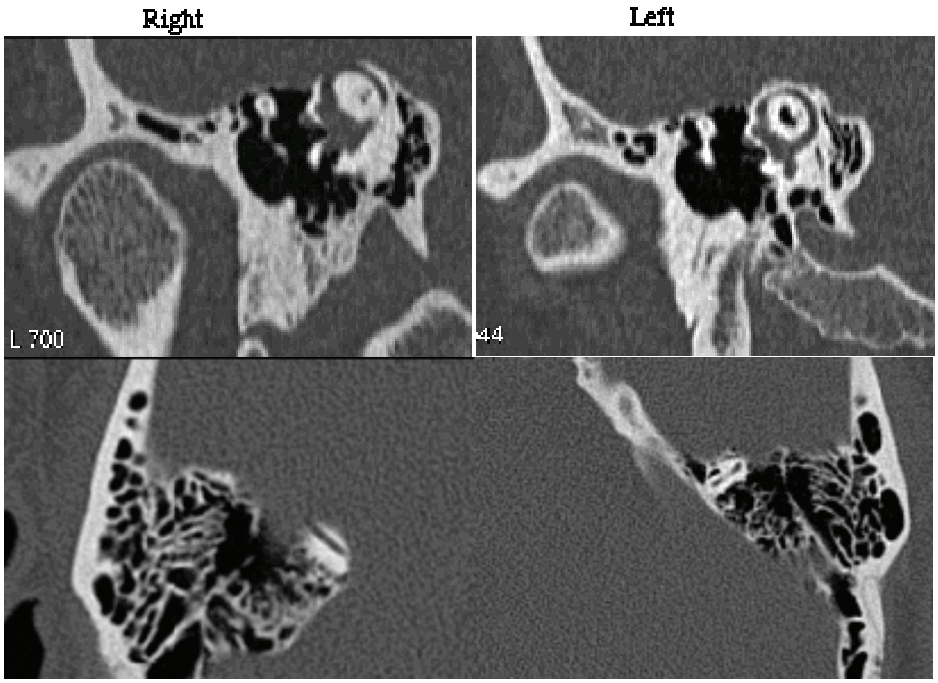

Figure 1. Computed tomography scan (CT scan) reconstruction in the plane of the superior semicircular canal of patient 3 with right-sided unilateral SCDS. Top panels show a reconstruction in the superior canal plane, bottom panels show the same canal in an axial coupe. In the right ear (left panels) a dehiscence of bone of 4-5 mm can be seen. The left superior canal of the same patient, which is intact, is shown in the right panels.

The eye movement recordings, the vestibular stimulation, the experimental set-up and the data analysis were performed as described in Chapter 3 (Goumans et al. accepted January 2010).

Results

Ocular stabilisation during 3D vestibular stimulation

Sinusoidal vestibular stimulation about horizontal axes resulted in compensatory eye movements with the usual quantitative differences in gain for the horizontal, vertical and torsional eye movement components. The relative contribution of each component to the overall gain depended on the orientation of the stimulus axis. In all four patients the gain and misalignment in light and darkness was not significantly different from the data of control subjects as described in Chapter 3 ($P > 0.05$). Figure 2 shows gain and misalignment of the patient with bilateral SCDS.

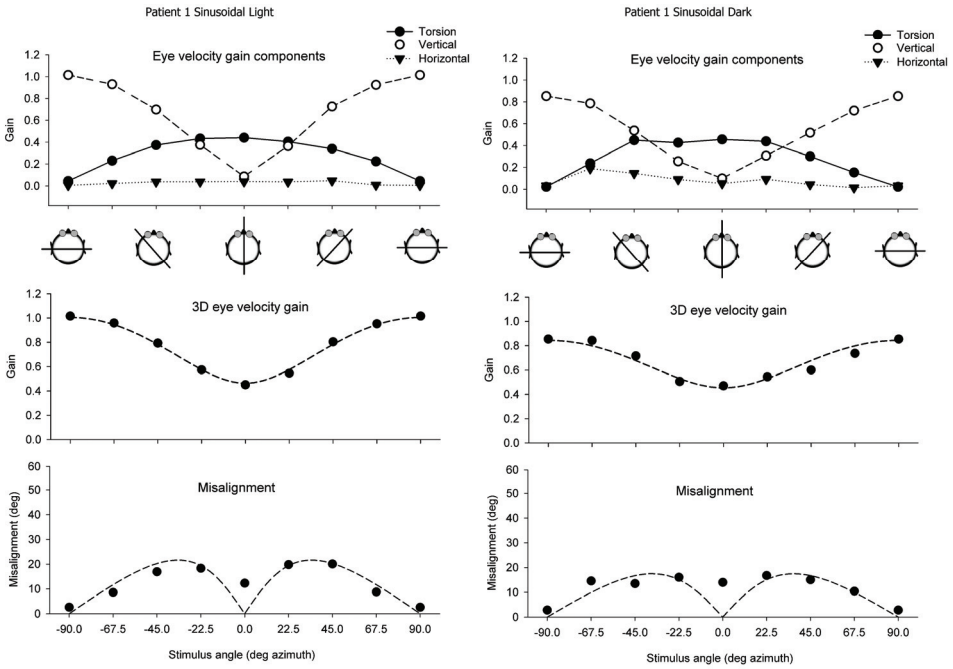

Figure 2. Results of horizontal axis sinusoidal stimulation for patient 1 in the light (left panel) and in the dark (right panel). Top panel: gain of the horizontal, vertical and torsion eye velocity components. Centre panel: 3D eye velocity at each tested stimulus axis orientation. The dashed line represents the vector eye velocity gain response predicted from the vertical and torsion components. Lower panel: misalignment of the response axis with respect to the stimulus axis. The dashed line in the lower panel represents the predicted misalignment calculated from the vector sum of only vertical and torsion eye velocity components in response to pure pitch and pure roll stimulation, respectively.

Ocular stabilisation during fixation

Heartbeat

Two patients complained about hearing their own heartbeat extremely loud in the affected ear (patient 1 and 3). They also observed that the environment was wobbling at the same rate as their own heartbeat. To quantify the relation between hearing the heartbeat in the affected ear and the eye movement responses, the heartbeat was measured in all patients and also in one control subject with an oxymeter attached to the index finger.
In the two patients who complained about hearing the heartbeat (patient 1 and 3) we indeed found that there was an oscillatory eye movement response at the same rate as their heartbeat (Figure 3). Mainly vertical oscillatory eye movements occurred with a rate of 96 beats per minute for patient 1 and with a rate of 84 beats per minute for patient 3. We also observed small horizontal and torsional eye movement components. Note that the horizontal oscillatory movements of the right and left eye were in opposite direction (vergence). This was in contrast to the other two patients (patient 2 and 4)

and the control subject who did not have eye movement responses correlated with heartbeat rate.

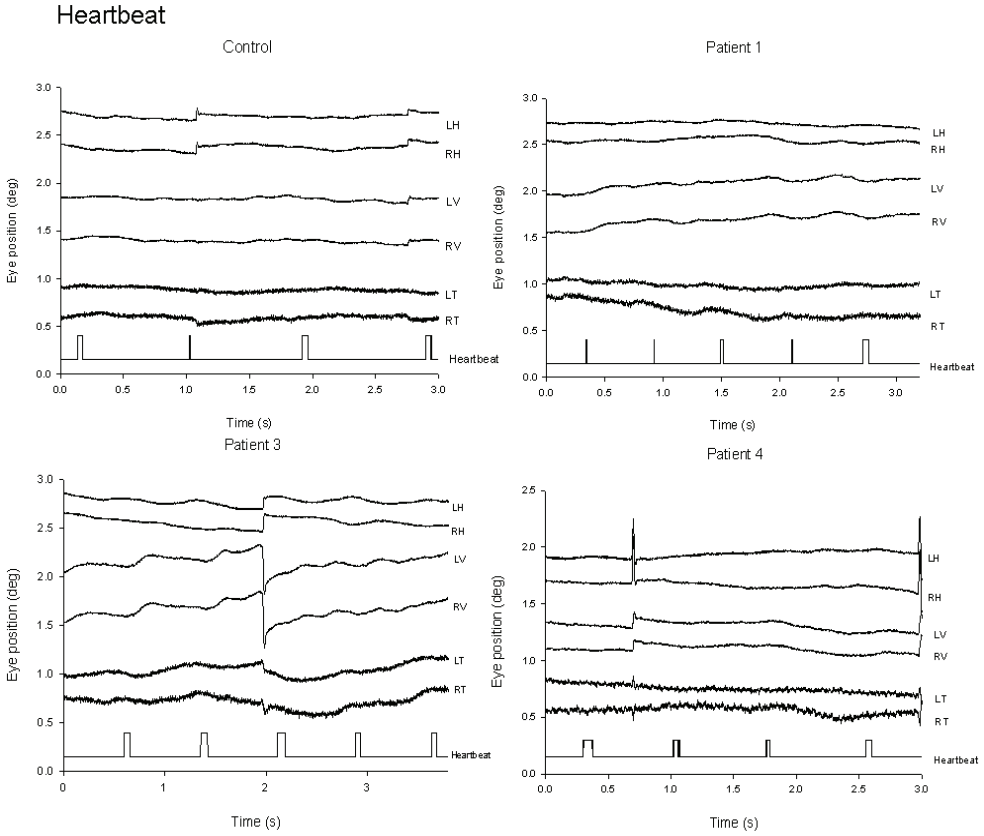

Figure 3. Effect of heartbeat on 3D eye movements. In the control subject (upper left panel) and patient 4 (lower right panel) normal eye responses are shown during fixation of the eyes. In patient 1 (upper right panel) and patient 3 (lower left panel) 3D oscillatory eye responses are shown. Note the vergence movements for horizontal eye responses. Eye movement components: LH = left horizontal, RH = right horizontal, LV = left vertical, RV = right vertical, LT = left torsional, RT = right torsional and Heartbeat = oximeter sign, digitised with threshold.

Hennebert sign

Two patients (2 and 3) complained about vertigo during pressure changes in the external ear canal. When they put their finger in the ear canal dizziness appeared in combination with wobbling of the visual world. In order to quantify the effect of pressure changes in the ear canal and eye movement responses, we tested all patients for the Hennebert sign in both ears. We found eye responses in reaction to pressure changes in the external ear (Hennebert sign) in all four patients, but the characteristics of the eye responses varied per patient (see Figure 4). Remarkably, in two patients (1 and 2) vertical-torsional oscillatory eye movement responses occurred. This was in contrast to patients 3 and 4: where a nystagmus with horizontal,

vertical and torsional components in reaction to the pressure change occurred. Note that the vertical eye movement component was downwards for patient 3 (right-sided dehiscence) and upwards for patient 4 (left sided dehiscence). Two patients (3 and 4), with one-sided dehiscence, showed also eye responses after pressure changes in the non-affected ear, but the amplitude of the eye movement responses were smaller. The patient with bilateral dehiscence (1) showed oscillatory eye movements after pressure stimulation in both ears.

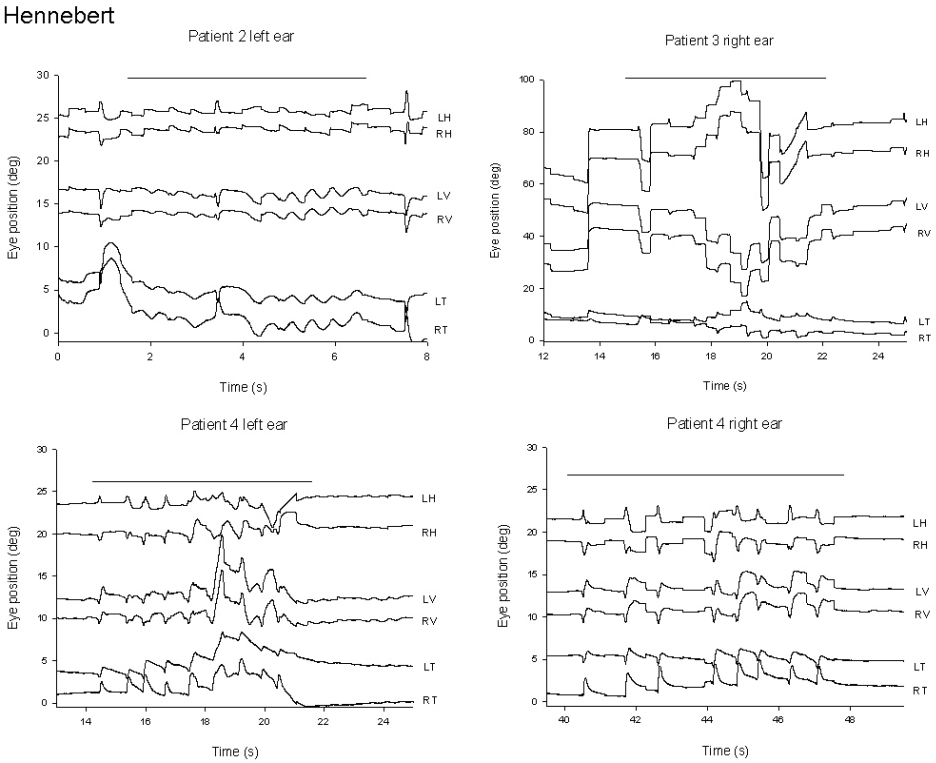

Figure 4. Effect of pressure change in the external ear canal (Hennebert sign) on 3D eye movements. The horizontal solid bar illustrates the period that the finger was in the ear canal. Patient 2 (upper left panel) had vertical-torsional oscillated eye movement responses. Patient 3 (upper right panel) had 3D nystagmus-like eye responses. Patient 4 (lower left and right panel) had nystagmus as well. Note that in both ears the Hennebert sign was positive but with greater responses in the affected ear (left ear). Eye movement components: LH = left horizontal, RH = right horizontal, LV = left vertical, RV = right vertical, LT = left torsional, RT = right torsional.

Tullio phenomenon

The Tullio phenomenon (for description see Chapter 5) was tested in patient 1, 2 and 3. A tone with a frequency of 600 Hz was presented to both ears in succession. In Figure 5 the 3D eye movement responses after stimulation of the right ear for patient 3 are shown. A nystagmus occurred with an upward vertical eye movement component and a clockwise torsional component. It is interesting to note that after cessation of the stimulus the individual torsional

eye responses rotated in the opposite direction. Furthermore, we observed the Tullio phenomenon also in patient 1.

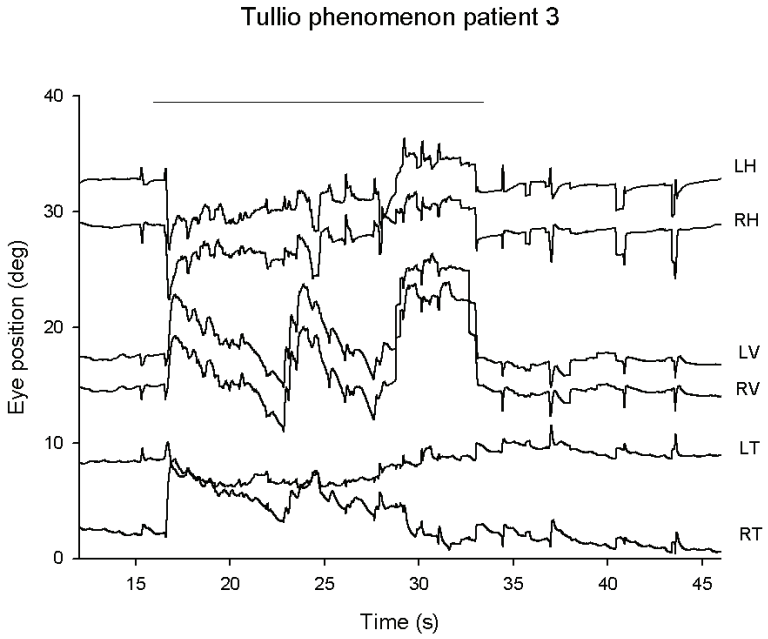

Figure 5. 3D eye movement responses for patient 3 in reaction to a tone of 600 Hz (Tullio phenomenon). The horizontal bar illustrates the time duration of the tone burst. Eye movement components: LH = left horizontal, RH = right horizontal, LV = left vertical, RV = right vertical, LT = left torsional, RT = right torsional.

Discussion

The first goal was to assess the effects of a superior canal dehiscence on 3D vestibular function by measuring 3D VOR.
The second goal was to quantify 3D ocular stability during fixation in rest and the variability of responses in 3D eye movements after active pressure changes in the middle ear cavity (Hennebert sign or Tullio phenomenon).

Ocular stability during 3D vestibular stimulation
Sinusoidal vestibular stimulation did not yield differences in gain and misalignment between control subjects and patients with SCDS, both in light and darkness.
The reason for this may be that during small amplitude sinusoidal stimulations no large changes in acceleration occur that could cause turbulence of the endolymph. When the inner and outer membrane of the semicircular canals are intact, 3D VOR is expected to be normal. Our data suggest that this is the case in all four SCDS patients.

Fixation, Hennebert sign and Tullio phenomenon
In Chapter 5 a review of the superior canal dehiscence syndrome is given as well as specific symptoms and signs experienced by patients are explained. Our findings demonstrate that the subjective complaints of visual instability in patients with SCDS during fixation have a direct measurable cause. In 2 out 4 patients heartbeat was detectable in the eye movement traces. This is most likely due to the heart rate pulsation of the cerebro-spinal fluid that causes an endolymph flow in the superior semicircular canal (Goumans et al. 2005). Because the endolymph of all semicircular canals form a closed system, eye movements are not restricted to the plane of the affected canal as has been claimed before (Cremer et al. 2000; Ostrowski et al. 2001). Hennebert sign was found in all patients, although only two patients (2 and 3) presented with this specific complaint during daily activities. We also found a positive, although weaker response in the not affected ear in two patients (3 and 4) who were diagnosed with a one-sided dehiscence of the superior canal. A possible explanation for this result may lay in the knowledge that in 1.4% of the temporal bone specimens the bone overlying the superior semicircular canal is extremely thin, which suggested a developmental anomaly (Carey et al. 2000). Thus even if there is no truly objective dehiscence an extremely thin part of bone may induce some disturbance in eye movements without the specific clinical symptoms for SCDS.
In contrast with the Hennebert sign, during sound stimulation the Tullio phenomenon was not observed in all patients. In patients 1 and 2 who also complained of vertigo due to specific sounds, the Tullio phenomenon was observed and objectified.

Clinical implications
Although in agreement with previous findings (Minor 2000; Brantberg et al. 2001), SCDS does not lead to problems of the 3D VOR, almost all patients with SCDS complain about a chronic form of dizziness. This has a strong effect on daily life (Banerjee et al. 2005; Minor 2000).
Because cerebro-spinal fluid pulsations are a source of 3D instability, patients should avoid heavy exercise, as the increase of heart rate may increase the frequency and amplitude of endolymph motion in the dehiscent canal.
During daily activities we are continuously exposed to loud sounds (e.g. in traffic), which cause pressure changes in the ear that are mediated to the endolymph of the semicircular canals. Because in SCDS patients the dehiscence seems to act as a release window, turbulence will occur in the semicircular canal endolymph fluid leading to 3D ocular instabilities.

References

Banerjee A., Whyte A., Atlas M.D. Superior canal dehiscence: review of a new condition. Clin otolaryngol. 2005; 30: 9-15.

Brantberg K., Bergenius J., Mendel L., Witt H., Tribukait., Ygge J. Symptoms, findings and treatment in patients with dehiscence of the superior semicircular canal. Acata Otolaryngol. 2001; 121: 68-75.

Carey J.P., Hirvonen T.P., Huller T.E., Minor L.B. Acoustic responses of vestibular afferents in a model of superior canal dehiscence. Otol Neurotol. 2004; 25(3): 345-52.

Carey J.P., Minor L.B., Nager G.T. Dehiscence or thinning of bone overlying the superior semicircular canal in a temporal bone survey. Arch Otolaryngol Head Neck Surg. 2000; 126: 127-47.

Cremer P.D., Minor L.B., Carey J.P. della Santina C.C. Eye movements in patients with superior canal dehiscence syndrome align with abnormal canal. Neurology. 2000; 55: 1833-1841.

Deutschlander A., Strupp M., Jahn K., Jager L., Quiring F., Brandt T. Vertical oscillopsia in bilateral superior canal dehiscence syndrome. Neurology. 2004; 62(5): 684-5.

Goumans J., Boumans LJ, van der Steen J., Feenstra L. Superior-canal dehiscence syndrome. Ned Tijdschr Geneeskd, 2005; 149:1320-1325.

Goumans J.,Houben M.M.J., Dits J., van der Steen J. Peaks and troughs of three dimensional vestibulo ocular reflex in humans. JARO, 2010 accepted for publication.

Hirvonen T.P., Carey J.P, Liang C.J., Minor L.B. Superior canal dehiscence; mechanisms of pressure sensitivity in a chinchilla model. Arch Otolaryngol Head Neck Surg. 2001; 127: 1331-1336.

Minor L.B. Superior canal dehiscence syndrome. Am J Otol. 2000; 21: 9-19.

Minor L.B. Clinical manifestations of superior semicircular canal dehiscence. Laryngoscope. 2005; 115: 1717-27.

Minor L.B., Cremer P.D., Carey J.P., Della Santina C.C., Streubel S-O., Weg N. Symptoms and signs in superior canal dehischence syndrome. Ann N Y Acad Sci. 2001; 942: 259-273.

Minor L.B., Solomon D., Zurich J.S., Zee D.S. Sound- and /or pressure-induced vertigo due to bone dehiscence of the superior semicircular canal. Arch Otolaryngol Head Neck Surg. 1998; 124: 249-58.

Ostrowski V.B., Byskosh A., Hain T.C. Tullio phenomenon with dehiscence of the superior semicircular canal. Otol Neurotol. 2001; 22: 61-5.

Rosowski J.J., Songer J.E., Nakajima H.H., Brinsko K.M., Merchant S.N. Clinical, experimental, and theoretical investigations of the effect of superior semicircular canal dehiscence on hearing mechanisms. Otol Neurotol. 2004; 25: 323-32.

Songer J.E., Rosowski J.J. The effect of superior canal dehiscence on cochlear potential in response to air-conducted stimuli in chinchilla. Hear Res. 2005; 210: 53-62.

Tilikete C., Krolak-Salmon P., Truy E., Vighetto A. Pulse-synchronous eye oscillations revealing bone superior canal dehiscence. Ann Neurol. 2004; 56(4): 556-60.

Watson S.R., Halmagyi G.M., Colebatch J.G. Vestibular hypersensitivity to sound (Tullio phenomenon): structural and functional assessment.

Neurology. 2000; 54(3): 722-737.
Younge B.R., Khabie N., Brey R.H., Driscoll C.L. Rotatory nystagmus synchronous with heartbeat: a treatable form of nystagmus. Trans Am Ophthalmol Soc. 2003; 101: 113-8.

Chapter 7

Extensive admittance testing in the diagnostic work-up of superior canal dehiscence syndrome

Reincke HA, Goumans J

submitted

Abstract

The objectives of this study were to analyse the findings of an extended audiometric test battery in patients with superior canal dehiscence syndrome (SCDS). Five patients with confirmed SCDS were included, four with a unilateral SCDS and one with a bilateral SCDS. Each patient underwent an extended battery of audiometric tests. Our results for the 'standard' audiometric tests were in accordance with the literature. Two-component tympanometry showed a pattern contra-indicative of a more than average stiffness-controlled middle ear system. Pulse synchronous deviations in the continuous registration of the admittance were noted in three of four tested affected ears. ABR testing did not show any abnormalities. Standard tympanometry and stapedius reflex testing do not distinguish SCDS ears from non-affected ears. Two-component tympanometry at 678 Hz and continuous registration of the admittance seem to be more valuable tests in this respect. The results of these tests in SCDS ears are in accordance with the third window hypothesis. We advise addition of continuous registration of the admittance and two-component tympanometry at 678 Hz to the ´standard´ audiometric test battery for the diagnostic work-up of SCDS.

Introduction

Superior canal dehiscence syndrome (SCDS) is a disorder affecting the organ of hearing and balance. Since it was described in 1998 by Minor et al. (Minor et al. 1998), the incidence and etiology of this syndrome (Carey et al. 2000; Carey & Amin 2006; Tsunoda & Terasaki 2002), as well as the diagnostic work-up (Minor 2005; Banerjee et al. 2005; Brantberg et al. 2001) has been studied extensively. A definite diagnosis of SCDS is based on the finding of a dehiscence of the bone overlying the superior semicircular canal with high-resolution computed tomography scan (CT scan) of the temporal bone (Minor 2005; Belden et al. 2003) on the one hand and the clinical signs and symptoms on the other hand. Common signs and symptoms of SCDS fall into two categories: signs and symptoms related to balance and those related to hearing. Most patients have vestibular symptoms or both vestibular and hearing symptoms. Few patients have only hearing symptoms (Minor 2005; Mikulec et al. 2004).
Common symptoms related to the balance organ are vertigo in relation to coughing, sneezing or Valsalva manoeuvres and vertigo in response to sound stimulation or external pressure changes (Brantberg et al. 2001; Hillman et al. 2006; Ostrowski et al. 2001; Minor 2005). Most patients however report chronic vestibular problems (Mikulec et al. 2004; Minor 2005). Patients with SCDS often have abnormally large sound-induced vestibular-evoked myogenic potentials (VEMP) with a lower threshold on the affected side than on the healthy side (Brantberg et al. 2004; Brantberg et al. 1999; Streubel et al. 2001).
Hearing complaints are attributed to an increased sensitivity for bone conducted sounds, a decreased sensitivity for air conducted sounds or both (Mikulec et al. 2004; Minor et al. 2003). A typical audiogram of an ear with SCDS has a low-frequency air-bone gap, much like in otosclerotic patients. Patients with SCDS may also report autophony, including tinnitus. This autophony, which is believed to be due to the increased sensitivity to bone-conduction signals, can be quite extreme, with patients hearing their own eyes blink or the impact of footsteps while running or even walking (Minor 2000; Banerjee et al. 2005). A relatively large number of patients complain of pulse-synchronous tinnitus (Banerjee et al. 2005).

The 'standard' audiometric test battery for SCDS according to literature includes pure tone audiometry and often also speech audiometry. In particular when an air-bone gap is found in the audiogram, Weber testing, standard tympanometry and acoustic reflex testing are added to this test battery. Patients usually show a low frequency conductive hearing loss, normal speech discrimination scores, a normal tympanogram and intact acoustic reflex responses (Banerjee et al. 2005; Brantberg et al. 2001; Mikulec et al. 2004; Minor et al. 2003). Since the audiogram of a typical SCDS ear often mimics the audiogram found in patients suffering from otosclerosis, there is a significant risk of mis-diagnosing a SCDS patient if only these tests are used. Some patients even have had a middle-ear surgery, which significantly increases the risk of sensorineural hearing loss, after potential SCDS repair surgery in a later stage (Limb et al. 2006). It is therefore considered important to increase the sensitivity of the audiometric

test battery in order to reduce the chance of missing the SCDS diagnosis and performing unnecessary surgery.
In this study, we carried out extended audiometric testing on five patients with a SCDS confirmed by CT scan in one or both ears. In order to get more understanding of the nature of the often observed air-bone gap, we added two-component tympanometry with a 678 Hz probe tone to the aforementioned 'standard' test battery. Besides, we tried to objectify the often observed pulsatile tinnitus by carrying out a continuous registration of the middle ear admittance. ABR testing was done in order to see whether there are any abnormalities in the response that could be related to the SCDS. The goal of this study is to see whether this extended audiometric test battery can aid in the diagnostic work-up of SCDS.

Methods

Patients

Five patients with superior canal dehiscence syndrome participated in the experiment. In four of them the diagnosis of superior semicircular canal dehiscence was confirmed on high-resolution CT scans of the temporal bone. A fifth patient who participated in our study already had his SCDS radiologically confirmed elsewhere. No patients had neurological, cardiovascular or ophthalmic disorders and none of them had a history of middle ear problems. Otoscopic examination was normal. All patients gave their informed consent and the experimental procedure was approved by the Medical Ethics Committee of the Erasmus University Medical Centre and adhered to the Declaration of Helsinki for research involving human patients. The patient characteristics, subjective symptoms, as well as the clinical findings apart from audiometry, are summarised in Table 1.

Patient	Gender	Age	SCDS side	Subjective hearing loss	Autophony and tinnitus	Subjective sound induced balance symptoms by	Objective sound induced balance symptoms	Other subjective auditory symptoms
1	male	36	right	none	voice, footsteps, heartbeat, eyeblinks and chewing	loud sounds	right-sided positive Hennebert	none
2	female	47	left	none	voice, humming tinnitus	shrill sounds	left-sided positive Hennebert	sounds sound 'hollow'
3	male	54	both	right-sided deafness, left-side hearing is diminished	voice, footsteps, heartbeat, eye blinks	loud sounds	positive Tullio and bilateral positive Hennebert	loud noise is painful
4	female	28	left	left ear feels clogged	none	loud sounds	positive Tullio	own voice 'resonates'
5	female	25	left	left-side hearing is diminished	tinnitus	none	left-sided positive Hennebert	some sounds sound 'strange'

Table 1. Patient characteristics, relevant symptoms and clinical findings, apart from audiometry, for our five patients with SCDS.

Experimental design

Our audiometric test battery consisted of the 'standard' tests: pure tone and speech audiometry, Weber testing, standard single-component 226 Hz tympanometry and stapedius reflex tests and was extended with click-evoked ABR testing, two-component tympanometry at 226 and 678 Hz and continuous registration of the middle ear admittance. Both ears were tested, irrespective of the presence or absence of SCDS at that ear.

Weber testing, pure tone and speech audiometry were performed in a standard audiometric, sound treated test booth using a Madsen OB-822 clinical audiometer with a Radio ear B71 bone conductor and Telephonics TDH-39P headphones. For the Weber testing, amplitude modulated pure tones were used with frequencies of 0.5, 1, 2 and 4 kHz in a procedure starting subliminally. Air conduction thresholds were determined at octave frequencies from 0.25-8 kHz. Bone conduction thresholds were determined at the same frequencies, except for 8 kHz. Speech audiometry was performed using the same audiometer and a recording of the Dutch NVA CVC word lists (Bosman, 1989). Full performance curves were measured. Masking on the contralateral ear was applied whenever appropriate for both tone and speech audiometry.

All admittance and stapedius reflex testing was carried out using a Grason Stadler GSI 33 v.2. tympanometer. Standard tympanometry was carried out with a 226 Hz probe tone. Ear canal volume, static compliance, middle ear pressure and peak width were registered and compared to a standard type A tympanogram (Hall, 1994). Additionally, two-component (acoustic susceptance, B, and conductance, G) tympanograms were measured at probe frequencies of 226 Hz and 678 Hz. These B / G tympanograms were interpreted qualitatively, using the guidelines given in the literature (Van Camp et al, 1983; Shanks & Shelton, 1991; Gerull et al, 1979; Creten et al, 1985; Van Camp et al, 1986; Van de Heyning et al, 1982; Shone & Moffat, 1986; Zhao et al, 2002; Shahnaz & Polka, 1997). Especially the number and height of peaks in the B and G tympanogram measured at a probe frequency of 678 Hz were considered. Stapedius reflex thresholds were determined at stimulus frequencies of 0.5, 1 and 2 kHz, both for ipsi- and contra-lateral stimulation after compensation for abnormal middle ear pressure. The maximum stimulus level used was 100 dB HL. In the continuous admittance registration, the admittance of both ears was recorded continuously for 10 seconds, without presenting a stimulus. Any deviation from baseline, periodic or not, was noted. For periodic deviations, it was checked whether or not these were pulse-synchronous.

Click-evoked ABR testing was carried out in an electromagnetical shielded, sound treated test booth. Two-channel recordings were collected with electrodes on the vertex, both mastoids and the forehead. A band-pass filter with cut-off frequencies of 20 Hz and 3 kHz was used to improve the signal to noise ratio. Responses with high noise levels were rejected using an artefact-rejection window of 20 μV for the same reason. A broadband click stimulus with alternating polarity and a repetition frequency of 23 Hz was used as a stimulus, at levels of 90 and 70 dBnHL (levels relative to mean behavioural thresholds in normal hearing listeners). If possible, the stimulus level was decreased in steps of 10 dB down to determine response thresholds. The latencies were compared to our clinical reference values. The latency-level curves were then used to estimate the conductive component in the hearing

loss, using the method of Van der Drift et al (Van der Drift et al, 1989). In this method, the conductive component of the hearing loss was estimated by the horizontal shift in the patient's latency-level curve relative to the latency-level curve for normal hearing listeners. This technique is the standard technique of interpretation of ABR responses in our clinic. The same experienced clinical audiologist carried out the interpretation of all ABR responses.

Results

The test results of all measurements are summarised in Table 2 for each patient. Weber tests, pure tone audiometry and stapedius reflex threshold tests were completed for all patients. Speech audiometric results were obtained for all patients except for patient 1 as he was not a native Dutch speaker. Standard tympanometric results were obtained for all ears, except for the left ear of patient 1. An airtight seal could not be obtained in this ear canal at the time. Two-component tympanometry at 226 and 678 Hz and continuous admittance measurements were completed for all patients. ABR recordings could not be obtained for patients 1 and 4. Patient 1 was a patient from Switzerland who visited our department only once, and thus did not have enough time to complete all tests. Patient 4 underwent a series of clinical tests in the diagnostic process and declined to complete extra tests for reasons of clinical research. For the same reason we did not complete ABR threshold measurements for patient 5, however, we did complete the ABR recordings at high stimulus levels thus giving us information on the possible presence of a conductive loss.

	Affected side						Non-affected side			
Test	Patient 1 right	Patient 2 left	Patient 3 right	Patient 3 Left	Patient 4 left	Patient 5 left	Patient 1 left	Patient 2 right	Patient 4 right	Patient 5 right
Pure tone AC thresholds (dB HL)	10, 10, 0, 0, 10, 10	20, 25, 15, 20, 20, 30	>80, >85, >95, >100, >120, >100	40, 20, 15, 15, 20, 40	15, 20, 10, 10, 5, 10	75, 70, 55, 40, 25, 45	0, 0, 5, -5, 10, 5	5, 10, 5, 10, 15, 25	0, 0, -5, 0, 5, 15	10, 15, 5, 10, 10, 15
Pure tone BC thresholds (dB HL)	0, 5, 0, 15, 10	0, 10, -5, 15, 25	>45, >60, >70, >75, >75	0, 5,0, 20, 20	0, 10, -10, 20, 15	>65, 50, 55, 45, 45	5, 0, 10, 10, 10	5, 20, 5, 20, 25	20, 0, -10, 0, 10	0, 30, 5, 10, 30
Weber lateralisation	yes	yes	nr	nr	yes	no	no	no	no	yes
Shift speech audiogram (dB)	-	20	>70	15	15	30	-	10	5	10
Tympanogram type	A	A	Ad	Ad	A	A	-	C	A	A
B/G 678 Hz tympanogram type	3B1G	3B3G	3B3G	3B1G	3B1G	1B1G	3B1G	1B1G	1B1G	1B1G
B/G 678 Hz: B negative?	yes	yes	yes	yes	no	no	yes	no	no	no
Pulse-synchronous deviations in continuous admittance?	yes	yes	yes	yes	yes	no	yes	no	no	no
Stapedius reflex thresholds	normal	ipsi / contra not elicitable	not measurable due to strong spontaneous fluctuations	not measurable due to strong spontaneous fluctuations	ipsi not measured / contra not elicitable	normal	normal	ipsi normal / contra not elicitable	ipsi / contra not elicitable	normal
ABR latencies	-	normal	-	normal	-	normal	-	normal	-	normal
ABR threshold	-	20 dBnHL	-	= <20 dBnHL	-	-	-	20 dBnHL	-	-
ABR cond. component	-	10 dB	-	0 dB	-	-	-	10 dB	-	-

Table 2. Results of the audiometric tests for the 5 SCDS patients. The left side of the table shows the results for the SCDS ears, the right side for the unaffected ears. In the first row the pure tone air conduction thresholds are given in dB HL at the octave frequencies 250, 500, 1000, 2000, 4000 and 8000 Hz respectively. In the second row, the bone conduction thresholds are given in dB HL at the same frequencies except 8 kHz. 'Shift speech audiogram' is the curve shift in dB of the speech audiometry performance curve, relative to the reference curve for normal hearing listeners. 'Tympanogram type' is the type of the single-component tympanogram (226 Hz probe tone) according to the classification by Jerger (Hall 1994), wherein 'A' is the standard tympanogram, 'Ad' is a tympanogram with a large compliance and 'C' is a tympanogram with a lowered middle ear pressure. 'B/G 678 Hz tympanogram type' presents the number of peaks in B and G in the multi-component B/G tympanogram

(678 Hz probe tone), for instance 3B1G means 3 peaks (minima or maxima) in the B-curve and 1 peak in the G-curve. 'B/G 678 Hz: B negative:' means: the minimum peak in the B-curve is lower than the 'tails' of the curve. 'ABR latencies' are the latencies of peak V for the 90 dBnHL stimulus and considered normal if they fall within 2 standard deviations of our clinical reference values. 'ABR cond. component' is the estimated conductive component in the hearing loss, using the methods described in Experimental design.

Tone and speech audiometry and Weber testing

In five of the six tested SCDS ears a low-frequency air-bone gap was present (see Figure 1, left side for an example), with a range of 8 to 28 dB for the LF-AB gap. In the sixth ear this could not be measured since that ear was deaf. Note that patient 5 showed a mainly sensorineural hearing loss, most prominent in the low frequencies. In none of the affected ears was a better than normal sensitivity for bone conducted sounds measured. For speech audiometry, a shift in the discrimination curve was noted approximately equal to the PTA for patient 2, 3, 4, and 5. For patient 5, some high level regression was seen in the discrimination curve and 100% discrimination was not attained. This was possibly due to the fact that in this ear a low-frequency sensorineural hearing loss was present. Weber testing lateralized to the affected ear in all patients except patient 5, who has a moderate sensorineural hearing loss in the affected ear and normal hearing in the other ear. For patient 3, Weber testing lateralizes to the better hearing ear.

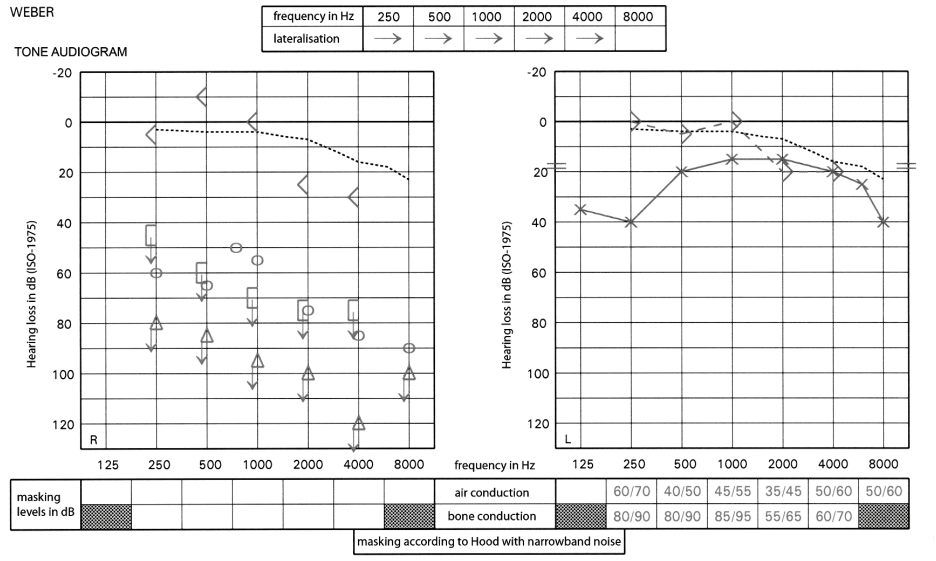

Figure 1. Tone audiogram of patient 3, showing a low-frequency conductive loss left and a deaf ear at the right. The dotted line shows the 50th percentile threshold for the age group of this patient.

Single and two-component tympanometry, stapedius reflex threshold testing and continuous admittance registration

Standard tympanometry showed a type A or type Ad tympanogram for the affected ears and a type A or type C for the unaffected ear. A striking observation was that for both patients 1 and 3, applying pressure to the right ear canal (affected side for patient 1 and one of the affected sides for patient 3), immediately resulted in strong vertigo complaints.
Two-component tympanometry at 678 Hz showed a 3B3G or 3B1G type in four of the five affected ears tested. The minimum for the B curve reached a negative value in all of these ears (see Figure 2 for an example). This is a strong indication of a mass-controlled middle ear system, in contrast to a stiffness-controlled middle ear system as is usually seen in otosclerotic ears. The sixth affected ear showed a 1B1G type. In this case however the B peak was lower than the G peak, which is considered normal at this probe frequency and therefore not an indication of a more than average stiffness-controlled middle ear system.

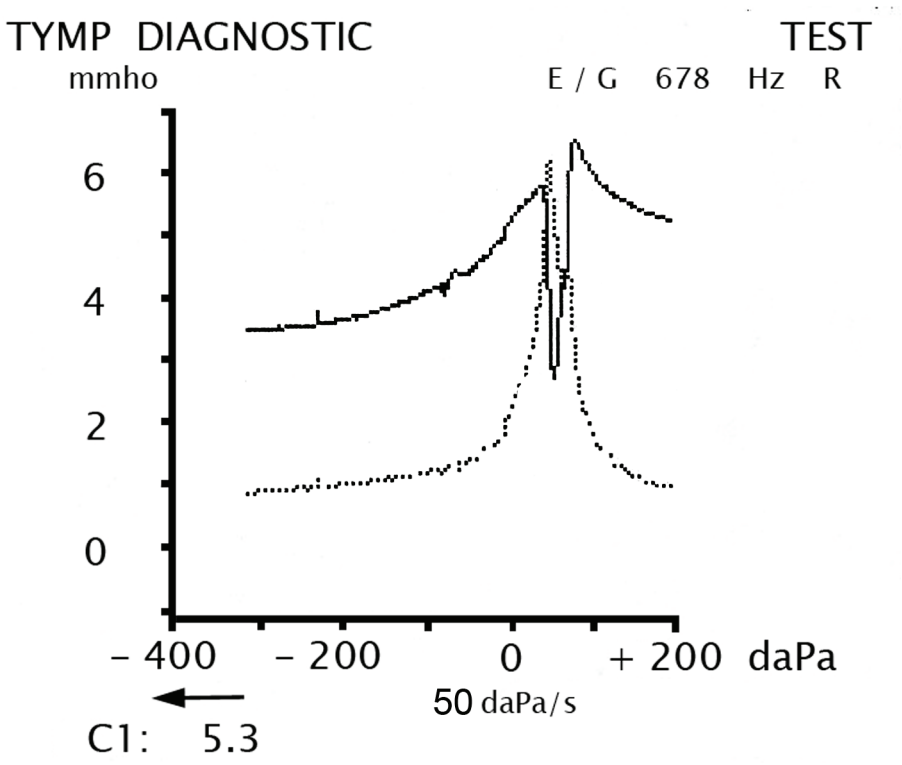

Figure 2. Two-component tympanogram at 678 Hz, measured in the SCDS ear of patient 1, showing a 3B1G type. The minimum peak for B reaches a negative value.

Only one of the four tested non-affected ears showed a 3B1G type, in which the minimum peak for B reached a negative value indicating a mass-controlled middle ear system. The other three tested non-affected ears showed a 1B1G type, all with a larger G than B indicating a normal stiffness-controlled middle ear system.
For the affected ears, stapedius reflexes could be elicited in two ears and could not be elicited in two other ears. The same holds for the non-affected ears. In two of the six affected ears, it is unclear whether or not the reflexes could be elicited, due to strong spontaneous fluctuations in the registration. Pulse synchronous deviations in the continuous registration of the admittance, as shown in Figure 3, were noted in five of the six tested affected ears and in one of the four tested non-affected ears.

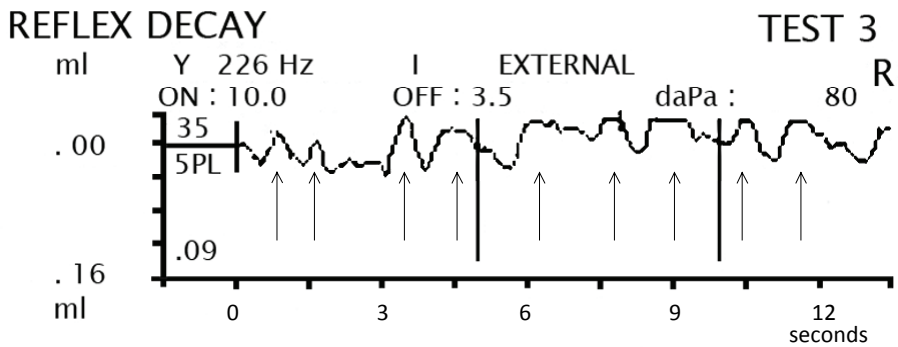

Figure 3. A strong, spontaneous fluctuation synchronous to the heartbeat is seen during continuous registration of the admittance for patient 1. The 'reflex decay' registration mode was used with the reflex eliciting stimulus set to external, since in this mode the 'spontaneous' (without reflex eliciting stimulus) admittance variations can be shown over a period of 10 seconds.

ABR measurement

In all tested affected and non-affected ears, the ABR latencies were normal. No abnormality was noted in any of the responses. Specifically, there were no signs of significantly prolonged peak latencies as found in ears with conductive losses (Van der Drift et al. 1989). There were also no signs of the presence of a sound-evoked short latency negative response.

Discussion

Audiometric results

In this study, we explored the diagnostic value of a number of audiometric tests in five patients with SCDS. Some of these tests have to our knowledge not been used before in the diagnosis of SCDS. Our results with Weber testing, pure tone audiometry and speech audiometry are in agreement with the literature (Banerjee et al. 2005; Brantberg et al. 2001; Mikulec et al. 2004; Minor et al. 2003). A problem in the diagnosis is the similarity of audiograms with those of otosclerotic patients. In our findings, standard tympanometry and stapedius reflex tests, advocated in the literature to diagnose SCDS, do not distinguish affected ears from non-affected ears. We extended the standard audiometric test battery with ABR testing, two-component tympanometry at 678 Hz and continuous registration of the admittance.

Two-component tympanometry at 678 Hz showed a curve-pattern not indicative of a more than average stiffness-controlled middle ear system in all tested ears, both affected and non-affected. This finding is not indicative of otosclerosis. Five of the six affected ears showed a 3B3G type, the sixth ear showed a 1B1G type. The minimum peak for B reached a negative value in four of these six ears. This negative minimum peak in the B-curve is an indication of a mass-controlled middle ear system, which is even considered to be a strong contra-indication of otosclerosis (Shanks & Shelton 1991; Gerull et al. 1979). Based on these results, two-component tympanometry at 678 Hz is considered a useful test in the diagnostic work-up for SCDS. It is furthermore a test that can easily be performed on most standard clinical tympanometers.

A second striking finding that has to our knowledge not been previously reported is the finding of spontaneous pulse-synchronous deviations in the continuous registration of the admittance. These deviations were noted in five of the six tested affected ears and in only one of the four tested non-affected ears. There was no clear relation between the spontaneous deviations and the clinical symptom of pulsatile tinnitus: in only two of the five affected ears where the spontaneous deviations were noted, patients indeed reported pulsatile tinnitus. There was one affected ear in which the clinical symptom of pulsatile tinnitus was present, but the spontaneous deviations were not seen in the continuous admittance registration. The relation with the clinical symptom of autophony was stronger: in four of the five affected ears where the spontaneous deviations were noted, the clinical symptom of autophony was present. The fifth ear was deaf and therefore the clinical symptom of autophony was not applicable. There was however also one non-affected ear where the spontaneous deviations were present but not the symptom of autophony. A pulse-synchronous spontaneous impedance change in the continuous registration of admittance for patients with autophony is not a new finding. It has already been described by Thiede et al. (Thiede et al. 2004), who found a significant correlation between high blood pressure and binaural pulse-synchronous spontaneous impedance changes. Thiede et al. carried out CT, Magnetic Resonance Imaging (MRI) or angiography in order to detect pathologies related to the presence of pulsatile tinnitus. They did not specifically search for a dehiscence of the superior semicircular canal. Thus the possibility that some of their patients suffered

from SCDS cannot be ruled out. Registration of the spontaneous admittance deviations is also a simple test that can be easily performed with most standard clinical tympanometers.
Auditory brainstem response (ABR) tests seem to be useful only to rule out retrocochlear pathology as a possible cause for the observed symptoms of SCDS (Schmidt et al. 2001; El-Kashlan et al. 2000). There were no signs of prolonged peak latencies as would have been expected in conductive hearing loss. No abnormalities were found in the responses that might aid in the diagnosis of SCDS.

Theoretical considerations
In several studies the hearing function in patients with SCDS has been studied, as described in the introduction. An increased sensitivity for bone conduction and a decreased sensitivity for air conduction have been reported. The third window hypothesis has proven most valuable in explaining both effects (Rosowski et al. 2004; Songer & Rosowski 2005). The alterations in the sensitivity for both air conducted and bone conducted sounds are generally attributed to the dehiscence that acts as a 'third mobile window' in the bony capsule of the inner ear (Rosowski et al. 2004; Songer & Rosowski 2005). According to this theory, air conducted sounds, especially those with frequencies below 2 kHz, are shunted away from the cochlea through this window. The changes in cochlear mechanics also give rise to an increased sensitivity for bone conduction, particularly for frequencies below 2 kHz. Rosowski et al. (Rosowski et al. 2004) performed experiments in which the sound-induced velocity of the tympanic membrane was measured using Laser Doppler Vibrometry (LDV). SCDS ears and ears with a confirmed ossicular discontinuity were compared to normal ears. They concluded that the mean conduction velocity of SCDS ears was significantly higher than the normal mean at the tested frequencies of 300, 500, 700 and 1000 Hz. The measured low-frequency velocities for the affected ears range between normal and ears with an ossicular discontinuity. They argued that an increased mobility of the ossicular chain in SCDS ears might be responsible. This suggests a superior semicircular dehiscence-induced decrease in the load on the tympanic membrane. Rosowski et al. also performed a model analysis of the human inner ear. Using this model, both the decrease in sensitivity for low-frequency air-conduction and the increase in sensitivity for low-frequency bone conduction, can be accurately predicted (Rosowski et al. 2004).
It is not easy to confirm the possible increased ossicular chain mobility in SCDS ears, as found by Rosowski et al. (Rosowski et al. 2004). LDV, the method used by Rosowski et al., is hardly applicable in a clinical setting. Standard tympanometry and stapedius reflex tests are neither very sensitive nor very specific in detecting increased ossicular-chain mobility. Two-component tympanometry at 678 Hz however showed a curve-pattern in the affected ears that are strongly indicative of a mass-controlled middle ear system and thus contra-indicative of a stiffness-controlled middle ear system. This makes otosclerosis very unlikely as a cause for the observed low-frequency conductive hearing loss in SCDS since the middle ear system in otosclerosis is more than average stiffness-controlled (Shahnaz & Polka 1997). The finding that the middle ear system is more than average mass-controlled can be explained as a consequence of leaking away of part of the acoustic energy through the dehiscence (Rosowski et al. 2004; Songer &

Rosowski 2005). This finding is thus in accordance with the third-window hypothesis. However, the acoustic admittance at the lateral surface of the tympanic membrane is determined not only by the mechanical admittance of the cochlea (which is affected by SCDS), but also by the mass and stiffness of the middle ear transmission system, by volume and pressure of air in middle ear and ear canal and by the tonus of the middle ear muscles. Therefore it cannot be concluded directly that when a middle ear is found to be more than average mass-controlled, this should be attributable to SCDS. Besides, a more than average mass-controlled middle ear system has also been measured in patients with scarred tympanic membranes and in patients with an enlarged vestibular aqueduct (EVA) for whom the cochlear impedance is also lowered by a third window (Sato 2002; Nakashima et al. 2000).
It is interesting to discuss the possible mechanism behind the spontaneous admittance deviations that were found in the affected ears of our patients. Since they appear to be pulse-synchronous, a possible cause might be the pulsations in the intracranial vessels causing travelling waves in the cerebrospinal fluid (CSF). These waves are then transmitted through the bony dehiscence into the cochlea stimulating the organ of Corti. These waves could lead to displacements of the stapedial footplate as well, giving rise to spontaneous impedance changes (SICs) of the middle ear, discernible by standard tympanometry (Thiede et al. 2004).
On theoretical grounds, prolonged peak latencies in the ABR responses with a click stimulus, could be expected in SCDS ears if part of the acoustic energy leaks away through the dehiscent semicircular canal. This is usually seen in ears with a conductive loss (Van der Drift et al. 1989). The prolongation of the peak latencies is related to the amount of acoustic energy that leaks away through the dehiscent semicircular canal especially in the 2-4 kHz frequency region, since the ABR responses are best correlated to hearing loss in those frequencies (Van der Drift et al. 1987). However we did not observe such effects in our patients. Another effect that can theoretically be expected is the presence of a sound-evoked short latency negative response possibly originating from the sacculus. The presence of this response has been reported in ABR recordings of ears with profound losses under intense stimulation (Nong et al. 2002; Ochi & Ohashi 2001). For normal ears and ears with mild to moderate hearing loss this response is absent. This is possibly due to the presence of peaks I to V that may prevent detection. When sound energy leaks away through the dehiscent semicircular canal it passes through the sacculus. This can possibly generate a larger response than found in normal ears and might consequently give a measurable ABR response. This effect however was not observed in our patients.

Conclusion

From our limited sample of SCDS patients, we conclude:
The ‘standard’ test battery proposed in the diagnosis of SCDS consisting of pure-tone audiometry, speech audiometry, standard tympanometry and stapedius reflex testing, does not distinguish between e.g. a patient with otosclerosis or one with SCDS. This can lead to errors in the surgical approach.

The addition of two-component tympanometry with a 678 Hz probe tone and of a continuous recording of the middle ear impedance can improve the differential diagnosis and make the diagnosis of SCDS, based purely on specific complaints, routine ENT examination and audiometry more robust. The observation of fluctuations synchronous to the heartbeat can be a strong indication of SCDS; it would be interesting to investigate its relationship with autophony.
We advise extending the 'standard' audiometric test battery with two-component tympanometry at 678 Hz and continuous registration of the spontaneous deviations in the admittance.

References

Banerjee A., Whyte A. & Atlas M.D. 2005. Superior canal dehiscence: review of a new condition. Clin otolaryngol, 30, 9-15.

Belden C.J., Weg N., Minor L.B. & Zinreich S.J. 2003. CT evaluation of bone dehiscence of the superior semicircular canal as a cause of sound- and/or pressure-induced vertigo. Radiology, 226, 337-43.

Bosman, A.J. 1989. Speech perception by the hearing impaired. Utrecht, Thesis Universiteit van Utrecht.

Brantberg K., Bergenius J. & Tribukait A. 1999. Vestibular-evoked myogenic potentials in patients with dehiscence of the superior semicircular canal. Acta Otolaryngol, 119, 633-40.

Brantberg K., Bergenius J., Mendel L., Witt H., Tribukait A. & Ygge J. 2001. Symptoms, findings and treatment in patients with dehiscence of the superior semicircular canal. Acta Otolaryngol, 121, 68-75.

Brantberg K., Lofqvist L. & Fransson P.A. 2004. Large vestibular evoked myogenic potentials in response to bone-conducted sounds in patients with superior canal dehiscence syndrome. Audiol Neurotol, 9, 173-82.

Brantberg K., Bagger-Sjöbäck D., Mathiesen T., Witt H. & Pansell T. 2006. Posterior canal dehiscence syndrome caused by an apex cholesteatoma. Otol Neurotol, 27, 531-4.

Carey J.P., Minor L.B. & Nager G.T. 2000. Dehiscence or thinning of bone overlying the superior semicircular canal in a temporal bone survey. Arch Otolaryngol Head Neck Surg, 126, 137-47.

Carey J. & Amin N. 2006. Evolutionary changes in the cochlea and labyrinth: solving the problem of sound transmission to the balance organs of the inner ear. Anat Rec A Discov Mol Cell Evol Biol, 288, 482-9.

Creten W.L., Van de Heyning P.H. & Van Camp K.J. 1985. Immittance audiometry. Normative data at 220 and 660 Hz. Scand Audiol, 14, 115-21.

El-Kashlan H.K., Eisenmann D. & Kileny P.R. 2000. Auditory brain stem response in small acoustic neuromas. Ear Hear, 21, 257-62.

Gerull G., Giesen M. & Mrowinski D. 1979. Die komplexe Trommelfellimpedanz bei verschiendenen Mittelohrschaden. *Laryngol Rhinol,* 58, 25-32.

Hillman T.A., Kertesz T.R., Hadley K. & Shelton C. 2006. Reversible peripheral vestibulopathy: the treatment of superior canal dehiscence. Otolaryngol Head Neck Surg, 134, 431-6.

Hall J.W. & Chandler D. 1994. Tympanometry in clinical audiology. In: Katz J. (ed.) Handbook of clinical audiology, fourth edition. Baltimore: Williams & Wilkins, pp. 283-99.

Krombach G.A., DiMartino E., Schmitz-Rode T., Prescher A. & Haage P. et al. 2003. Posterior semicircular canal dehiscence: a morphologic cause of vertigo similar to superior semicircular canal dehiscence. Eur Radiol, 13, 1444-50.

Limb C.J., Carey J.P., Srireddy S. & Minor L.B. 2006. Auditory function in patients with surgically treated superior semicircular canal dehiscence. Otol Neurotol, 27, 969-80.

Mikulec A.A., McKenna M.J., Ramsey M.J., Rosowski J.J. & Herrmann B.S. et al. 2004. Superior semicircular canal dehiscence presenting as

conductive hearing loss without vertigo. Otol Neurotol, 25, 121-9.
Mikulec A.A. & Poe D.S. 2006. Operative management of a posterior semicircular canal dehiscence. Laryngoscope, 116, 375-8.
Minor L.B., Solomon D., Zurich J.S. & Zee D.S. 1998. Sound- and/or pressure-induced vertigo due to bone dehiscence of the superior semicircular canal. Arch Otolaryngol Head Neck Surg, 124, 249-58.
Minor L.B. 2000. Superior canal dehiscence syndrome. Am J Otol, 21, 9-19.
Minor L.B., Carey J.P., Cremer P.D., Lustig L.R. & Streubel S.O. 2003. Dehiscence of bone overlying the superior canal as a cause of apparent conductive hearing loss. Otol Neurotol, 24, 270-8.
Minor L.B. 2005. Clinical manifestations of superior semicircular canal dehiscence. Laryngoscope, 115, 1717-27.
Modugno G.C., Magnani G., Brandolini C., Savastio G. & Pirodda A. 2006. Could vestibular evoked myogenic potentials (VEMPs) also be useful in the diagnosis of perilymphatic fistula? Eur Arch Otorhinolaryngol, 263, 552-5
Nakashima T., Ueda H., Furuhashi A., Sato E., Asahi K., Naganawa S. & Beppu R. 2000. Air-bone gap and resonant frequency in large vestibular aqueduct syndrome. Am J Otol, 21, 671-4.
Nong D.X., Ura M., Kyuna A., Owa T. & Noda Y. 2002. Saccular origin of acoustically evoked short latency negative reponse. Otol Neurotol, 23, 953-7.
Ochi K. & Ohashi T. 2001. Sound-evoked myogenic potentials and responses with 3-ms latency in auditory brainstem response. Laryngoscope, 111, 1818-21.
Ostrowski V.B., Byskosh A. & Hain T.C. 2001. Tullio phenomenon with dehiscence of the superior semicircular canal. Otol Neurotol, 22, 61-5.
Rosowski J.J., Songer J.E., Nakajima H.H., Brinsko K.M. & Merchant S.N. 2004. Clinical, experimental, and theoretical investigations of the effect of superior semicircular canal dehiscence on hearing mechanisms. Otol Neurotol, 25, 323-32.
Sato E., Nakashima T., Lilly D.J., Fausti S.A. & Ueda H. et al. 2002. Tympanometric findings in patients with enlarged vestibular aqueducts. Laryngoscope, 112, 1642-6.
Schmidt R.J., Sataloff R.T., Newman J., Spiegel J.R. & Myers D.L. 2001. The sensitivity of auditory brainstem response testing for the diagnosis of acoustic neuromas. Arch Otolaryngol Head Neck Surg, 127, 19-22.
Shahnaz N. & Polka L. 1997. Standard and multifrequency tympanometry in normal and otosclerotic ears. Ear Hear, 18, 326-41.
Shanks J. & Shelton C. 1991. Basic principles and clinical applications of tympanometry. Otolaryngol Clin North Am. 24, 299-328.
Shone G.R. & Moffat A. 1986. Oto-admittance measurements in the diagnosis of otosclerosis. *J Laryngol Otol*, 100, 149-54.
Songer J.E. & Rosowski J.J. 2005. The effect of superior canal dehiscence on cochlear potential in response to air-conducted stimuli in chinchilla. Hear Res, 210, 53-62.
Streubel S.O., Cremer P.D., Carey J.P., Weg N. & Minor L.B. 2001. Vestibular-evoked myogenic potentials in the diagnosis of superior canal dehiscence syndrome. Acta Otolaryngol Suppl, 545, 41-9.
Thiede O., Stoll W. & Schmal F. 2004. Clinical and experimental

investigations of spontaneous impedance changes of the middle ear. Ann Otol Rhinol Laryngol, 113, 577-81.
Tsunoda A. & Terasaki O. 2002. Dehiscence of the bony roof of the superior semicircular canal in the middle cranial fossa. J Laryngol Otol, 116, 514-8.
Van Camp K.J., Creten W.L., Van de Heyning P.H., Decraemer W.F. & Vanpeperstraete P.M. 1983. A search for the most suitable immittance components and probe tone frequency in tympanometry. Scand Audiol, 12, 27-34.
Van Camp K.J., Shanks J.E. & Margolis RH. 1986. Simulation of pathological high impedance tympanograms. J Speech Hear Res, 29, 505-14.
Van de Heyning P.H., Van Camp K.J., Creten W.L. & Vanpeperstraete P.M. 1982. Incudo-stapedial joint pathology: a tympanometric approach. J Speech Hear Res, 25, 611-8.
Van der Drift J.F., Brocaar M.P. & Van Zanten G.A. 1987. The relation between the pure-tone audiogram and the click auditory brainstem response threshold in cochlear hearing loss. Audiology, 26, 1-10.
Van der Drift J.F., Van Zanten G.A. & Brocaar M.P. 1989. Brainstem electric response audiometry: estimation of the amount of conductive hearing loss with and without use of the response threshold. Audiology, 28, 181-93.
Zhao F., Wada H., Koike T., Ohyama K., Kawase T. & Stephens D. 2002. Middle ear dynamic characteristics in patients with otosclerosis. Ear Hear, 23, 150-8.

Chapter 8

General discussion

General discussion

The vestibular system is necessary to have a stable projection of the visual world on the retina during head movements. To stabilise the eye when moving the head in any direction, the vestibular system registers head movements in three dimensions. The vestibular system achieves this by making use of two specialised structures, i.e. the semicircular canals and the otoliths. The semicircular canals detect angular accelerations; the otoliths organs detect translational accelerations. Both convey three-dimensional (3D) information to the brain leading to the generation of compensatory eye movements, the angular and translational vestibulo-ocular reflex (VOR), respectively. In addition visual information is used to stabilise the eyes to optimise stable vision. This so called optokinetic system works closely together with the vestibular system. Dysfunction in any of these systems results in inadequate compensatory eye movements with a decrement in stable vision. Rotations and translations of the head in every direction generally accompany daily activities. Because retinal image stabilization is a process with six degrees of freedom, it seems logical to test the visio-vestibular function in all six directions. Until now practical and technical difficulties prevented a full range assessment of 3D VOR. To assess vestibular dysfunction in standard clinical practice, only the horizontal VOR is generally measured, using of the rotating chair and caloric stimulation. Sinusoidal stimulation has been used to test the VOR both in clinical setting as well as in research.
Recently, new technologies have become available allowing for extension of the range of testability of man. E.g. the head impulse test has been developed to test the initial VOR response. With this test the heads receives a high acceleration impulse delivered by hand or torque helmet, during which the VOR is registered continuously. The advantage of this new technology is that the VOR is not influenced by the visual system or by cognitive processes during the first 100 ms. However, disadvantages are (1) the possible influences of the neck afferents, (2) the difficulty to induce linear motion, (3) the difficulty to stimulate exactly in the plane of any one of the three semicircular canals and (4) to repeat any stimulation with exactly the same acceleration profile.

Taking advantage of new technological developments, the overall objectives of this thesis were (1) to get insight into the natural variability in the accuracy of the 3D VOR and (2) to quantify changes that occur in 3D vestibulo-ocular stabilization in patients with various types of unilateral vestibular disorders that may explain the presence of dizziness in these patients during their daily activities.

To address these questions, our first goal was to decide on the best method for measuring the 3D VOR.
In our laboratory we used a new device to investigate the function of the 3D VOR. This device consists of a motion platform with six degrees of freedom that allows for stimulation of each of the three semicircular canals and/or otoliths in any direction and in any combination. The motion platform delivers whole body motions avoiding the influences of neck afferents. Another important advantage of our motion platform is the accurate repeatability of

the acceleration stimulus in strength of impulse and direction, making it a reliable technique.

To register the compensatory eye movements after stimulation in any direction two possible systems are feasible: 3D video-oculography (Chronos) and 3D scleral search coils. In order to make our choice between these two systems we tested them in an experiment described in Chapter 2.
The scleral search coil technique is the international golden standard for measuring eye movements. It consists of two separate windings of copper wire embedded in a soft silicon annulus, which is put on one of the eyes and which works in a magnetic field. This technique registers eye movements extreme precisely, with a very high signal to noise ratio. Due to its discomfort the maximal measurement time is approximately thirty minutes. The other technique, video-oculography, has the advantage of being non-invasive with no restrictions in measuring time. The main problem of 3D infrared eye measurement systems in the past was its low frame sampling rate (typically about 50 Hz). However, the Chronos device we used permitted a frame rate of 200 Hz.
In our validation experiments we compared the performance of the video based infrared 3D eye tracker device (Chronos) with the scleral search coil technique during fixation, saccades, optokinetic stimulation and vestibular stimulation. One important finding was that even the improved frame rate of 200 Hz with the Chronos turned out to be not high enough to measure fast eye movements such as saccades or during vestibular stimulation. With the Chronos apparatus it was difficult to track eye positions continuously in dark conditions due to the enlarged pupils in the dark and increased eyelid closure. Especially the torsion eye movement component was less accurate with the Chronos than the coil technique.
The surplus value of this experiment was the movability of the motion platform in any direction, making possible not only sinusoidal motions, but acceleration impulses as well. These additions in movability present important information about vestibular (dys)function. The system allows for the measurement in any position of the torsion eye movement component. Although video-oculography is a good alternative for static tests, we selected the 3D scleral search coil technique for our other experiments as this guaranteed the best accuracy and reliability.

The choice of the scleral search coil technique restricted us to relatively short measurement times of thirty minutes only. We therefore designed a combination of stimuli that we expected to provide an efficient test of the vestibular function. We tested both in light and dark conditions with healthy subjects and with patients. Our stimulus set consisted of sinusoidal rotations in the three cardinal axes: rostra-caudal (yaw), interaural (pitch) and naso-occipital (roll). We extended the experiments with sinusoidal rotations in intermediate horizontal axes (between pitch and roll) with increments of 22.5 degrees. This offered the opportunity for quantitative measurements of the accuracy of the oculomotor rotation axis in a single canal plane pair with its corresponding set of eye muscle pairs, and also for different combinations of canals and muscle pairs. We also applied acceleration rotation impulses in the dark in yaw, pitch, roll and the vertical canal planes testing the vestibular function in a more natural way and without interference of visual information.

The usual way to quantify the vestibular function is the so-called gain, which is defined as the ratio between head velocity and the compensatory eye velocity. We also took misalignment into account. Misalignment is the difference in alignment of the eye rotation axis in respect to the head rotation axis. Errors occurring both in gain and misalignment can be responsible for compromising the quality of image stabilization (sharp vision).

The results described in Chapter 3 give important insight in the processing of vestibular afferent information in healthy subjects. An interesting result is that the misalignment for sinusoidal rotation in light showed minimum values for the cardinal axes pitch and roll, but maximum values with stimulation about the vertical canal plane pairs. These values are consistent with a co-ordinate system with a fixed head's pitch and torsion axis that reflects optimised strategies for foveal vision. However, our results also showed that during sinusoidal rotation in darkness and during acceleration rotation impulses, this head-fixed co-ordination system is not persistent, but depends on visual feedback. The misalignment increased dramatically over the whole range of tested axes. The plausible explanation for this is that during horizontal axis stimulation the orientation of the horizontal semicircular canals is not earth horizontal oriented and therefore a horizontal eye movement component interferes. This influence maximises during roll stimulation, because the relatively low velocity gain for torsion in combination with this extra horizontal eye velocity component has a major effect on the misalignment.
An important conclusion from the experiment described in Chapter 3 is that even in healthy subjects, misalignments in the vestibular function response have to be partially corrected by vision. We conclude that an intact and active integration of visual and vestibular afferent information is necessary to have optimal vestibular function. Because of the important role of the orientation of the horizontal semicircular canals in vestibular compensation reactions this might explain the different reactions to vestibular stimulation between individuals.

Another goal was to explore the possible changes that occur in 3D vestibulo-ocular stabilization in patients with unilateral vestibular function loss.
In Chapter 4 the effects are described of a one-sided vestibular Schwannoma on the vestibular function. A comparison was made between three patients who had a stable right-sided Schwannoma for several years with three patients who had been operated on a right-sided Schwannoma several years earlier. This comparison gives more insight into the plasticity of the vestibular system and thereby some insight into the complaints of these patients. This is of clinical importance as the treatment policy for patients with Schwannoma is changed. A more conservative treatment in the form of 'wait and see' policy is nowadays the first choice of treatment. Thus, gathering additional information on vestibular complaints is important as the usual criterion for surgical or radiotherapeutical intervention is mainly the tumour's size. Complaints of dizziness – be it prior or after the therapy - is usually not considered an important factor in the therapeutic decision. However, dizziness has a major effect on daily activity and quality of life. An important finding was that the oculomotor performance of the three operated patients was much better than of the non-operated patients, both in light and

darkness. Taking the small number of patients into account, it seems to be better for vestibular revalidation to have one single functional labyrinth, instead of two labyrinths of which one is malfunctioning. Therefore we propose that in considering the optimal treatment for an vestibular Schwannoma – apart from the tumour's size and level of hearing loss – the degree of vestibular function loss should probably be taken into account as well. Another interesting result was the finding of drift and instabilities in the torsional eye movement component that have a major effect on the ocular stability in patients with vestibular Schwannoma. Until now mainly horizontal drifts have been reported to be important in dizziness in patients with unilateral vestibular deafferentiation. Due to our testing system allowing for measurements in 3D VOR in several axes in the horizontal plane, we consistently observed both in gain and misalignment an important role of the torsional eye movement component in maintaining vestibular function. This stresses the importance to measure 3D VOR in the clinical setting as well. Otherwise one may probably overlook valuable information in both the diagnostic work-up as well as the correct treatment proposal.

In chapter 6 and 7 the effects of a dehiscence of the superior canal are described for both the vestibular functions and the audiometry.
As described in chapter 5, the superior canal dehiscence syndrome (SCDS) is a relatively new entity, which has been described for the first time in 1998. It is caused by a partial or complete absence of bone overlying the superior semicircular canal of the equilibrium organ, which results in both dizziness and/or hearing complaints. The provoking factors to induce dizziness and/or hearing problems can be a sound stimulus (Tullio phenomenon) or pressure changes applied to the external ear canal (Hennebert sign) and/or Valsalva manoeuvre.
The fact that the SCDS has been described rather recently implies that it probably is not easy to diagnose with the current clinical tests. It has been demonstrated that the dehiscence can be shown most reliably on CT-scan slices of 0.5 mm combined with projections in the plane of the superior semicircular canal. In addition, specific signs and symptoms have been described such as Tullio phenomenon, hyperacusis, normal electronystagmography results, lateralized tuning fork tests of Weber to the affected ear and conductive hearing loss on the affected ear. We aimed to define a practical and easy diagnostic test battery for diagnosing SCDS. We examined patients with pure tone and speech audiometry, Weber tests, standard single component tympanometry, stapedius reflex tests with two-component tympanometry, continuous registration of the admittance and ABR-tests. Patients usually have a conductive hearing loss, which mimics the audiometric findings of otosclerosis, leading to unnecessary stapedotomies and occasionally sensorineural hearing loss. The normal tympanometry and stapedius reflex tests do not separate otosclerosis from SCDS, but two-component tympanometry at 678 Hz showed in almost all affected ears a minimum peak for B-curve, indicating a mass-controlled middle ear system in stead off a stiffness-controlled middle ear system as observed in otosclerosis. Two component tympanometry therefore seems to be a simple and worthy additional test, which can discem otosclerosis from SCDS.
We suggest that these tests should be added to the diagnostic work up of SCDS. Another interesting finding was that during continuous registration

spontaneous pulse-synchronous deviations in impedance were registered in those patients who also complained about autophony. Continuous registration is a simple test with valuable information on SCDS.
With our motion platform with six degrees of freedom and the possibility to apply sinusoidal stimulation in several axes in the horizontal plane it was possible to explore the influences of impairment of just one part of the equilibrium organ. We found that sinusoidal stimulation both in light and in darkness did not show any abnormalities compared with healthy subjects for the 3D VOR. This is actually an expected result, because the function of the equilibrium organ itself is not impaired by the bony dehiscence. The majority of patients with SCDS complain about a chronic form of dizziness. In daily life, normally occurring short fast head movements appear to be the major cause to impair ocular stability.

General conclusions

Overall we can make some general conclusions. Because in the light the vestibular system functions as a head fixed co-ordinated system, which fails in darkness or during fast head movements, optimisation by visual feedback system is then needed. This explains the natural occurring variability in accuracy of the 3D VOR.
Secondly, the torsional eye movement component has despite its low gain a major influence on ocular stability in both healthy subjects and in patients. Therefore, the 3D VOR is an important diagnostic test in a patient with complaints of dizziness.

Chapter 9

Summary / Samenvatting

Summary

Maintaining balance and spatial orientation during voluntary and involuntary motions is a joint effort between three sensory systems – visual, vestibular and propriocepsis – which are integrated in the brain. If there is a failure somewhere in this process of sensory-motor integration, complaints of dizziness and/or unsteadiness occur. It is of clinical importance to analyse in which sensory system(s) the problem(s) arise(s). Because complaints of dizziness are hard to describe for a patient and also because it is not unthinkable that more than one ailment can be active within a patient at the same time, it is important to have a specific diagnostic test for each sensory system. The aim of this thesis was to get more insight into the naturally occurring variability's in 3D vestibulo-ocular stabilisation and to find the changes that occur in 3D vestibulo-oculular stabilisation in patients with various types of unilateral vestibular disorders.
The sense of equilibrium consists of three semicircular canals and two otolith organs in each petrosal bone (os petrosum of the os temporale) of the skull. The function of the semicircular canals is to register angular accelerations during three-dimensional head movements. The function of the otoliths is to register linear accelerations in 3D and detect changes with respect to gravity. To test the function of the vestibular function the vestibulo-ocular reflex (VOR) is used. The VOR is a reflexive eye movement that makes possible that during a head movement the visual image stabilises on the retina. There are two types of VOR. The angular VOR is generated by the semicircular canals and the linear VOR by the otoliths. The usually used measure to quantify VOR is 'gain', which is the ratio between head velocity and the compensatory eye velocity.

In chapter 2 the 3D infrared video eye registration system (Chronos) is compared with the 3D scleral search coil technique, the golden standard in eye movement registration. 3D eye movements are simultaneously registered with both eye registration systems in four healthy subjects during fixation, saccades, optokinetic stimulation and vestibular stimulation. Because of the lower time resolution and lower stability of the cameras of the Chronos, the conclusion can be made that the scleral search coil technique is the preferred method for measurements with high precision or measurements with fast head movements. The estimate of the torsion component of the eye movement is also less accurate with the video method than with the scleral search coil technique.

In chapter 3 we describe 3D eye movement measurements in six healthy subjects during whole body sinusoidal rotation stimulation and constant accelerated impulses in light and darkness on a six degrees of freedom platform. We measured both gain and misalignment. Misalignment is the angular difference between the eye and the head rotation axis. The healthy subjects were rotated at the vertical axis and axes in the horizontal plane with steps of 22.5 degrees. Impulses were given in the cardinal axes and in the direction of the vertical canal plane.
An interesting result is that the misalignment for sinusoidal rotation in light showed minimum values for the cardinal axes pitch and roll, but maximum values with stimulation about the vertical canal plane pairs. These values are consistent with a co-ordinate system with a fixed head's pitch and torsion

axis that reflects optimised strategies for foveal vision. However, our results also showed that during sinusoidal rotation in darkness and during acceleration rotation impulses, this head-fixed co-ordination system is not persistent but depends on visual feedback. Even in healthy subjects misalignments in the vestibular function response have to be partially corrected by vision. We conclude that an intact and active integration of visual and vestibular afferent information is necessary to have optimal vestibular function.

In chapter 4 three patients operated for a vestibular Schwannoma were compared with three patients with a not operated vestibular Schannoma with respect to 3D ocular stability. The gain and misalignment of the 3D VOR were calculated after whole body sinusoidal rotary stimulation and impulses. The gain and misalignment of the not operated patients were mild to severe. This contrasted with the operated patients where nearly normal values were found. Probably a drift in the torsion component is responsible for the odd misalignment. This suggests that compensatory mechanisms in the repair of the VOR can only be effective in a stable situation if there is a permanent loss of function of the labyrinth.

In chapter 5 an overview is given of the superior canal dehiscence syndrome (SCDS) first described in 1998. A dehiscence of the bony canal of the superior vertical canal acts as a 'third window' through which dizziness and oscillopsia can be generated after a sound and/or pressure stimulus in the affected ear. This dehiscence is visible on a CT scan. A characteristic symptom is that after a sound stimulus, during Valsalva manoeuvre or after pressure changes in the external ear canal an eye movement with vertical/torsional component can be seen.

In chapter 6 we examined four patients with SCDS. The effects of the dehiscence on 3D ocular stability were analysed during vestibular stimulation, fixation, pressure changes in the external ear canal (Hennebert sign) and sound stimulus (Tullio phenomenon). The gain and misalignment of the 3D VOR was calculated after 'whole body' sinusoidal rotary stimulation. All patients had a positive Hennebert sign. In two patients eye movements were found to oscillate at the same rate as their heartbeat during the fixation task. The gain and misalignment were not impaired during sinusoidal stimulation in light and in darkness.

In chapter 7 the audiometric results of five patients with SCDS are described. The standard test battery (pure tone and speech audiometry, Weber testing, tympanometry and stapedius reflex test) presented with results according to literature. We extended this with two-component tympanometry, continuous registration and click-evoked ABR testing. ABR testing did not show any abnormalities. Two-component tympanometry at 678 Hz showed a pattern contra-indicative of a more than average stiffness-controlled middle ear system. During continuous registration pulse synchronous deviations were observed in the affected ear. The results of two-component tympanometry and continuous registration are in accordance with the 'third window' hypothesis. Therefore these tests are an improvement in the diagnostic work up when SCDS is suspected.

The general conclusions from this thesis are: (1) for 3D ocular stability torsion eye movements play a prominent role in maintaining 3D stability. Small changes in this component have a major influence on the stability of the VOR in terms of alignment of the eye rotation axis with respect to the head rotation axis. In this way torsion has, despite its low gain, a large impact on our sense of equilibrium. (2) Because in the light the vestibular system functions as a head fixed co-ordinated system, which fails in darkness or during fast head movements, optimisation by visual feedback system is then needed. This explains the natural occurring variability in accuracy of the 3D VOR.

Samenvatting

Het behoud van het evenwicht en de ruimtelijke oriëntatie tijdens willekeurige en onwillekeurige bewegingen is een nauw samenspel tussen drie zintuigsystemen – visus, vestibulair systeem en propriocepsis – die geïntegreerd worden in de hersenen. Als ergens in het proces van de sensomotorische integratie iets mis gaat, uit zich dat in duizeligheid of wankelheid. Het is van klinisch belang een onderscheid te kunnen maken in welk van deze zintuigsystemen het probleem is gelokaliseerd. Omdat voor een patiënt klachten van duizeligheid moeilijk in woorden zijn uit te drukken en het ook niet ondenkbaar is dat meer dan één oorzaak in een patiënt tegelijk kan voorkomen, is het belangrijk een gerichte onderzoeksmethode te hebben per zintuigsysteem. Het doel van dit proefschrift was om meer inzicht te krijgen in de natuurlijke variaties in 3D vestibulo-oculaire stabilisatie en om de veranderingen hierin in 3D vestibulo-oculaire stabilisatie te vinden bij patiënten met verschillende vormen van eenzijdige vestibulaire afwijkingen. Het evenwichtsorgaan bestaat uit drie halfcirkelvormige kanalen en twee otoliet - organen in elk rotsbeen (os petrosum van het os temporale) van de schedel. De functie van de halfcirkelvormige kanalen is driedimensionaal (3D) de hoekversnellingen tijdens hoofdbeweging op te merken. De functie van de otolieten is lineaire versnellingen op te merken in 3D en veranderingen ten opzichte van de zwaartekracht vast te stellen. Om de functie van het vestibulaire systeem te toetsen wordt gebruik gemaakt van de vestibulo-oculaire reflex (VOR). De VOR is een reflexmatige oogbeweging die ervoor zorgt dat tijdens een hoofdbeweging het gezichtsbeeld op het netvlies stabiliseert. Er zijn twee typen VOR. De angulaire VOR wordt opgewekt door de halfcirkelvormge kanalen en de lineaire VOR door de otolieten. De van oudsher gebruikte maat om de VOR te kwantificeren is ‘gain’. ‘Gain’ is de verhouding tussen de snelheid van de oogbeweging en de snelheid van de hoofdbeweging.

In hoofdstuk 2 wordt het 3D infrarood video oogregistratie systeem (Chronos) vergeleken met de 3D ‘scleral search coil’ techniek, de gouden standaard in de registratie van oogbewegingen. 3D oogbewegingen worden gelijktijdig vastgelegd met beide oogregistratie systemen in vier gezonde proefpersonen tijdens fixatie, saccades, optokinetische stimulatie en vestibulaire stimulatie. Vastgesteld kan worden dat vanwege de lagere tijdsresolutie en de geringe stabiliteit van de camera’s van de Chronos, de coil techniek de voorkeur heeft tijdens metingen waarvoor een hoge precisie noodzakelijk wordt geacht of metingen met snelle hoofdbewegingen. De kwaliteit van de torsie component van de oogbeweging is ook minder nauwkeurig te meten met de Chronos dan met de coil techniek.

In hoofdstuk 3 werden bij zes gezonde proefpersonen, tijdens ’whole body’ sinusoïdale rotatie stimulatie en constant geaccelereerde impulsen in licht en donker, opgewekt door een platform met zes vrijheidsgraden, de 3D oogbewegingen gemeten. De maat van uitkomst is ‘gain’, maar ook ‘misalignment’ (asafwijking). De asafwijking is het hoekverschil tussen de oogas en hoofdrotatie as. De gezonde proefpersonen werden rondgedraaid rond de verticale as en rond assen in het horizontale vlak met stappen van 22.5 graden. Impulsen werden gegeven in de kardinale assen en de richting van het verticale kanaalvlak. Een belangrijk resultaat is dat de asafwijking bij

sinusoïdale rotatie in het licht minimum waarden geeft voor de kardinale assen 'pitch' (afgeleid van het Engelse woord voor stampen van een schip) en 'roll' (afgeleid van het Engelse woord voor slingeren van een schip), maar maximale waarden bij stimulering van de verticale kanaalassen. De gemeten waarden passen bij een coördinatie systeem waarbij de hoofdassen gefixeerd zijn, passend bij geoptimaliseerde strategieën voor foveaal (scherp) zien. De resultaten van de metingen in het donker en tijdens impulsstimulatie laten zien dat dit coördinatiesysteem onvoldoende functioneert en een visuele terugkoppeling noodzakelijk maakt. Zelfs in gezonde personen worden asafwijkingen deels gecompenseerd door visuele terugkoppeling. Wij constateren, dat een intacte en actieve integratie van zowel visuele als vestibulaire informatie nodig is voor optimale vestibulaire functie.

In hoofdstuk 4 worden drie patiënten die geopereerd waren aan een vestibulair Schwannoom vergeleken met drie niet geopereerde patiënten voor wat betreft de 3D oculaire stabiliteit. De 'gain' en asafwijking van de 3D VOR werd berekend na 'whole body' sinusoïdale rotatie stimulatie en impulsen. De 'gain' en asafwijking van de niet geopereerde patiënten waren matig tot ernstig verstoord. Dit is in tegenstelling met de geopereerde patiënten, waarbij bijna normale waarden werden gevonden. Waarschijnlijk is een drift in de torsie component verantwoordelijk voor de gevonden asafwijking. Dit wekt de indruk dat compensatoire mechanismen in het herstel van de VOR alleen resultaat hebben in een stabiele toestand, zoals bij blijvend functieverlies van een labyrint.

In hoofdstuk 5 wordt een overzicht gegeven van het superior canal dehiscence syndroom (SCDS), dat in 1998 voor het eerst is beschreven. Een 'dehiscentie' (onderbreking) van het benige kanaal van het voorste verticale kanaal werkt als een 'derde venster' waardoor duizeligheid en oscillopsia opgewekt kunnen worden tijdens een geluid en/of drukstimulus in het aangedane oor. Deze 'dehiscentie' is zichtbaar op een CT scan. Karakteristiek is ook dat na een geluidstimulus, tijdens een Valsalva manoeuvre of door drukveranderingen in de uitwendige gehoorgang een oogbeweging met verticale/torsie component kan worden gezien.

In hoofdstuk 6 wordt bij vier patiënten met SCDS het effect van de 'dehiscentie' op de 3D oculaire stabiliteit bepaald tijdens vestibulaire stimulatie, fixatie, drukveranderingen in de uitwendige gehoorgang (teken van Hennebert) en na geluidstimulus (Tullio fenomeen). De 'gain' en asafwijking van de 3D VOR werd berekend na 'whole body' sinusoïdale rotatie stimulatie. Alle patiënten hadden een positief teken van Hennebert. Bij twee patiënten werd tijdens fixatie een oscillerende oogbeweging vastgesteld met hartslagfrequentie. De 'gain' en asafwijking waren niet afwijkend tijdens sinusoïdale stimulatie in het licht en donker.

In hoofdstuk 7 worden de audiometrische resultaten beschreven van vijf patiënten met SCDS. De gebruikelijke testbatterij (toon/spraakaudiometrie, stemvorkproef volgens Weber, tympanometrie en stapedius reflexmeting) was conform de literatuur. Wij hebben twee-componenten tympanometrie, continue registratie en hersenstam onderzoek hieraan toegevoegd.

Het hersenstam onderzoek toonde geen afwijkingen. Twee-componenten tympanometrie met 678 Hz liet een patroon zien dat pleit tegen een verhoogde stijfheid van het middenoorsysteem. Tijdens continue registratie werden pols-synchrone deviaties waargenomen in het aangedane oor. De resultaten van twee-componenten tympanometrie en continue registratie komen overeen met de 'derde venster' hypothese. Daardoor kunnen deze onderzoeken waardevol zijn in het vaststellen van de diagnose SCDS.

De algemene conclusies van dit proefschrift zijn: (1) dat voor 3D oculaire stabiliteit de torsie oogbewegingen een belangrijke rol spelen in het behoud van de oculaire stabiliteit; kleine veranderingen hierin hebben grote invloed op de stabiliteit van de VOR, dat wil zeggen in het vasthouden ('alignment') van de oogrotatie as ten opzichte van de hoofdrotatie as. Hierdoor oefent torsie, ondanks zijn lage 'gain', een grote invloed uit op ons evenwichtsorgaan. (2) Omdat in het licht het vestibulaire systeem functioneert als een coördinatie systeem waarbij de hoofdassen gefixeerd zijn, dat tijdens stimulatie in het donker of tijdens snelle hoofdbewegingen faalt, is een visuele terugkoppeling nodig. Dit verklaart de natuurlijk voorkomende variabiliteit in de nauwkeurigheid van de 3D VOR.

Dankwoord

Toen we (Hans, Mark en ik) begonnen met ons 'evenwichtslab' bestond dit uit een kale ruimte met een groot apparaat erin en veel maar dan ook veel computers. Terugkijkend kunnen we trots zijn dat we dit tot zo'n mooi en functioneel laboratorium hebben weten te ontwikkelen.
Werkend aan dit proefschrift kom je tot het besef dat dit alleen tot stand kan komen door de inzet van en samenwerking met vele anderen.
Daarom wil ik dan ook iedereen bedanken die meegewerkt heeft aan de totstandkoming van dit werk.
Tevens wil ik nu de gelegenheid nemen om een aantal mensen in het bijzonder te bedanken:

Dr. J. van der Steen, beste Hans, mijn copromotor en bovenal directe begeleider in al die jaren, jouw inspiratie en absolute volharding was me tot steun. Je bent een wetenschapper in hart en nieren en ik heb veel van je geleerd. Soms moest je me een beetje temperen en ik zal dan ook jouw opmerking niet vergeten: 'Janine, jij altijd met je "even"!'

Prof. dr. L. Feenstra, geachte professor en promotor, u bent voor mij een persoon waarvoor ik een groot respect koester. Uw veelzijdigheid en diepgang, maar ook de snelle en deskundige respons als ik weer iets naar u mailde ter beoordeling werkte stimulerend. U wist me te blijven motiveren.

Prof. dr. J.G.G. Borst, geachte professor en promotor, in één woord bijzonder dat u altijd precies die punten eruit wist te halen die nog extra aandacht vroegen. Erg inspirerend.

Dr. M.M.J. Houben, beste Mark, het was leerzaam om met jou het onderzoek vorm te geven en je onderzoekservaring daarin mee te nemen. Belangrijk voor mij was je gezelligheid en humor tijdens het werk.

Prof. dr. R.J. Baatenburg de Jong, bedankt dat u tijdens mijn KNO-opleiding het belang van het doen van wetenschappelijk onderzoek hebt onderstreept.

Dr. L.J.J.M. Boumans en Ronald Maas, jullie enthousiasme voor het vestibulaire systeem is bijzonder en werkte aanstekelijk, bedankt hiervoor.

Drs H.A. Reincke, beste Hermerik, het was fijn om met jou samen te werken.

Beste Raymond Haans, Joyce Dits en Arjen deJongste, bedankt voor jullie hulp bij de vele experimenten en analyses.

(Oud) assistenten KNO: Nadjah, Liane, Marjolein, Marc W, Jeroen, Katja, Paul, Floris, Claire, Saskia, Marieke, Froukje, Quirine, Frank, Charlotte, Tom, Laura, Gulnez, Stijn, Marc S, Thijs, allen bedankt voor jullie gezelligheid en goede samenwerking.

Mijn paranimfen ir. G. Goumans en drs. T. Drescher, lieve Guido en Tamar, fijn dat ik altijd op jullie steun kan rekenen en met name nu ook in deze bijzondere periode rondom het tot stand komen van dit proefschrift. En niet te vergeten de blijvende support.

Lieve papa en mama, lieve Rik en de rest van familie en vrienden, bedankt voor jullie begrip en geduld in de afgelopen jaren als ik weer eens niet kon komen, omdat…….
Dit wordt vanaf nu allemaal anders!

Curriculum Vitae

Janine Goumans werd geboren op 1 april 1978 te Amsterdam. Na een start op de 1e Montessori school te Nieuwegein, heeft zij de laatste vier jaar van het basisonderwijs gevolgd op de Kathedrale Koorschool te Utrecht. Op de Koorschool stond naast het basisonderwijs ook muziekeducatie centraal. Hier is dan ook haar passie voor muziek en vioolspelen ontstaan. Het eindexamen gymnasium bèta werd in 1996 behaald aan het Christelijk Gymnasium te Utrecht.
In datzelfde jaar begon zij met de studie Geneeskunde aan de Erasmus Universiteit Rotterdam (EUR). Tijdens haar studie heeft ze o.a. keuzevakken gevolgd in medische geschiedenis en ethiek. Haar afstudeeronderzoek 'Measurements error in grip and pinch force measurements in patients with hand injuries' deed zij aan de afdeling Revalidatie Geneeskunde van het Erasmus Medisch Centrum.
Naast de reguliere co-schappen liep zij een keuze co-schap in het 's Lands Hospitaal, Parimaribo te Suriname, op de afdeling Gynaecologie en Verloskunde. Het tweede keuze co-schap op de KNO/Hoofd-Halschirurgie in het Haga Ziekenhuis, lokatie Leyweg, werd gecombineerd met het aanleggen van een data bestand van hoofdhalstumoren gericht op de kenmerken van patiënten en tumoren gekoppeld aan behandelingsresultaten. In maart 2003 werd cum laude het artsexamen afgelegd.
Sinds één april 2003 is zij werkzaam als arts-assistent op de afdeling Keel-Neus- en Oorheelkunde van het Erasmus Medisch Centrum onder leiding van Prof.dr. L. Feenstra en later Prof.dr. R.J. Baatenburg de Jong. Onder begeleiding van dr. J. van der Steen, Prof.dr. J.G.G. Borst en Prof.dr. L. Feenstra werkte zij als arts-onderzoeker op de afdeling Neurowetenschappen van de EUR aan het onderzoek naar 3D oculaire stabiliteit, beschreven in dit proefschrift.
In de loop van 2010 zal ze naar verwachting haar opleiding tot KNO-arts voltooien.

List of publications

Larsen M, de Boer AA, Dijkstra M , van Eekelen FCA, Goumans J, Kruys RM, Veenstra N. De methode-Montignac; een ethische toetsing. Ned Tijdschr Geneeskund studenten-editie, juli 1999 (3);2:38-41.

Schreuders TAR, Roebroeck ME, Goumans J, van Nieuwenhuijzen JF, Stijnen TH, Stam HJ. Measurements error in grip and pinch force measurements in patients with hand injuries. Physical therapy, september 2003 (83);9:806-815.

Goumans J, Teepe RGC, Kuypers KC, Baarsma EA. Een hypopharynxcarcinoom geassocieerd met acanthosis nigricans, een paraneoplastisch verschijnsel. Nederlands tijdschrift KNO-heelkunde, april 2004(10);2:83-86.

Houben MM, Goumans J, deJongste AH, van der Steen J. Angular and linear vestibulo-ocular responses in humans. Ann N Y Acad Sci, april 2005;1039:68-80.

Goumans J, Boumans LJ, van der Steen J, Feenstra L. Superior-canal dehiscence syndrome. Ned Tijdschr Geneeskd, juni 2005 11;149(24):1320-5.

Houben MM, Goumans J, van der Steen J. Recording three-dimensional eye movements: scleral search coils versus video oculography. Invest ophthalmol Vis Sci, january 2006; 47(1):179-87.

Goumans J, Houben MMJ, Dits J, van der Steen J. Peaks and troughs of three-dimensional vestibulo-ocular reflex in humans. J Assoc Res Otolaryngology, accepted January 2010.

List of abbreviations

ABR	Auditory Brainstem Response
ADC	Analog to Digital Converter
B	Acoustic Susceptance
CCW	Counter Clock Wise
Chronos	Video-based infrared three-dimensional eye tracker device
CSF	Cerebro Spinal Fluid
CT scan	Computed Tomography scan
CW	Clock Wise
dB	Decibel
dBnHL	Decibel Hearing Level
EVA	Enlarged Vestibular Aqueduct
FFT	Fast Fourier Transformation
G	Conductance
IR	Infra Red
LDV	Laser Doppler Vibrometry
LED	Light Emitting Diode
LF AB gap	Low Frequency Air-Bone gap
MLF	Medial Longitudinal Fascicle
MRI	Magnetic Resonance Imaging
NVA CVC list	Consonant-Vowel-Consonant word list, by the Dutch Society of Audiology
N. VIII	Nervus Statoacusticus, Nervus Octavus, Nervus Vestibulocochlearis
Pitch	Rotational axis along the interaural axis
PTA	Pure Tone Average
PVC	Poly Vinyl Chloride
Roll	Rotational axis along the naso-occipital axis
SCDS	Superior Canal Dehiscence Syndrome
SICs	Spontaneous Impedance Changes
TEOAEs	Transient Evoked Otoacoustic Emissions
UVD	Unilateral Vestibular De-afferentiation
VOR	Vestibulo-Ocular Reflex
VEMP's	Vestibular Evoked Myogenic Potentials
Yaw	Rotational axis along the rostro-caudal or vertical axis
2D	Two-Dimensional
3D	Three-Dimensional
6DF	Six Degrees of Freedom